GREAT MODELS THINK ALIKE AND THIS UNDERMINES AI OVERSIGHT

Shashwat Goel[1,2] **Joschka Strüber**[3,4] **Ilze Amanda Auzina**[3,4] **Karuna K Chandra**[5]
Ponnurangam Kumaraguru[5] **Douwe Kiela**[6,7] **Ameya Prabhu**[3,4] **Matthias Bethge**[3,4]
Jonas Geiping[1,2,3]

[1]ELLIS Institute Tübingen [2]Max Planck Institute for Intelligent Systems [3]Tübingen AI Center
[4]University of Tübingen [5]IIIT Hyderabad [6]Contextual AI [7]Stanford University

ABSTRACT

As Language Model (LM) capabilities advance, evaluating and supervising them at scale is getting harder for humans. There is hope that other language models can automate both these tasks, which we refer to as "AI Oversight". We study how model similarity affects both aspects of AI oversight by proposing *Chance Adjusted Probabilistic Agreement* (CAPA): a metric for LM similarity based on overlap in model mistakes. Using CAPA, we first show that LLM-as-a-judge scores favor models similar to the judge, generalizing recent self-preference results. Then, we study training on LM annotations, and find complementary knowledge between the weak supervisor and strong student model plays a crucial role in gains from "weak-to-strong generalization". As model capabilities increase, it becomes harder to find their mistakes, and we might defer more to AI oversight. However, we observe a concerning trend – model mistakes are becoming more similar with increasing capabilities, pointing to risks from correlated failures. Our work underscores the importance of reporting and correcting for model similarity, especially in the emerging paradigm of AI oversight.

1 INTRODUCTION

Machine Learning model capabilities have improved immensely over the last few years. Scaling up the amount of data used for training has played a crucial role in these improvements (Kaplan et al., 2020). Initially, most of the gains in Language Model (LM) capabilities came from scaling pretraining data (Llama Team, 2024a). Recently, there is increasing interest in post-training, either with human preferences (Ouyang et al., 2022), or task-specific expert annotations (Lightman et al., 2023). Collecting human preferences or annotations is slow and expensive. Therefore, with increasing model capabilities, an attractive alternative is to use LMs to annotate training data (Gilardi et al., 2023) and score model outputs (Zheng et al., 2023), to boost both training (Stiennon et al., 2020) and evaluation (Li et al., 2024b). In this paper, we refer to both these techniques together as *AI oversight*[1].

Can we rely on AI oversight going forward? This remains a topic of much debate. In this work, we study oversight from the perspective of model similarity. When assessing or teaching humans, it is well recognized that individuals have different strengths and weaknesses. Similarly, two models with 50% accuracy may misclassify completely different samples and thus be highly dissimilar (having different 'strengths'). To measure model similarity, we build on *error consistency* (Geirhos et al., 2020), which measures overlap in the samples where two models err beyond what is expected by chance due to the two models' accuracies. In Section 2, we extend the error consistency metric in two crucial ways – 1) by counting differences in predictions rather than correctness for each sample, and 2) incorporating output probabilities. In this way, our novel similarity metric, *Chance Adjusted Probabilistic Alignment* (CAPA), allows us to quantify functional similarity between models. We use this to analyze both evaluation and training using AI oversight as depicted in Figure 1:

1. LLM-as-a-Judge. Prior work has shown that LM judges are biased towards their own generations (Liu et al., 2024; Panickssery et al., 2024). It might seem possible to avoid this concern by simply using a different model as the judge. However, just like human evaluators prefer candidates

[1]The term is inspired by "scalable oversight" (Bowman et al., 2022), which studies human-in-the-loop mechanisms for AI Safety.

with similar traits (Bagues & Perez-Villadoniga, 2012), could LM judges also exhibit this *affinity bias*? In Section 3, we study this using CAPA, finding LM judges indeed assign higher scores to models that are more similar to themselves.

2. Training LMs on annotations of other LMs. Next, we study the effect of similarity on inter-LM training setups, where one model annotates data used to train another model. We hypothesize that performance gained through such training leverages complementary knowledge among models, and is thus inversely proportional to CAPA. We investigate this hypothesis in Section 4, following the weak-to-strong generalization setup (Burns et al., 2024), where a strong (larger) student model is shown to outperform the weaker (smaller) supervisor whose annotations it is fine-tuned on. Indeed, we find performance gains are higher when the supervisor and the student model are more different. Moreover, our findings indicate a higher performance ceiling for this setting than previously estimated, if the weak supervisor's complementary knowledge is leveraged effectively.

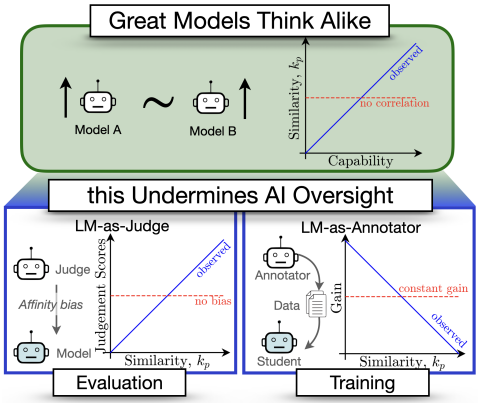

Figure 1: **Our Main Contributions.** We introduce CAPA (κ_p), a probabilistic model similarity metric adjusting for chance agreement. Using CAPA, we find: (1) LLM-as-a-judge scores favor similar models, (2) Weak-to-strong generalization improves when models differ more, and (3) Model errors become more correlated as capabilities rise.

3. With increasing LM capability errors are becoming more correlated. AI oversight is gaining popularity as capabilities increase. The above results show the benefits of diverse models for AI oversight – less similarity between models reduces bias in LLM-as-a-judge, and also leads to greater gains when training on LM annotations. Unfortunately, in Section 5 we find that as frontier LMs become more capable, their mistakes converge as captured by CAPA. This trend indicates a risk of common blind-spots and failure modes when using AI oversight, which is concerning for safety (Kenton et al., 2024).

Overall, our work proposes a novel probabilistic metric for model similarity, and demonstrates the risks of correlated mistakes in the emerging paradigm of AI oversight. We hope the community shifts towards releasing sample-wise model predictions alongside benchmark scores (Burnell et al., 2023; Ghosh et al., 2024), as they enable richer analysis like measuring similarity.

2 Methodology: Measuring LM Similarity

2.1 Background

Functional similarity: Prior work on model similarity has focused on two classes of similarity measures: representational and functional similarity (see Klabunde et al. (2024) for a recent survey). *Representation similarity* metrics focus on the weights and activations of the networks (Kornblith et al., 2019), comparing how features are represented internally. In contrast, *functional similarity* metrics focus on the input–output behavior of the model. Functional similarity metrics are more broadly applicable than representation metrics as (1) they allow comparisons across model families and architectures and (2) are applicable for models behind an API (where weights are not released). Functional similarity metrics are more interpretable because they operate on data samples rather than noisy, complex internal representations (Golechha & Dao, 2024). Despite large architectural differences across models and model families, their outputs can still be fairly similar. Moreover, Geirhos et al. (2020) argue models with similar internal mechanisms make similar mistakes, and thus mistakes can proxy whether models use similar internal mechanisms. Therefore, in the present work we focus on functional similarity metrics.

Error Consistency: A popular similarity metric designed in the context of comparing mistakes of image-classifiers to humans is error consistency (Geirhos et al., 2020). It quantifies the overlap on samples where two models make mistakes while normalizing for chance overlap due to accuracy. First, they define c_{obs} as the "observed error overlap" i.e., the fraction of samples on which both

models are correct or both models are wrong. This itself is used a metric in recent work on LM similarity, Dutta et al. (2024). However, as Geirhos et al. (2020) point out, c_{obs} has a crucial shortcoming: two independent models with high accuracy will have a higher c_{obs} by chance than two models with low accuracy (❶). An independent model here is one that is correct on a uniform random subset (size corresponding to accuracy) of samples, and wrong on the others. For instance, two independent models with 90% accuracy will agree on at least 81% of the samples by chance, whereas for two models with 50% accuracy, the lower-bound on chance agreement drops to 25%. Consequently, to account for this, Geirhos et al. (2020) calculate the "expected error overlap" (c_{exp}) as $c_{\text{exp}} = \text{acc}_1 \cdot \text{acc}_2 + (1 - \text{acc}_1)(1 - \text{acc}_2)$ where acc_i is the accuracy of model i. Similar to Cohen's κ (Cohen, 1960), error consistency (Eq. 1) is then defined as the fraction of excess agreement observed ($c_{\text{obs}} - c_{\text{exp}}$) from what is possible beyond chance ($1 - c_{\text{exp}}$):

$$k = \frac{c_{\text{obs}} - c_{\text{exp}}}{1 - c_{\text{exp}}}, \tag{1}$$

Table 1: **Comparison of Functional Similarity Metrics**. Only CAPA satisfies all three desiderata:
❶ *Adjusts for accuracy* – Does not inflate scores for model pairs with lesser scope to disagree due to higher accuracy.
❷ *Distinguishes different mistakes* – Considers different wrong predictions as a disagreement.
❸ *Incorporates probabilities* – Uses the probability distribution over predictions models provide.

Metric	Adjusts for Accuracy	Distinguishes different mistakes	Incorporates Probabilities
%Flips $= 1 - c_{\text{obs}}$ (Dutta et al., 2024)	✗	✗	✗
Cohen's κ, Scott's π, Fleiss κ	✗	✓	✗
%Agreement (Zheng et al., 2023)	✗	✓	✗
Error Consistency (Geirhos et al., 2020)	✓	✗	✗
Pearson / Matthew's Correlation of Errors	✓	✗	✗
Divergence metrics like KL, JSD	✗	✓	✓
CAPA (Ours)	✓	✓	✓

2.2 Our Contribution

We identify two key limitations of error consistency (k):

Does not distinguish differing mistakes (❷): If two models make wrong but different predictions, error consistency still counts that as an agreement. For example, two models that are always wrong, even in different ways, have perfect error consistency ($k = 1$). It thus overestimates similarity.

Does not capture probability information (❸): For comparison to humans, error consistency assumes a single top prediction, whereas models inherently output a probability distribution. Ignoring these probabilities can lead to incorrect conclusions about model similarity. Consider two models whose outputs are $[0.49, 0.51]$ and $[0.51, 0.49]$. Despite their small differences, binary labels would classify them as making entirely different predictions (0 and 1). Conversely, models with predictions $[0.99, 0.01]$ and $[0.51, 0.49]$ may share the same binary output (0 and 0) but differ significantly in confidence distribution.

Novel Metric. We redefine c_{obs} and c_{exp} to address the above limitations. For clarity we adjust the notation of our agreement metrics to c^p_{obs} and c^p_{exp}. To compute c^p_{obs} we directly use the model output probabilities (Eq.2), thus accounting for disagreement on incorrect options and better capturing model similarity. This approach lets us calculate c^p_{obs} without sample-wise ground-truth annotations. For c^p_{exp}, we take into account that the model output predictions can span over multiple options rather than only looking at sample-wise accuracy.

Definition. We define κ_p in the context of Multiple Choice Questions (MCQs), which is the format of many popular benchmarks for LMs. We provide a detailed derivation in Appendix A.1, with extensions to classification and exact match evaluations in Appendix A.3.

Observed Agreement (c^p_{obs}): It represents the probability of agreement if the model's predictions were sampled based on the *observed* likelihoods assigned over options. Formally,

$$c^p_{\text{obs}} = \frac{1}{|D|} \sum_{x \in D} \sum_{o_i \in O(x)} p_1(o_i) \cdot p_2(o_i), \tag{2}$$

where $p_1(o_i)$ and $p_2(o_i)$ are the output probabilities for model 1 and 2, respectively, on a data sample x for option o_i. $O(x)$ are the possible options: $O(x) = [o_i, \ldots, o_n]$, and $|D|$ is the number of samples.

Chance Agreement (c^p_{exp}): To account for higher accuracies inflating c^p_{obs}, we normalize by the agreement expected from two *independent* models. First, we define $\overline{p_j}$ as the average probability model j assigns to the correct option across all samples. For a perfectly calibrated model $\overline{p_j}$ approaches accuracy, thus aligning with the motivations in error consistency. Then, we define independent models as assigning $\overline{p_j}$ probability to the correct option, and uniformly distributing the remaining $1 - \overline{p_j}$ probability over the incorrect options. The latter is necessary, as there is no coherent concept of "classes" for MCQ data, i.e. the options can be permuted. This prevents us from computing class marginals for the remaining options, such as in inter-annotator agreement metrics like Cohen's Kappa, Scott's Pi (Scott, 1955), Fleiss' Kappa (Fleiss et al., 1981). Formally,

$$c^p_{exp} = \underbrace{\overline{p_1} \cdot \overline{p_2}}_{\text{chance agreement on correct option}} + \underbrace{(1 - \overline{p_1}) \cdot (1 - \overline{p_2}) \cdot \frac{1}{|D|} \sum_{x \in D} \frac{1}{|O(x)| - 1}}_{\text{chance agreement on incorrect option}}, \tag{3}$$

where $|O(x)|$ is the number of options in question x. Finally, the equation for CAPA is:

$$\kappa_p = \frac{c^p_{\text{obs}} - c^p_{\text{exp}}}{1 - c^p_{\text{exp}}} \tag{4}$$

Interpretation. We prove κ_p is bounded between -1 and 1 in Appendix A.6. A value of 0 means the models have the same agreement as independent models given their accuracies. A negative value means the models disagree, and a positive value indicates they agree beyond independent models with their accuracy. *As κ_p increases, it means models make more similar mistakes, their errors become more correlated, and they are functionally less different*. We use these interpretations interchangably.

Alternatives and Justification. We summarize comparisons to existing functional similarity measures based on key desiderata (1-3) in Table 1. In Appendix A.4 we justify design choices for CAPA, comparing it with various alternatives like using Jensen Shannon Distance (JSD), or defining c^p_{exp} using assumptions similar to Scott's π instead of Cohen's κ. We provide plots with alternative similarity metrics for our main empirical takeaways throughout the Appendix, and find consistent trends. In each case, κ_p shows the trend most clearly, with the least noise. CAPA can also be used when probabilities are unavailable by assigning probability 1 to the predicted option and 0 to the others. We use this to prove κ_p is a strict generalization of error consistency, and reduces to it for binary classification (Appendix A.1). Furthermore, κ_p can be extended beyond pairwise comparisons to multiple models, (Appendix A.2). For completeness, we present probabilistic extensions for Cohen's κ, Scott's π, Fleiss' κ_F in Appendix A.5 and show comparisons to CAPA on illustrative examples and synthetic data in Appendix A.7.

3 Affinity Bias in LLM-as-a-Judge

Evaluating free-response model generations automatically at scale is tricky (Biderman et al., 2024). This has led to popular leaderboards like Arena-hard-auto (Li et al., 2024b), AlpacaEval 2.0 (Dubois et al., 2024), and AidanBench (McLaughlin et al., 2024) adopting LLM-as-a-Judge for scoring. Recent work cautions that language models are biased towards their own outputs (Liu et al., 2024; Panickssery et al., 2024), and these leaderboards assume that excluding the judge model from the rankings circumvents this problem. However, it has been shown that human interviewers are biased towards candidates with similar knowledge and traits, a phenomenon called *affinity bias* (Bagues & Perez-Villadoniga, 2012). We study whether LMs also exhibit a bias toward similar models. This would indicate that it is not sufficient to just use a held-out LM as the judge; one must account for the confounder of similarity.

3.1 Experimental Setup

To study whether LM judges prefer more similar models, we evaluate a large set of judges and models on MMLU-Pro (Wang et al., 2024), a benchmark for hard problem solving questions across 14 domains. We filter 8,707 questions that can also be answered in a free-text response style, without options, following Myrzakhan et al. (2024).

Each question is posed to every evaluated model as an MCQ and as an open-style question. The per-sample results of the former are used to compute the similarities of judge-model pairs, whereas responses to the latter are given to an LLM-as-a-judge. The judge has to make a binary decision on whether a free-text response is correct or wrong. This is done based on its own internal knowledge without access to a ground-truth solution. We call the average of binary judgments across the benchmark the model's *Judgment Score* for a given judge. Using a parallel MCQ evaluation with ground-truth answers allows us to compare the judgment scores with verifiable accuracy measurements (details and comparisons to alternatives are in Appendix B.2), consistent with prior scalable oversight research (Bowman et al., 2022). We compute pairwise similarity with CAPA, κ_p, across 9 judge and 39 model pairs. For a complete overview of models investigated, the question filtering process, the inference setup and the prompts used for judges see Appendix B.

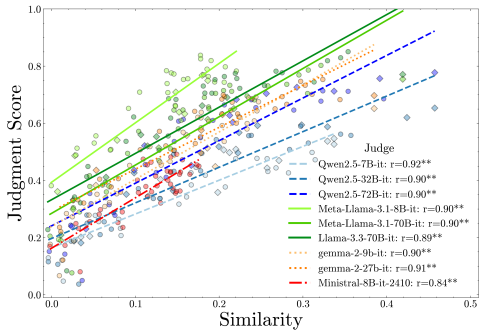

Figure 2: **Judgment Score vs. Model Similarity.** Regression lines fit judgment and similarity scores for model-judge pairs. Points represent pairs, $\diamond$ indicates same-family models. Pearson correlation values r show significant positive correlation ($**$: $p < 0.01$).

3.2 Results & Discussion

Q1: Do LM Judges favor more similar models? As a motivating example, `Qwen2.5-72B-Instruct` as a judge scores `Qwen2.5-7B-Instruct` as being 71% correct, while the more capable (41% vs 51% MCQ accuracy) `Llama-3.1-70B-Instruct` is deemed less accurate at 67%. In Figure 2 we show that model favoritism extends beyond *self-* or *family-* preference to *all* models that are functionally similar. We find a significant ($p < 0.01$) positive correlation (average Pearson r=0.84) between LLM-as-a-judge scores and model similarity (κ_p) for all judges.

Q2: Is this merely due to better accuracy? Note that while κ_p adjusts for inflation in agreement of highly accurate models, we do expect models with lower accuracy to be less similar with highly capable judge models, and thus have lower κ_p. To control for the accuracy of the evaluated model we perform multiple regression and partial correlation analysis (see Table 2). The multiple regression analysis shows that both, accuracy and similarity, have a significant positive effect on the judge score. The coefficient of accuracy increases for more capable judge models, consistent with prior work showing improved alignment with human judges (Thakur et al., 2024). The partial correlation results control for accuracy and confirm that there is still a significant effect of similarity on judgment scores even for the best judge models. Altogether, the statistical analysis confirms that judgment scores are confounded by affinity bias.

Table 2: **Partial Correlation and Multiple Regression Results.** The table reports partial correlation results between judgment scores and model similarity when controlling for accuracy (r - Pearson correlation), as well as multiple regression results between judgment scores (DV) $\sim$ similarity (IV) and accuracy (IV). $*$ and $**$ indicate significance level p<0.05 and p<0.01 respectively. Across all judges we find a significant partial correlation, which implies that after controlling for accuracy there remains a relationship between judge score and model similarity. With respect to Multiple regression, across all judges we find a significant effect of both IV on judgment scores while holding the other constant, suggesting a strong positive relationship (for details, see Appendix B.3).

Judge	Partial Cor.	Multiple Reg.	
	r	sim	acc
Qwen2.5-7B-It	0.60^{**}	0.59^{**}	0.51^{**}
Qwen2.5-32B-It	0.43^{**}	0.41^{**}	0.86^{**}
Qwen2.5-72B-It	0.42^{**}	0.47^{**}	1.04^{**}
Meta-Llama-3.1-8B-It	0.65^{**}	1.15^{**}	0.53^{**}
Meta-Llama-3.1-70B-It	0.45^{**}	0.61^{**}	0.92^{**}
Llama-3.3-70B-It	0.35^{*}	0.50^{*}	1.02^{**}
gemma-2-9b-It	0.65^{**}	0.76^{**}	0.69^{**}
gemma-2-27b-It	0.65^{**}	0.71^{**}	0.68^{**}
Ministral-8B-It-2410	0.60^{**}	0.82^{**}	0.43^{**}

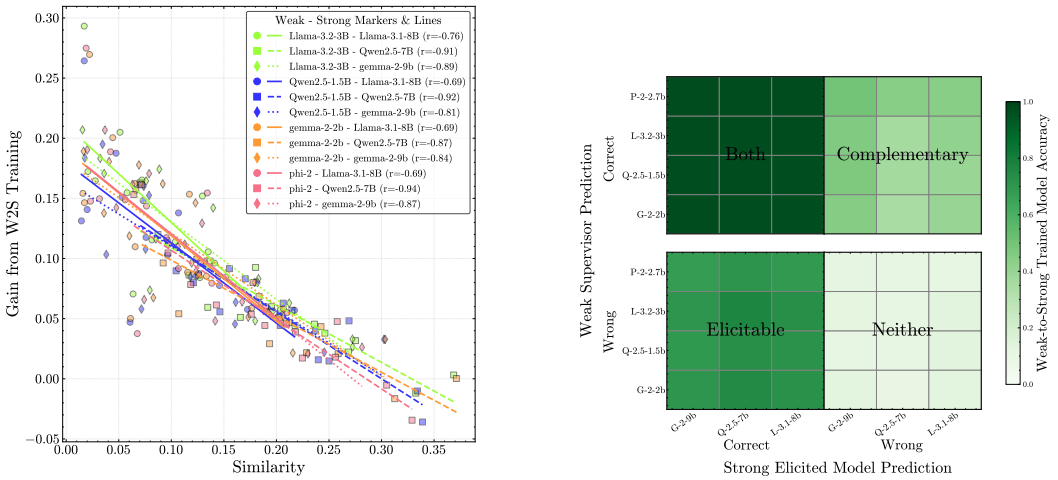

Figure 3: **Analysis of weak-to-strong generalization.** (a) The strong student gains more from weak-to-strong training across 12 model pairs on tasks where it differs more from the weak supervisor ($p < 0.01$). (b) Complementary knowledge transfer enhances performance beyond mere elicitation, as test accuracy is partitioned by the correctness of a weak supervisor and an oracle strong model (averaged over 15 tasks).

4 Learning from Complementary Knowledge of LM Annotators

We now study the role of similarity in AI supervising training. This can allow scaling up training data by reducing reliance on costly and time-intensive expert human inputs. There is hope that models can learn from other models to improve further even on tasks where they surpass human capabilities (Hughes et al., 2024). Where could this improvement come from? We hypothesize that the existence of complementary knowledge or capabilities between two LMs can be one mechanism for driving improvements from LM annotations, if effectively leveraged. This complement can exhibit itself in the form of differing predictions on training data, and can thus be quantified using functional similarity between the supervisor and student model. Lower κ_p is indicative of more complementary knowledge, and as an implication of our hypothesis, should inversely correlate with the performance gain of a student model when trained on the supervisor's annotations.

4.1 Experimental Setup

Burns et al. (2024) study training a larger student model on annotations from a small task-finetuned "expert" teacher. They find the student can outperform the supervisor, a phenomenon they call "weak to strong generalization". We study this setup as it can seem counter-intuitive when viewed from the lens of accuracies. How can training a 60% accuracy student on a 70% accuracy task-finetuned teacher lead to 75% accuracy? To investigate this, we adopt a lens of complementary knowledge.

We measure similarity between the weak supervisor and base student model on the validation set. We then perform weak-to-strong training on the student model, using the confidence-weighted finetuning objective proposed in Burns et al. (2024). We investigate if similarity is an apriori predictor of performance gained on the test set. For our experiments, we study 4 weak models in the $1-3$B parameter range, and 3 strong models in the $7-9$B parameter range, for a total of 12 model pairs, and 15 of the NLP tasks studied in Burns et al. (2024), specified in Table 17. The full setup is consistent with the open-weight model reproduction by (Scherlis et al., 2024), and is described in Appendix C.1.

4.2 Results & Discussion

Q1: Does Complementary Knowledge Influence Performance Gain? Figure 3a shows that for all model combinations, similarity between the weak supervisor and initial strong student inversely correlates with the improvement obtained from weak-to-strong training ($r = -0.85$). Even after using partial correlation analysis to control for the accuracy gap between the weak supervisor and strong student, similarity is inversely correlated with weak-to-strong gain ($r = -0.35, p < 0.01$). Thus,

tasks where the supervisor and student make less correlated errors tend to yield greater improvements. This contributes towards understanding why gains from weak to strong training vary across tasks, an open question posed by Burns et al. (2024).

Q2. Does Complementary Knowledge Add Beyond Elicitation? The original explanation for performance gains from weak-to-strong generalization is that the weak supervisor "elicits" the latent knowledge in the superior representations of the stronger student (Burns et al., 2024). To investigate whether complementary knowledge adds to this explanation or is subsumed within it, we first obtain the strong model with "upper-bound" elicitation by finetuning it on ground-truth annotations. We refer to this as the *strong elicited* model. We can then separate the test data into four parts based on whether the strong elicited and weak supervisor model were correct or wrong, measuring average accuracy of the weak-to-strong model on each part to disentangle gains from different factors. The experiment setup is discussed further in Appendix C.2.

Table 3: **Accuracy gains possible from weak-to-strong training.** We average accuracies across 15 datasets and 12 model pairs and report gaps to the student model's initial accuracy. Complementary knowledge transfer can enable higher gains than the previously considered ceiling estimate from elicitation.

Model	**Accuracy Gap**
Initial Strong Student	75.1%
Weak Supervisor	+4.1
Weak to Strong Trained Student	+7.4
Ceiling Estimate	
Ground-truth Elicitation (previous)	+11.2
Elicitation ∪ Complementary (ours)	+14.1

Figure 3b reports aggregate values across 15 tasks for 12 model pairs. Accuracy on the bottom-left quadrant (avg. 71.9%) can only be due to successful elicitation, as here the weak supervisor was wrong. Accuracy on the top-right quadrant (avg. 42.2%) can only be due to complementary knowledge transfer as here the upper-bound elicitation model was wrong. This confirms that elicitation plays an important role in weak-to-strong generalization, with complementary knowledge transfer from the weak supervisor also contributing to significant gains.

Q3. Where can weak-to-strong training improve? The strong elicited model is considered to represent upper-bound performance, but as shown in Table 3, the actual ceiling is significantly higher if complementary knowledge of the weak supervisor is fully leveraged. Interestingly, on the training set, the weak-to-strong trained model shows similar accuracy on the top-left and bottom-right quadrants as shown in Figure 11. Yet, when generalizing to unseen samples, it falls back more often to its initial priors. We hope this analysis guides future work on improving weak-to-strong training methodology, by highlighting complementary knowledge as a concrete avenue for improvement.

5 Models are making more similar mistakes as capabilities increase

The previous two sections highlighted two major advantages of having access to more diverse LMs: a) it leads to less biased judges, b) it can drive more performance gains from training on LM annotations. This points to the importance of diversity, or lower model similarity, for AI oversight. As AI oversight becomes increasingly relevant with advancing capabilities, we now study similarity trends in existing LMs across different levels of capability. It has been shown model representations across modalities are converging with increasing capabilities (Huh et al., 2024). This raises the question as to whether this also leads to more similar mistakes?

5.1 Experimental Setup

We collect sample-wise evaluation files for 130 official models from the OpenLLM Leaderboard 2 released by HuggingFace, listed in Appendix D.5. We use MMLU-Pro (Wang et al., 2024) and Big Bench Hard (BBH) (Suzgun et al., 2023) as they measure a broad range of capabilities using MCQ, and frontier models have reasonable accuracies while not saturating these datasets. We first bucket these models into five performance percentile ranges. Then, for each model, we compute its mean similarity (κ_p) with models in the same bucket from different developers, to prevent confounding from distillation or continual training. More setup details are provided in Appendix D.1. In Appendix D.3 we also report pairwise results, and using the extension of κ_p for sets of $M > 2$ models.

5.2 Results & Discussion

Q1. Are model errors becoming more correlated with improving capabilities? Figure 4 shows a strong positive correlation between model capabilities and κ_p, which measures similarity beyond chance agreement due to accuracy. In Appendix D.4 we find this also holds across individual categories in both datasets, not just in aggregate.

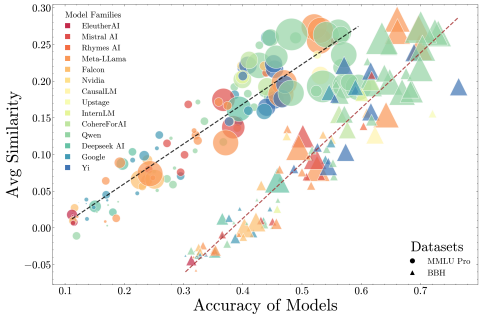

Figure 4: **Average Similarity (κ_p) vs Model Capability**. We split 130 LMs into 5 buckets based on their accuracy percentile. For each LM we compute its mean similarity within the bucket (across models from different developers), and plot it against model accuracy. The size of the scatter points is proportional to model size. As κ_p measures overlap in mistakes, the positive correlation indicates LM mistakes are getting more correlated with increasing capabilities.

Potential Implications. If this trend continues, it could mean greater affinity bias when using LM judges, and lower potential for gains from inter-LM training in the context of our earlier results. It could amplify collective biases, and undermine benefits of independence when using LM juries. Most concerningly, our results indicate that as model blind-spots get harder to detect, making us defer more to AI oversight, models also make more similar mistakes, posing safety risks from correlated failures.

Q2. Why are model errors becoming more correlated? This is an interesting research direction in itself. We perform a preliminary analysis in Appendix D.2, summarizing key conclusions here. First, we observe only a slight increase in similarity for harder questions, indicating difficulty is not a significant confounder for this trend. We find this trend is stronger in instruction-tuned models, and using alternative architectures like Mamba (Gu & Dao, 2023) may not be enough to increase diversity.

6 Related Work

There is increasing interest in finding differences between models for applications like visual tools for comparative analytics (Strobelt et al., 2021; Kahng et al., 2024), efficient human evaluation (Boubdir et al., 2023), comparing learning algorithms (Shah et al., 2023), identifying side-effects of API updates (Eyuboglu et al., 2024) or quantization (Dutta et al., 2024). Prior work has also looked at qualitatively describing differences between data distributions (Zhong et al., 2022; 2023; Dunlap et al., 2024b;a). Our work proposes metrics to quantify LM differences (or similarity). Huh et al. (2024) used representation similarity metrics (Kornblith et al., 2019; Bansal et al., 2021) to show convergence in visual representations and their alignment with language representations. In contrast, we show model mistakes are becoming more correlated as capabilities improve, using sample level evaluations (Burnell et al., 2023) such as those available on OpenLLMLeaderboard (Myrzakhan et al., 2024) and HELM (Bommasani et al., 2023). Geirhos et al. (2020) proposed measuring "error consistency" between image classifiers and humans, with Geirhos et al. (2021) showing an early trend of data-rich models making more similar mistakes to humans. We enrich this metric, distinguishing between different mistakes and incorporating probabilistic information.

Our results on AI judges fall in a broader line highlighting their pitfalls (Zheng et al., 2024). These include biases such as favoring verbose texts or options at certain positions (Koo et al., 2024; Ye et al., 2024). Interestingly, these biases are also sometimes found in human annotators (Chen et al., 2024). In fact, there is rich literature documenting biases in human judgements of other humans. One such bias is affinity bias, where recruiters prefer candidates with similar knowledge and skills as them (Bagues & Perez-Villadoniga, 2012). We show LM judges also systematically favor other models that make similar mistakes, generalizing previous results that showed LMs favor their own outputs (Liu et al., 2024; Panickssery et al., 2024). Overall, we believe AI evaluators should be accompanied with formal checks like consistency (Fluri et al., 2024).

A second aspect of AI oversight is using another model's supervision to train better models. This is similar to training on text generated by an LM (Chiang et al., 2023) with ongoing debates about its benefits (Kazdan et al., 2024), and an emerging paradigm of exploiting a gap in difficulty between solution generation and evaluation (Song et al., 2024). In this paper, we study the more

established setup of training LMs on LM annotations, where Burns et al. (2024) demonstrated the phenomenon of weak to strong generalization, and it has been leveraged for other applications like image classification (Guo et al., 2024) and aligning models (Zhu et al., 2024). Prior work has attempted to understand weak to strong generalization, notably using "misfit error" (Charikar et al., 2024), which shows that the student's disagreement with the weak supervisor *after* weak to strong training correlates with its accuracy gap from the weak supervisor. Instead, we show similarity between the weak supervisor and strong student can *apriori* predict gains from weak-to-strong training. The benefit of model diversity has previously been discussed in related settings like knowledge distillation for image classifiers (Roth et al., 2024) and training chess models that outperform the humans they are trained on (Zhang et al., 2024).

7 Conclusion, Limitations, Future Work

Our paper shows the importance of measuring functional similarity for language models. We derive a novel, probabilistic metric for model similarity, CAPA (κ_p). We then use it to study the implications of similarity for AI oversight – showing affinity bias in AI judges, and the role of complementary knowledge when training on LM annotations, such as in weak-to-strong generalization. AI oversight will become more relevant as capabilities improve, so our finding that increasing capabilities could lead to more correlated errors is particularly concerning. Thus, we believe measuring and accounting for model similarity is going to be increasingly important. We now list some limitations of our work, and avenues for developing a better understanding of model similarity and its implications.

Establishing Causation: We established similarity correlates with both aspects of AI oversight – evaluation and training supervision. To establish causality, we need methods to make a model less similar without harming capabilities, which is itself a challenging open problem.

Extending to similarity metrics for free-text outputs: Everyday use of generative models is based on their free-text responses. Like much work on benchmarking, we had to limit to MCQ tasks as the science of precisely evaluating free-text is still evolving (Biderman et al., 2024). For example, both model-free (Papineni et al., 2002) and model-based metrics (Pillutla et al., 2021) suffer from a wide range of syntax and style sensitivity issues (Kocmi et al., 2021; He et al., 2023). We hope the community takes up the challenge of designing similarity metrics for free-response text and reasoning. This would allow studying the role of similarity using more promising oversight setups like debate (Kenton et al., 2024) and process supervision (Lightman et al., 2023).

Generator-Verifier gap: AI oversight has recently shown promise for tasks where it is easier to validate a solution than generate it (Song et al., 2024). Similarity may continue to play a role here. (1) In evaluations, similarity in stylistic preferences of the generated solution may influence judge scores. (2) In training, the generator-verifier gap may be larger if models are more different.

Safety implications: Researchers separately develop many post-training interventions to reduce harmfulness, dual-use knowledge, dishonesty etc. In real world model deployments, all these problems have to be tackled at once, which can benefit from composing interventions (Kolbeinsson et al., 2024). If the benefits are decorrelated, composing would lead to greater compound safety. If the side effects are correlated, composing would lead to lower accumulation. More broadly, measuring LM similarity post-intervention can help characterize decorrelation in research bets, for granters (Canton, 2025). For example, LM unlearning was recently found to be functionally similar to refusal training (Łucki et al., 2024), even though it was proposed as a complementary safeguard (Li et al., 2024a). Finally, as we transition towards language agents, similarity can help understand collective "blind spots" (He et al., 2023), and could lead to better cooperation (Lowe et al., 2017) but also scheming (Balesni et al., 2024) between multiple agents.

Qualitative analysis of model differences: We developed quantitative methods for measuring LM similarity on a given data distribution. One exciting direction is to use these metrics to provide qualitative difference descriptors (Dunlap et al., 2024a) between models, by describing data distributions where models are least similar.

REFERENCES

Loubna Ben Allal, Anton Lozhkov, Elie Bakouch, Gabriel Martín Blázquez, Lewis Tunstall, Agustín Piqueres, Andres Marafioti, Cyril Zakka, Leandro von Werra, and Thomas Wolf. Smollm2 - with great data, comes great performance. https://github.com/huggingface/smollm, 2024.

Manuel Bagues and Maria J Perez-Villadoniga. Do recruiters prefer applicants with similar skills? evidence from a randomized natural experiment. *Journal of Economic Behavior & Organization*, 82(1):12–20, 2012.

Mikita Balesni, Marius Hobbhahn, David Lindner, Alexander Meinke, Tomek Korbak, Joshua Clymer, Buck Shlegeris, Jérémy Scheurer, Charlotte Stix, Rusheb Shah, Nicholas Goldowsky-Dill, Dan Braun, Bilal Chughtai, Owain Evans, Daniel Kokotajlo, and Lucius Bushnaq. Towards evaluations-based safety cases for ai scheming, 2024. URL https://arxiv.org/abs/2411.03336.

Yamini Bansal, Preetum Nakkiran, and Boaz Barak. Revisiting model stitching to compare neural representations. *NeurIPS*, 2021.

Stella Biderman, Hailey Schoelkopf, Lintang Sutawika, Leo Gao, Jonathan Tow, Baber Abbasi, Alham Fikri Aji, Pawan Sasanka Ammanamanchi, Sidney Black, Jordan Clive, Anthony DiPofi, Julen Etxaniz, Benjamin Fattori, Jessica Zosa Forde, Charles Foster, Jeffrey Hsu, Mimansa Jaiswal, Wilson Y. Lee, Haonan Li, Charles Lovering, Niklas Muennighoff, Ellie Pavlick, Jason Phang, Aviya Skowron, Samson Tan, Xiangru Tang, Kevin A. Wang, Genta Indra Winata, François Yvon, and Andy Zou. Lessons from the trenches on reproducible evaluation of language models, 2024. URL https://arxiv.org/abs/2405.14782.

Rishi Bommasani, Percy Liang, and Tony Lee. Holistic evaluation of language models. *Annals of the New York Academy of Sciences*, 2023.

Meriem Boubdir, Edward Kim, Beyza Ermis, Marzieh Fadaee, and Sara Hooker. Which prompts make the difference? data prioritization for efficient human llm evaluation, 2023. URL https://arxiv.org/abs/2310.14424.

Samuel R. Bowman, Jeeyoon Hyun, Ethan Perez, Edwin Chen, Craig Pettit, Scott Heiner, Kamilė Lukošiūtė, Amanda Askell, Andy Jones, Anna Chen, Anna Goldie, Azalia Mirhoseini, Cameron McKinnon, Christopher Olah, Daniela Amodei, Dario Amodei, Dawn Drain, Dustin Li, Eli Tran-Johnson, Jackson Kernion, Jamie Kerr, Jared Mueller, Jeffrey Ladish, Joshua Landau, Kamal Ndousse, Liane Lovitt, Nelson Elhage, Nicholas Schiefer, Nicholas Joseph, Noemí Mercado, Nova DasSarma, Robin Larson, Sam McCandlish, Sandipan Kundu, Scott Johnston, Shauna Kravec, Sheer El Showk, Stanislav Fort, Timothy Telleen-Lawton, Tom Brown, Tom Henighan, Tristan Hume, Yuntao Bai, Zac Hatfield-Dodds, Ben Mann, and Jared Kaplan. Measuring progress on scalable oversight for large language models, 2022. URL https://arxiv.org/abs/2211.03540.

Ryan Burnell, Wout Schellaert, John Burden, Tomer D. Ullman, Fernando Martinez-Plumed, Joshua B. Tenenbaum, Danaja Rutar, Lucy G. Cheke, Jascha Sohl-Dickstein, Melanie Mitchell, Douwe Kiela, Murray Shanahan, Ellen M. Voorhees, Anthony G. Cohn, Joel Z. Leibo, and Jose Hernandez-Orallo. Rethink reporting of evaluation results in ai. *Science*, 2023. URL https://www.science.org/doi/abs/10.1126/science.adf6369.

Collin Burns, Pavel Izmailov, Jan Hendrik Kirchner, Bowen Baker, Leo Gao, Leopold Aschenbrenner, Yining Chen, Adrien Ecoffet, Manas Joglekar, Jan Leike, Ilya Sutskever, and Jeffrey Wu. Weak-to-strong generalization: Eliciting strong capabilities with weak supervision, 2024. URL https://openreview.net/forum?id=ghNRg2mEgN.

Erik Canton. A portfolio approach to research funding. *Research Policy*, 2025. URL https://www.sciencedirect.com/science/article/pii/S0048733324001781.

Moses Charikar, Chirag Pabbaraju, and Kirankumar Shiragur. Quantifying the gain in weak-to-strong generalization, 2024. URL https://arxiv.org/abs/2405.15116.

Guiming Hardy Chen, Shunian Chen, Ziche Liu, Feng Jiang, and Benyou Wang. Humans or LLMs as the judge? a study on judgement bias. In *EMNLP*, 2024. URL https://aclanthology.org/2024.emnlp-main.474/.

Wei-Lin Chiang, Zhuohan Li, Zi Lin, Ying Sheng, Zhanghao Wu, Hao Zhang, Lianmin Zheng, Siyuan Zhuang, Yonghao Zhuang, Joseph E. Gonzalez, Ion Stoica, and Eric P. Xing. Vicuna: An open-source chatbot impressing gpt-4 with 90%* chatgpt quality, March 2023. URL https://lmsys.org/blog/2023-03-30-vicuna/.

Davide Chicco, Matthijs J Warrens, and Giuseppe Jurman. The matthews correlation coefficient (mcc) is more informative than cohen's kappa and brier score in binary classification assessment. *IEEE Access*.

Christopher Clark, Kenton Lee, Ming-Wei Chang, Tom Kwiatkowski, Michael Collins, and Kristina Toutanova. BoolQ: Exploring the Surprising Difficulty of Natural Yes/No Questions. In *NAACL*, 2019.

Jacob Cohen. A coefficient of agreement for nominal scales. *Educational and psychological measurement*, 1960.

Yann Dubois, Balázs Galambosi, Percy Liang, and Tatsunori B Hashimoto. Length-controlled alpacaeval: A simple way to debias automatic evaluators. *arXiv preprint arXiv:2404.04475*, 2024.

Lisa Dunlap, Krishna Mandal, Trevor Darrell, Jacob Steinhardt, and Joseph E Gonzalez. Vibecheck: Discover and quantify qualitative differences in large language models, 2024a. URL https://arxiv.org/abs/2410.12851.

Lisa Dunlap, Yuhui Zhang, Xiaohan Wang, Ruiqi Zhong, Trevor Darrell, Jacob Steinhardt, Joseph E. Gonzalez, and Serena Yeung-Levy. Describing differences in image sets with natural language, 2024b. URL https://arxiv.org/abs/2312.02974.

Abhinav Dutta, Sanjeev Krishnan, Nipun Kwatra, and Ramachandran Ramjee. Accuracy is not all you need. In *The Thirty-eighth Annual Conference on Neural Information Processing Systems*, 2024. URL https://openreview.net/forum?id=QVG7j29Sta.

Sabri Eyuboglu, Karan Goel, Arjun Desai, Lingjiao Chen, Mathew Monfort, Chris Ré, and James Zou. Model changelists: Characterizing updates to ml models. FAccT '24, 2024. URL https://doi.org/10.1145/3630106.3659047.

Joseph L Fleiss, Bruce Levin, Myunghee Cho Paik, et al. The measurement of interrater agreement. *Statistical methods for rates and proportions*, 1981.

Lukas Fluri, Daniel Paleka, and Florian Tramèr. Evaluating superhuman models with consistency checks. In *2024 IEEE Conference on Secure and Trustworthy Machine Learning (SaTML)*, pp. 194–232. IEEE, 2024.

Leo Gao, Jonathan Tow, Baber Abbasi, Stella Biderman, Sid Black, Anthony DiPofi, Charles Foster, Laurence Golding, Jeffrey Hsu, Alain Le Noac'h, Haonan Li, Kyle McDonell, Niklas Muennighoff, Chris Ociepa, Jason Phang, Laria Reynolds, Hailey Schoelkopf, Aviya Skowron, Lintang Sutawika, Eric Tang, Anish Thite, Ben Wang, Kevin Wang, and Andy Zou. A framework for few-shot language model evaluation, 12 2023. URL https://zenodo.org/records/10256836.

Robert Geirhos, Kristof Meding, and Felix A Wichmann. Beyond accuracy: quantifying trial-by-trial behaviour of CNNs and humans by measuring error consistency. In *NeurIPS*, 2020.

Robert Geirhos, Kantharaju Narayanappa, Benjamin Mitzkus, Tizian Thieringer, Matthias Bethge, Felix A. Wichmann, and Wieland Brendel. Partial success in closing the gap between human and machine vision. In *NeurIPS*, 2021. URL https://proceedings.neurips.cc/paper_files/paper/2021/file/c8877cff22082a16395a57e97232bb6f-Paper.pdf.

Gemma Team. Gemma 2: Improving open language models at a practical size, 2024. URL https://arxiv.org/abs/2408.00118.

Adhiraj Ghosh, Sebastian Dziadzio, Ameya Prabhu, Vishaal Udandarao, Samuel Albanie, and Matthias Bethge. Onebench to test them all: Sample-level benchmarking over open-ended capabilities. *arXiv preprint arXiv:2412.06745*, 2024.

Fabrizio Gilardi, Meysam Alizadeh, and Maël Kubli. Chatgpt outperforms crowd workers for text-annotation tasks. *Proceedings of the National Academy of Sciences*, 120(30):e2305016120, 2023.

Satvik Golechha and James Dao. Challenges in mechanistically interpreting model representations. In *ICML 2024 Workshop on Mechanistic Interpretability*, 2024.

Albert Gu and Tri Dao. Mamba: Linear-time sequence modeling with selective state spaces. *arXiv preprint arXiv:2312.00752*, 2023.

Jianyuan Guo, Hanting Chen, Chengcheng Wang, Kai Han, Chang Xu, and Yunhe Wang. Vision superalignment: Weak-to-strong generalization for vision foundation models, 2024. URL https://arxiv.org/abs/2402.03749.

Tianxing He, Jingyu Zhang, Tianle Wang, Sachin Kumar, Kyunghyun Cho, James Glass, and Yulia Tsvetkov. On the blind spots of model-based evaluation metrics for text generation. In *ACL*, 2023. URL https://aclanthology.org/2023.acl-long.674/.

Dan Hendrycks, Collin Burns, Steven Basart, Andrew Critch, Jerry Li, Dawn Song, and Jacob Steinhardt. Aligning AI with shared human values. *arXiv preprint arXiv:2008.02275*, 2020.

Dan Hendrycks, Collin Burns, Steven Basart, Andy Zou, Mantas Mazeika, Dawn Song, and Jacob Steinhardt. Measuring massive multitask language understanding. In *International Conference on Learning Representations*, 2021. URL https://openreview.net/forum?id=d7KBjmI3GmQ.

Edward J Hu, Yelong Shen, Phillip Wallis, Zeyuan Allen-Zhu, Yuanzhi Li, Shean Wang, Lu Wang, and Weizhu Chen. Lora: Low-rank adaptation of large language models. *arXiv preprint arXiv:2106.09685*, 2021.

Lifu Huang, Ronan Le Bras, Chandra Bhagavatula, and Yejin Choi. Cosmos QA: Machine reading comprehension with contextual commonsense reasoning. *arXiv preprint arXiv:1909.00277*, 2019.

Edward Hughes, Michael Dennis, Jack Parker-Holder, Feryal Behbahani, Aditi Mavalankar, Yuge Shi, Tom Schaul, and Tim Rocktaschel. Open-endedness is essential for artificial superhuman intelligence, 2024. URL https://arxiv.org/abs/2406.04268.

Minyoung Huh, Brian Cheung, Tongzhou Wang, and Phillip Isola. The platonic representation hypothesis. *ICML*, 2024.

Minsuk Kahng, Ian Tenney, Mahima Pushkarna, Michael Xieyang Liu, James Wexler, Emily Reif, Krystal Kallarackal, Minsuk Chang, Michael Terry, and Lucas Dixon. Llm comparator: Visual analytics for side-by-side evaluation of large language models, 2024. URL https://arxiv.org/abs/2402.10524.

Jared Kaplan, Sam McCandlish, Tom Henighan, Tom B Brown, Benjamin Chess, Rewon Child, Scott Gray, Alec Radford, Jeffrey Wu, and Dario Amodei. Scaling laws for neural language models. *arXiv preprint arXiv:2001.08361*, 2020.

Joshua Kazdan, Rylan Schaeffer, Apratim Dey, Matthias Gerstgrasser, Rafael Rafailov, David L. Donoho, and Sanmi Koyejo. Collapse or thrive? perils and promises of synthetic data in a self-generating world, 2024. URL https://arxiv.org/abs/2410.16713.

Zachary Kenton, Noah Y. Siegel, János Kramár, Jonah Brown-Cohen, Samuel Albanie, Jannis Bulian, Rishabh Agarwal, David Lindner, Yunhao Tang, Noah D. Goodman, and Rohin Shah. On scalable oversight with weak llms judging strong llms. 2024. URL https://arxiv.org/abs/2407.04622.

Daniel Khashabi, Snigdha Chaturvedi, Michael Roth, Shyam Upadhyay, and Dan Roth. Looking beyond the surface: A challenge set for reading comprehension over multiple sentences. In *Proceedings of the 2018 Conference of the North American Chapter of the Association for Computational Linguistics: Human Language Technologies, Volume 1 (Long Papers)*, pp. 252–262, 2018.

Max Klabunde, Tobias Schumacher, Markus Strohmaier, and Florian Lemmerich. Similarity of neural network models: A survey of functional and representational measures, 2024. URL https://arxiv.org/abs/2305.06329.

Tom Kocmi, Christian Federmann, Roman Grundkiewicz, Marcin Junczys-Dowmunt, Hitokazu Matsushita, and Arul Menezes. To ship or not to ship: An extensive evaluation of automatic metrics for machine translation. In *Proceedings of the Sixth Conference on Machine Translation*, 2021. URL https://aclanthology.org/2021.wmt-1.57/.

Arinbjorn Kolbeinsson, Kyle O'Brien, Tianjin Huang, Shanghua Gao, Shiwei Liu, Jonathan Richard Schwarz, Anurag Vaidya, Faisal Mahmood, Marinka Zitnik, Tianlong Chen, and Thomas Hartvigsen. Composable interventions for language models, 2024. URL https://arxiv.org/abs/2407.06483.

Ryan Koo, Minhwa Lee, Vipul Raheja, Jong Inn Park, Zae Myung Kim, and Dongyeop Kang. Benchmarking cognitive biases in large language models as evaluators. In *ACL*, 2024. URL https://aclanthology.org/2024.findings-acl.29/.

Simon Kornblith, Mohammad Norouzi, Honglak Lee, and Geoffrey Hinton. Similarity of neural network representations revisited. In *ICML*, 2019.

Klaus Krippendorff. Reliability in content analysis: Some common misconceptions and recommendations. *Human communication research*, 2004.

Woosuk Kwon, Zhuohan Li, Siyuan Zhuang, Ying Sheng, Lianmin Zheng, Cody Hao Yu, Joseph E. Gonzalez, Hao Zhang, and Ion Stoica. Efficient memory management for large language model serving with pagedattention. In *Proceedings of the ACM SIGOPS 29th Symposium on Operating Systems Principles*, 2023.

Nathaniel Li, Alexander Pan, Anjali Gopal, Summer Yue, Daniel Berrios, Alice Gatti, Justin D. Li, Ann-Kathrin Dombrowski, Shashwat Goel, Gabriel Mukobi, Nathan Helm-Burger, Rassin Lababidi, Lennart Justen, Andrew Bo Liu, Michael Chen, Isabelle Barrass, Oliver Zhang, Xiaoyuan Zhu, Rishub Tamirisa, Bhrugu Bharathi, Ariel Herbert-Voss, Cort B Breuer, Andy Zou, Mantas Mazeika, Zifan Wang, Palash Oswal, Weiran Lin, Adam Alfred Hunt, Justin Tienken-Harder, Kevin Y. Shih, Kemper Talley, John Guan, Ian Steneker, David Campbell, Brad Jokubaitis, Steven Basart, Stephen Fitz, Ponnurangam Kumaraguru, Kallol Krishna Karmakar, Uday Tupakula, Vijay Varadharajan, Yan Shoshitaishvili, Jimmy Ba, Kevin M. Esvelt, Alexandr Wang, and Dan Hendrycks. The WMDP benchmark: Measuring and reducing malicious use with unlearning. In *ICML*. PMLR, 2024a. URL https://proceedings.mlr.press/v235/li24bc.html.

Tianle Li, Wei-Lin Chiang, Evan Frick, Lisa Dunlap, Tianhao Wu, Banghua Zhu, Joseph E. Gonzalez, and Ion Stoica. From crowdsourced data to high-quality benchmarks: Arena-hard and benchbuilder pipeline, 2024b. URL https://arxiv.org/abs/2406.11939.

Yuanzhi Li, Sébastien Bubeck, Ronen Eldan, Allie Del Giorno, Suriya Gunasekar, and Yin Tat Lee. Textbooks are all you need ii: phi-1.5 technical report, 2023. URL https://arxiv.org/abs/2309.05463.

Hunter Lightman, Vineet Kosaraju, Yura Burda, Harri Edwards, Bowen Baker, Teddy Lee, Jan Leike, John Schulman, Ilya Sutskever, and Karl Cobbe. Let's verify step by step. *arXiv preprint arXiv:2305.20050*, 2023.

Yiqi Liu, Nafise Moosavi, and Chenghua Lin. LLMs as narcissistic evaluators: When ego inflates evaluation scores. In *ACL*, 2024. URL https://aclanthology.org/2024.findings-acl.753/.

Llama Team. The llama 3 herd of models, 2024a. URL https://arxiv.org/abs/2407.21783.

Llama Team. Llama 3.2 model card. https://github.com/meta-llama/llama-models/blob/main/models/llama3_2/MODEL_CARD.md, 2024b.

Llama Team. Llama 3.3 model card. https://github.com/meta-llama/llama-models/blob/main/models/llama3_3/MODEL_CARD.md, 2024c.

Ryan Lowe, Yi I Wu, Aviv Tamar, Jean Harb, OpenAI Pieter Abbeel, and Igor Mordatch. Multi-agent actor-critic for mixed cooperative-competitive environments. *NeurIPS*, 2017.

Aidan McLaughlin, James Campbell, Anuja Uppuluri, and Yiming Yang. Aidanbench: Stress-testing language model creativity on open-ended questions. In *NeurIPS 2024 Workshop on Language Gamification*, 2024.

Microsoft Research. Phi-4 technical report. Technical report, Microsoft, 2024. URL https://www.microsoft.com/en-us/research/publication/phi-4-technical-report/.

Mistral AI. Ministral 8b instruct model card. https://huggingface.co/mistralai/Ministral-8B-Instruct-2410, 2024.

Aidar Myrzakhan, Sondos Mahmoud Bshaeat, and Zhiqiang Shen. Open-llm-leaderboard: From multi-choice to open-style questions for llms evaluation, benchmark, and arena. *arXiv preprint arXiv:2406.07545*, 2024.

Yixin Nie, Adina Williams, Emily Dinan, Mohit Bansal, Jason Weston, and Douwe Kiela. Adversarial NLI: A new benchmark for natural language understanding. *arXiv preprint arXiv:1910.14599*, 2019.

OpenAI. Gpt-4 technical report, 2024. URL https://arxiv.org/abs/2303.08774.

Long Ouyang, Jeff Wu, Xu Jiang, Diogo Almeida, Carroll L. Wainwright, Pamela Mishkin, Chong Zhang, Sandhini Agarwal, Katarina Slama, Alex Ray, John Schulman, Jacob Hilton, Fraser Kelton, Luke Miller, Maddie Simens, Amanda Askell, Peter Welinder, Paul Christiano, Jan Leike, and Ryan Lowe. Training language models to follow instructions with human feedback, 2022. URL https://arxiv.org/abs/2203.02155.

Arjun Panickssery, Samuel R. Bowman, and Shi Feng. LLM evaluators recognize and favor their own generations. In *NeurIPS*, 2024. URL https://openreview.net/forum?id=4NJBV6Wp0h.

Kishore Papineni, Salim Roukos, Todd Ward, and Wei-Jing Zhu. Bleu: a method for automatic evaluation of machine translation. In *ACL*, 2002. URL https://aclanthology.org/P02-1040/.

Mohammad Taher Pilehvar and Jose Camacho-Collados. WiC: the word-in-context dataset for evaluating context-sensitive meaning representations. *arXiv preprint arXiv:1808.09121*, 2018.

Krishna Pillutla, Swabha Swayamdipta, Rowan Zellers, John Thickstun, Sean Welleck, Yejin Choi, and Zaid Harchaoui. Mauve: Measuring the gap between neural text and human text using divergence frontiers. *NeurIPS*, 2021.

Qwen Team. Qwen2.5 technical report, 2025. URL https://arxiv.org/abs/2412.15115.

Alec Radford, Jeffrey Wu, Rewon Child, David Luan, Dario Amodei, Ilya Sutskever, et al. Language models are unsupervised multitask learners. *OpenAI blog*, 2019.

Anna Rogers, Olga Kovaleva, Matthew Downey, and Anna Rumshisky. Getting closer to AI complete question answering: A set of prerequisite real tasks. In *AAAI*, 2020.

Karsten Roth, Lukas Thede, A. Sophia Koepke, Oriol Vinyals, Olivier J Henaff, and Zeynep Akata. Fantastic gains and where to find them: On the existence and prospect of general knowledge transfer between any pretrained model. In *ICLR*, 2024. URL https://openreview.net/forum?id=m50eKHCttz.

Veli Safak. Min-mid-max scaling, limits of agreement, and agreement score. *arXiv preprint arXiv:2006.12904*, 2020.

Maarten Sap, Hannah Rashkin, Derek Chen, Ronan Le Bras, and Yejin Choi. Socialiqa: Commonsense reasoning about social interactions. *arXiv preprint arXiv:1904.09728*, 2019.

Adam Scherlis, Alex Mallen, Lucia Quirke, and Nora Belrose. Experiments in weak-to-strong generalization, 2024. URL https://blog.eleuther.ai/weak-to-strong/.

William A Scott. Reliability of content analysis: The case of nominal scale coding. *Public opinion quarterly*, 1955.

Harshay Shah, Sung Min Park, Andrew Ilyas, and Aleksander Madry. Modeldiff: A framework for comparing learning algorithms. In *ICML*, 2023.

Richard Socher, Alex Perelygin, Jean Wu, Jason Chuang, Christopher D Manning, Andrew Y Ng, and Christopher Potts. Recursive deep models for semantic compositionality over a sentiment treebank. In *Proceedings of the 2013 conference on empirical methods in natural language processing*, pp. 1631–1642, 2013.

Yuda Song, Hanlin Zhang, Carson Eisenach, Sham Kakade, Dean Foster, and Udaya Ghai. Mind the gap: Examining the self-improvement capabilities of large language models, 2024. URL https://arxiv.org/abs/2412.02674.

Nisan Stiennon, Long Ouyang, Jeffrey Wu, Daniel Ziegler, Ryan Lowe, Chelsea Voss, Alec Radford, Dario Amodei, and Paul F Christiano. Learning to summarize with human feedback. *Advances in Neural Information Processing Systems*, 33:3008–3021, 2020.

Hendrik Strobelt, Benjamin Hoover, Arvind Satyanaryan, and Sebastian Gehrmann. LMdiff: A visual diff tool to compare language models. In *EMNLP System Demonstrations 2021*, November 2021. URL https://aclanthology.org/2021.emnlp-demo.12.

Kai Sun, Dian Yu, Jianshu Chen, Dong Yu, Yejin Choi, and Claire Cardie. Dream: A challenge data set and models for dialogue-based reading comprehension. *Transactions of the Association for Computational Linguistics*, 7:217–231, 2019.

Mirac Suzgun, Nathan Scales, Nathanael Schärli, Sebastian Gehrmann, Yi Tay, Hyung Won Chung, Aakanksha Chowdhery, Quoc Le, Ed Chi, Denny Zhou, and Jason Wei. Challenging BIG-bench tasks and whether chain-of-thought can solve them. In *ACL Findings*, 2023. URL https://aclanthology.org/2023.findings-acl.824/.

Oyvind Tafjord, Matt Gardner, Kevin Lin, and Peter Clark. Quartz: An open-domain dataset of qualitative relationship questions. *arXiv preprint arXiv:1909.03553*, 2019.

Technology Innovation Institute. Welcome to the falcon 3 family of open models! https://huggingface.co/blog/falcon3, 2024.

Aman Singh Thakur, Kartik Choudhary, Venkat Srinik Ramayapally, Sankaran Vaidyanathan, and Dieuwke Hupkes. Judging the judges: Evaluating alignment and vulnerabilities in llms-as-judges, 2024. URL https://arxiv.org/abs/2406.12624.

Yubo Wang, Xueguang Ma, Ge Zhang, Yuansheng Ni, Abhranil Chandra, Shiguang Guo, Weiming Ren, Aaran Arulraj, Xuan He, Ziyan Jiang, Tianle Li, Max Ku, Kai Wang, Alex Zhuang, Rongqi Fan, Xiang Yue, and Wenhu Chen. MMLU-pro: A more robust and challenging multi-task language understanding benchmark. In *The Thirty-eight Conference on Neural Information Processing Systems Datasets and Benchmarks Track*, 2024. URL https://openreview.net/forum?id=y10DM6R2r3.

Alex Warstadt, Amanpreet Singh, and Samuel Bowman. Neural network acceptability judgments. *Transactions of the Association for Computational Linguistics*, 2019.

Johannes Welbl, Nelson F Liu, and Matt Gardner. Crowdsourcing multiple choice science questions. *arXiv preprint arXiv:1707.06209*, 2017.

Jiayi Ye, Yanbo Wang, Yue Huang, Dongping Chen, Qihui Zhang, Nuno Moniz, Tian Gao, Werner Geyer, Chao Huang, Pin-Yu Chen, Nitesh V Chawla, and Xiangliang Zhang. Justice or prejudice? quantifying biases in llm-as-a-judge. *arXiv preprint arXiv:2410.02736*, 2024.

Edwin Zhang, Vincent Zhu, Naomi Saphra, Anat Kleiman, Benjamin L. Edelman, Milind Tambe, Sham M. Kakade, and eran malach. Transcendence: Generative models can outperform the experts that train them. In *NeurIPS*, 2024. URL https://openreview.net/forum?id=eJG9uDqCY9.

Yuan Zhang, Jason Baldridge, and Luheng He. PAWS: Paraphrase Adversaries from Word Scrambling. In *Proc. of NAACL*, 2019.

Lianmin Zheng, Wei-Lin Chiang, Ying Sheng, Siyuan Zhuang, Zhanghao Wu, Yonghao Zhuang, Zi Lin, Zhuohan Li, Dacheng Li, Eric Xing, et al. Judging llm-as-a-judge with mt-bench and chatbot arena. *Advances in Neural Information Processing Systems*, 36:46595–46623, 2023.

Xiaosen Zheng, Tianyu Pang, Chao Du, Qian Liu, Jing Jiang, and Min Lin. Cheating automatic llm benchmarks: Null models achieve high win rates. *arXiv preprint arXiv:2410.07137*, 2024.

Ruiqi Zhong, Charlie Snell, Dan Klein, and Jacob Steinhardt. Describing differences between text distributions with natural language, 2022. URL https://arxiv.org/abs/2201.12323.

Ruiqi Zhong, Peter Zhang, Steve Li, Jinwoo Ahn, Dan Klein, and Jacob Steinhardt. Goal driven discovery of distributional differences via language descriptions. *Advances in Neural Information Processing Systems*, 36:40204–40237, 2023.

Ben Zhou, Daniel Khashabi, Qiang Ning, and Dan Roth. "Going on a vacation" takes longer than "Going for a walk": A Study of Temporal Commonsense Understanding. In *EMNLP*, 2019.

Wenhong Zhu, Zhiwei He, Xiaofeng Wang, Pengfei Liu, and Rui Wang. Weak-to-strong preference optimization: Stealing reward from weak aligned model, 2024. URL https://arxiv.org/abs/2410.18640.

Jakub Łucki, Boyi Wei, Yangsibo Huang, Peter Henderson, Florian Tramèr, and Javier Rando. An adversarial perspective on machine unlearning for ai safety, 2024. URL https://arxiv.org/abs/2409.18025.

Appendix

CONTENTS

A Metrics **19**
A.1 Derivation of CAPA . . . 19
A.2 Extending CAPA to more than two models . . . 20
A.3 How to use CAPA for classification and exact match settings? . . . 20
A.4 Detailed Discussion on Design Choices . . . 21
A.5 Probabilistic versions of popular agreement metrics . . . 23
A.6 Theoretical bounds for CAPA . . . 23
A.7 CAPA comparison with other inter-rater metrics . . . 25

B LLM-as-a-Judge **27**
B.1 Comparison of Judge Scores for Our Similarity vs Error Consistency . . . 28
B.2 Evaluating Judge Scores Against Ground-Truth . . . 28
B.2.1 MCQ Ground-Truth . . . 28
B.2.2 Judge Ensemble with Access to Reference Answers . . . 28
B.2.3 Judge Score Validity Against Reference-Based Ensemble . . . 29
B.3 Statistical Testing . . . 29
B.3.1 Quantifying Correlation Strength Using Partial Correlation . . . 30
B.3.2 Multiple Regression . . . 30
B.4 Experimental Setup for Filtering MMLU-Pro . . . 35
B.5 Experimental Setup to Perform Free-Form Inference on Filtered MMLU-Pro . . . 35
B.6 Experimental Setup for LLM-as-a-Judge on Filtered MMLU-Pro . . . 35
B.7 List of Judges and Evaluated Language Models . . . 36
B.8 Prompts . . . 36
B.8.1 LM-Judge Prompt without Reference Answer . . . 36
B.8.2 LM-Judge Prompt with MCQ Options . . . 47
B.8.3 Original MCQ CoT Prompt . . . 47
B.8.4 Open-style CoT Prompt . . . 49
B.8.5 Coarse Filtering Prompt . . . 50
B.8.6 Fine-grained Filtering Prompt . . . 51

C Weak-to-Strong Training **51**
C.1 Setup . . . 51
C.2 Elicitation vs Complementary Knowledge . . . 53
C.3 Effect of Different similarity metrics . . . 54

C.4 Accuracies in Weak-to-Strong training 55
C.5 Weak-to-strong Accuracy Value Details in Elicitation vs Complementary Knowledge Analysis 56

D Similarity Trends with Increasing Capabilities **56**
D.1 Setup Details 56
D.2 Why are model mistakes becoming more similar? A preliminary analysis 58
D.2.1 Instruction-tuning exacerbates the trend 58
D.2.2 Is the trend confounded by question difficulties? 58
D.2.3 Can changing architecture reduce model similarity? 58
D.3 Alternative Similarity Metrics 59
D.4 Model capability vs similarity across domains 60
D.5 List of models 61

A METRICS

The following section covers design details for CAPA κ_p. Firstly, we address derivation of CAPA in Section A.1 and its theoretical bounds in Section A.6. Secondly, we explain how to extend CAPA to multi-model set-up (Section A.2) and how to adapt CAPA to classification and exact match settings (Section A.3). Lastly, we introduce probabilistic versions of popular agreement metrics (Section A.5) and provide a comparison between them and CAPA (Section A.4).

A.1 DERIVATION OF CAPA

CAPA is intended to be used as a similarity metric in the context of model accuracies. As such, it extends Error consistency Geirhos et al. (2020), a metric that adjusts chance agreement by taking into account model accuracy. In particular, the same formula is used to define Cohen's κ, Scott's π, Fleiss' κ, Error Consistency and CAPA:

$$\frac{\text{observed agreement} - \text{chance agreement}}{\text{maximum possible agreement - chance agreement}}, \tag{5}$$

where the excess agreement is subtracted both from the numerator and denominator, essentially calculating the proportion of possible excess agreement that is observed between the two models. Across all metrics, the maximum possible agreement is 1. Where CAPA differs from the existing metrics is how we calculate the observed and change agreement.

We redefine *error consistency* Geirhos et al. (2020) by incorporating probabilistic information. To achieve this we introduce a probabilistic computation of the observed agreement, c_{obs} as c^p_{obs}, and the chance agreement, c_{exp} as c^p_{exp}. The new equation becomes:

$$\kappa_p = \frac{c^p_{\text{obs}} - c^p_{\text{exp}}}{1 - c^p_{\text{exp}}}. \tag{6}$$

Observed agreement c^p_{obs} : Given that we have the predicted output probabilities, $p_1(o_*)_x$, by a LM for all possible options, $O_x = [o_1, \ldots, o_N]$, for a data sample x, e.g. $p_1(o_*)_x \forall o_* \in O_x$, we can compute the relative observed overlap as:

$$c^p_{\text{obs}} \;=\; \frac{1}{|D|} \sum_{x=1}^{D} \sum_{i=1}^{O} p_1(o_i)_x \cdot p_2(o_i)_x \tag{7}$$

where $p_1(\cdot)$ is the predicted probability by model 1 and $p_2(\cdot)$ is the predicted probability by model 2. We would like to highlight that the above calculation is performed on **sample level** to avoid confusion with the common chance agreement p_e calculation in Cohen's kappa [2].

Agreement by chance c^p_{exp} To estimate the model chance agreement c^p_{exp} we first start by computing the average probability that a given model is correct $\overline{p_*}$:

$$\overline{p_*} = \frac{1}{|D|} \sum_{x=1}^{D} \sum_{i=1}^{O} \mathbb{I}[o_i = \text{gt}] p_*(o_i)_x \text{ where gt} = \text{ground truth} \tag{8}$$

Performing the above calculation per model accounts for the possibility that each model may have different marginal distributions. An assumption that is fair to assume in the context of LMs. Subsequently, given the $\overline{p_*}$ per model we can compute the probability that two models are **correct** by chance as: $\overline{p_1} \cdot \overline{p_2}$. Conversely, to account for model chance disagreement we (1) group all the remaining options as **incorrect** and (2) adjust for the number of options: $\frac{1}{|D|} \sum_{x=1}^{D} \frac{1}{|O_x|-1} (1 - \overline{p_1})(1 - \overline{p_2})$. These steps are necessary because (1) MCQ options can be permuted, therefore, class marginal probabilities cannot be computed, and (2) the chance disagreement without adjusting for the number of options overestimates the agreement by chance:

$$0 < \frac{1}{|D|} \sum_{x=1}^{D} \frac{1}{|O_x| - 1} (1 - \overline{p_1})(1 - \overline{p_2}) \leq (1 - \overline{p_1})(1 - \overline{p_2}) \tag{9}$$

[2] Cohen's kappa uses the marginal probabilities across categories to estimate p_e. However, in MCQ there are no 'class categories' as the options can be permuted across data samples. Therefore, marginal probabilities cannot be estimated.

In particular, if the number of options is ignored then the underlying assumption is that both models put their 'incorrect' probability mass on the same option, following a Dirac delta $\delta(o_*)$ distribution. This is a very strong assumption, that overestimates model error agreement. Therefore, we propose to adjust this by assuming that the distribution for the incorrect options follows a uniform distribution $\mathbf{U}\{o_1, o_{n-1}\}$ as adjusted by our normalizing factor $\frac{1}{|D|}\sum_{x=1}^{D}\frac{1}{|O_x|-1}$, where $|O_x|$ is the total number of options for a sample x. As such, the overall agreement by chance probability is:

$$c^p_{\text{exp}} = \underbrace{\overline{p_1}\overline{p_2}}_{\text{chance agreement correct}} + \underbrace{\frac{1}{|D|}\sum_{x=1}^{D}}_{\text{mean}} \underbrace{\frac{1}{|O_x|-1}}_{\text{uniformity assumption}} \underbrace{(1-\overline{p_1})(1-\overline{p_2})}_{\text{chance agreement incorrect}} \tag{10}$$

Moreover, for perfectly calibrated models the mean correct probability $\overline{p_*}$ would approach model accuracy, $\overline{p_*} \rightarrow \hat{p_*}$ and is upper bounded by it $\overline{p_*} < \hat{p_*}$ as $\overline{p_*}$ is computed based on probabilities ($\hat{p_*} = \frac{TP+TN}{|D|}$).

Reduction of CAPA to Error Consistency for binary classification In binary classification setting when the underlying probabilities are unavailable CAPA reduces to error consistency, as (1) $c^p_{\text{obs}} = \frac{1}{|D|}\sum_{x=1}^{D}\mathbb{I}[\text{arg max } p_1 = \text{arg max } p_2] = c_{\text{obs}}$, and (2) $c^p_{\text{obs}} = c_{\text{obs}}$ as $\overline{p_*} = acc_*$, and the normalizing factor simplifies to 1.

A.2 Extending CAPA to more than two models

In Section 2.2, we computed functional similarity between a pair of models. Here, we extend CAPA to multi-model comparisons. In the inter-annotator agreement literature, Fleiss' κ (Fleiss et al., 1981) is commonly used for this. However, it is ill suited to our modeling paradigm as it defines c^p_{exp} using the assumptions of Scott's π instead of Cohen's κ (this is problematic when measuring model similarity as discussed in the previous section). We derive CAPA for more than two models using first principles logic, similar to how Fleiss' κ was derived.

Suppose the number of models is $M > 2$. We still use the $\frac{c^p_{\text{obs}} - c^p_{\text{exp}}}{1 - c^p_{\text{exp}}}$ formula, but change the definition of c^p_{obs} and c^p_{exp}. For c^p_{obs}, Fleiss' κ measures the proportion of observed pairwise agreements from the total possible for each question, averaging across questions. This is equivalent to averaging the observed agreements for each pair of models when all models annotate all questions, which is true in our case[3]. This gives us $c^p_{\text{obs}} = \frac{2}{M(M-1)}\sum_{1\leq i<j\leq M}\frac{1}{|D|}\sum_{x=1}^{D}\sum_{k=1}^{O} p_i(o_k)_x \cdot p_j(o_k)_x$.

Second, for c^p_{exp}, Fleiss' κ measures the expected pairwise agreements if all M models were independent. This can be obtained by averaging the c^p_{exp} for two models across all possible pairs of M models. This gives us

$$c^p_{\text{exp}} = \frac{2}{M(M-1)}\sum_{1\leq i<j\leq M}(\overline{p_i}\cdot\overline{p_j} + (1-\overline{p_i})\cdot(1-\overline{p_j})\cdot(\frac{1}{|D|}\sum_{x=1}^{D}\frac{1}{|O_x|-1}))$$

.

A.3 How to use CAPA for classification and exact match settings?

In Section 2.2 we defined CAPA for MCQs as this is used throughout the paper, and more commonly for language models. For completeness, we now define CAPA for classification settings and exact match settings, which are alternate strategies for evaluating models.

Classification: Unlike MCQs, in this setting are coherent classes (categories), representing nominal data. The model output now is a probability distribution over C classes. Therefore, we compute c^p_{obs} across categories as follows:

$$c^p_{\text{obs}} = \frac{1}{|D|}\sum_{x\in D}\sum_{c_i\in C(x)} p_1(c_i)\cdot p_2(c_i), \tag{11}$$

[3]Fleiss κ is also defined when not all annotators respond to every question, as long as the number of respondents per question is fixed.

Metric	Formula	Description
Cohen's Kappa	$\kappa = \frac{P_o - P_e}{1 - P_e}$	Measures inter-rater reliability P_0 while accounting for chance agreement P_e.
Scott's Pi	$\pi = \frac{P_o - P_e}{1 - P_e}$	Similar to Kappa, but uses marginal probabilities for P_e.
Error Consistency	$k = \frac{c_{\text{obs}} - c_{\text{exp}}}{1 - c_{\text{exp}}}$	Adjusts for accuracy via $c_{\text{exp}} = acc_1 \cdot acc_2 + (1 - acc_1)(1 - acc_2)$
CAPA	$\kappa_p = \frac{c^p_{\text{obs}} - c^p_{\text{exp}}}{1 - c^p_{\text{exp}}}$	Accounts for sample level probabilities $c^p_{\text{obs}} = \frac{1}{\lvert D \rvert} \sum_{x=1}^{D} \sum_{i=1}^{O} p_1(o_i)_x \cdot p_2(o_i)_x$ and accounts for accuracy via $c^p_{\text{exp}} = \overline{p}_1 \cdot \overline{p}_2 + \frac{1}{\lvert D \rvert} \sum_{x=1}^{D} \frac{1}{\lvert O_x \rvert - 1}(1 - \overline{p}_1)(1 - \overline{p}_2)$

Table 4: Comparison of different inter-rater metrics

where $p_*(c_i)$ is the output probability for class c_i. For the computation of c^p_{exp} we follow the same definition as in the main paper, but now $\overline{p_j}$ is computed for the correct class and the chance agreement on the incorrect class is adjusted by the number of classes instead of number of options:

$$c^p_{\text{exp}} = \underbrace{\overline{p_1} \cdot \overline{p_2}}_{\text{chance agreement on correct class}} + \tag{12}$$

$$\underbrace{(1 - \overline{p_1}) \cdot (1 - \overline{p_2}) \cdot \frac{1}{|D|} \sum_{x \in D} \frac{1}{|C(x)| - 1}}_{\text{chance agreement on incorrect class}} \tag{13}$$

In principle, the above implementation could also be adjusted to further take into account the class categories by computing the marginal probabilities per class as:

$$\overline{p(c_i)_*} = \frac{1}{|D|} \sum_{i=1}^{D} p_*(c_i) \text{ where } c_i \neq \text{ground truth}, \tag{14}$$

and replacing the chance agreement on incorrect class with the product of per class 'incorrect' probabilities.

Exact or Fuzzy Match: Here, models are not provided categories or options to choose between, and instead provide an answer from an unconstrained set. The model's output string is matched with a reference answer. Here, the probability of independent models agreeing by chance approaches zero due to an unconstrained set of outputs. Further computing probabilistic agreement is difficult over conditional distributions across multiple tokens. We recommend calculating the discrete version of CAPA, where $c^{EM}_{\text{obs}} = \frac{1}{|D|} \sum_{x=1}^{D} \mathbb{I}[m_1(x) == m_2(x)]$, and $c^{EM}_{\text{exp}} = acc_1 \cdot acc_2$, finally computing $\frac{c^{EM}_{\text{obs}} - c^{EM}_{\text{exp}}}{1 - c^{EM}_{\text{exp}}}$.

A.4 Detailed Discussion on Design Choices

In this section, we discuss alternative design choices we could have taken. For an overview of the equations for each metric, see table 4.

Why not use inter-annotator agreement metrics like Cohen's κ? Cohen's κ, Scott's π, Krippendorf's α measure how people differ when answering survey questions, focusing on the reliability of those questions and the data (Krippendorff, 2004). They assume nominal data and computes marginal probability distributions per category. However, MCQs do not have an inherent category 'a' or 'b', i.e. options can be permuted, so we cannot compute such marginal probability distributions. Moreover, measuring LM similarity requires adjusting for chance agreement due to accuracy to avoid inflating similarity for high-accuracy models (Geirhos et al., 2020). For inter-annotator agreement metrics stemming from human survey studies — where there is no built-in concept of accuracy — and thus they are unsuitable for LM analysis without additional modification.

Should c^p_{exp} be defined similarly to Cohen's κ or Scott's π? When measuring similarity between LM Judges and human annotators, Thakur et al. (2024) recommend using Scott's π over Cohen's κ, as it is a better metric for inter-annotator agreement studies (Krippendorff, 2004). The two differ in

how they compute c_{exp}, Scott's π assumes that the two human raters are sampled from a common distribution, estimating it by averaging the marginal probabilities of the two raters. This is in contrast to Cohen's κ, which assumes the given different marginal distributions for the two raters. In our case, we wish to account for chance agreement due to accuracies rather than the marginal distribution over classes. To see the relative comparison of how Cohen's κ and Scott's π behave in our setting, we consider an example.

Suppose we have a binary classification problem, where both models always agree when they are both wrong as there is only one incorrect option. We now consider two pairs of models. Pair 1 has accuracies $0.2, 0.8$, whereas in pair 2, both models have accuracies 0.5. Intuitively, if both pairs were to have the same observed agreement, it would be more surprising if this happened for pair 1 than pair 2, given the vast difference in their accuracy. In other words, models in pair 2 are more similar than expected for independent models with the given accuracies than pair 1. We want this to be reflected in our similarity metric.

For pair 1, Scott's π, c_{exp} would be computed assuming a joint accuracy of $\frac{0.2+0.8}{2} = 0.5$, and for pair 2 with the same joint accuracy $\frac{0.5+0.5}{2} = 0.5$, giving $c_{\text{exp}} = 0.5^2 + (1-0.5)^2 = 0.5$. Cohen's κ of pair 2 would be computed as $0.5 \cdot 0.5 + (1-0.5) \cdot (1-0.5) = 0.5$ too. However, for Cohen's κ of pair 1, $c_{\text{exp}} = 0.2 \cdot 0.8 + 0.8 \cdot 0.2 = 0.32$. This means for a fixed observed agreement c_{obs}, say 0.5, $\pi = \frac{0.5-0.5}{1-0.5} = 0$ for both models, and similarly $\kappa = 0$ for pair 2. However, for pair 1, $\kappa = \frac{0.5-0.32}{1-0.32} = 0.264$. Indeed, Scott's π would lead us to think both pairs are equally similar, whereas κ indicates pair 2 is more similar, beyond chance agreement arising due to accuracy. Thus κ has the more desirable behavior.

More broadly, we do not wish to assume both models are drawn from a joint distribution, assigning them a common mean accuracy. However, Scott's π does this, which makes sense when calculating reliability of surveys or measuring alignment between human and LLM judges. However, this does not make sense in our setting where we wish to adjust for chance agreement expected due to the two model's given accuracies. Hence, we choose to define c_{exp} similar to Cohen's κ, where we retain the difference in the two model's accuracies when computing chance agreement.

Why not use Matthews Correlation Coefficient: We could take a completely different approach by computing the Pearson or Matthews Correlation Coefficient of the binary vectors of sample-wise correctness for the two models (Chicco et al.). However, it would be difficult to incorporate probabilistic information, and that models can be incorrect and still disagree by predicting different options. In other words, it suffers from the same issues as error consistency, and we found it more difficult to extend.

Why not use regression analysis? We could have performed a multinomial regression using the probabilities of the first model to predict probabilities of the second model, using this predictability as a measure of similarity. However, it is unclear whether a linear model would be enough. Ideally this prediction should also be contextualized on the input sample, but for this we would need a model-based metric to obtain a representation of the input sample. We chose to stick to a more interpretable, closed-form metric.

Why not use divergence metrics like KL or JSD? KL-divergence or Jensen–Shannon Distance (JSD) can measure the divergence between probability distributions assigned by models to the options with lucrative information-theoretic properties. Further, JSD is a valid distance metric, and normalized between 0 and 1. We could use the mean JSD over all questions as a model similarity metric. However, higher-accuracy models are expected to have lower JSD simply because they have more correct answers, i.e, end up assigning more probability mass to correct options across samples. Retaining the information-theoretic properties of JSD while adjusting for chance agreement due to accuracy remains an interesting open problem.

Why not use JSD of the two distributions instead of overlap in computing CAPA?: We could have plugged $1 - JSD$ into c^p_{obs} in the κ_p formula. It is also possible to define c^p_{exp} by computing JSD between the two independent model distributions defined and subtracting from 1. However, JSD instead of probabilistic overlap is not intuitively interpretable, especially when divided by the possible excess agreement as in κ_p. c^p_{obs} computes the expected agreement when sampling from both models based on the probability distribution they assign to the options. Intuitively, it gives us the fraction of times the two models would agree if we kept sampling predictions from these distributions infinitely.

A.5 PROBABILISTIC VERSIONS OF POPULAR AGREEMENT METRICS

We now provide probabilistic versions of Cohen's κ , Scott's π, and Fleiss' κ_F, so that the interested reader can contrast them with CAPA.

Probabilistic Cohen's κ One can obtain a probabilistic Cohen's κ by computing P_0 as c^p_{obs}, therefore accounting for the observed agreement based on model output probabilities. While $P_e = \sum_{i=1}^{C} \frac{1}{|D|} \sum_{x=1}^{D} p_1(c_i)_x \cdot \frac{1}{|D|} \sum_{x=1}^{D} p_2(c_i)_x$ where we compute the product of marginals for each class.

Probabilistic Scott's π Similarly to Cohen's κ to compute the observed agreement probabilistically we compute the average product across probabilities for 2 models, meaning P_0 becomes c^p_{obs}. While we adjust P_e computation as follows: $P_e = \sum_{i=1}^{C} (\frac{1}{2}(\frac{1}{|D|} \sum_{x=1}^{D} p_1(c_i)_x + \frac{1}{|D|} \sum_{x=1}^{D} p_2(c_i)_x))^2$, where we now compute the sum of the marginal probabilities per class as we assume that both models have a shared marginal distribution.

Probablistic Fleiss' Kappa (κ_F): It extends the $\frac{c_{\text{obs}} - c_{\text{exp}}}{1 - c_{\text{exp}}}$ formula to more than two models, where the observed and chance agreement is computed across pairs of two in the set of models. Like π it assumes chance predictions are sampled from a common combined distribution. While generally Fleiss' Kappa allows a partial random subset of annotators for each question, in our work we assume all models annotate all questions. Let M be the number of models, and $|C|$ be the number of classes. Let m_{xi} be the number of models that put sample x in class i. Let $P_x = \frac{1}{M(M-1)} \sum_{i \in C} m_{xi}(m_{xi} - 1)$ be the proportion of observed pairwise agreements for each question. $c_{\text{obs}} = \frac{1}{|D|} \sum_{x \in D} P_x$. For the chance agreement, $c_{\text{exp}} = \sum_{i \in C} (\frac{\sum_{1 \leq j \leq M} p_j(i)}{M})^2$.

Let M be the number of models, and $|C|$ be the number of classes. Let m_{xi} be the number of models that put sample x in class i. Let $P_x = \frac{1}{M(M-1)} \sum_{i \in C} m_{xi}(m_{xi} - 1)$ be the proportion of observed pairwise agreements for each question. $c_{\text{obs}} = \frac{1}{|D|} \sum_{x \in D} P_x$. For the chance agreement, $c_{\text{exp}} = \sum_{i \in C} (\frac{\sum_{1 \leq j \leq M} p_j(i)}{M})^2$.

A.6 THEORETICAL BOUNDS FOR CAPA

Bounds for c^p_{obs}. Compared to Geirhos et al. (2020) the resulting observed agreement is strictly greater than 0, as all probabilities are positive values, and strictly smaller than 1, as the sum of probability products is strictly smaller than the sum of probabilities:

$$0 < c^p_{\text{obs}} < 1 \tag{15}$$

Theorem: If $0 < a < 1$ and $0 < b < 1$, and $a + b = 1$, then $a^2 + b^2 < a + b$

Proof:

$$\begin{aligned} a^2 + b^2 &< a + b \\ a^2 - a + b^2 - b &< 0 \\ a(a-1) + b(b-1) &< 0 \end{aligned}$$

For $0 < a < 1$, $a > 0$ and $a - 1 < 0$, therefore, $a(a-1) < 0$. For $0 < b < 1$, $b > 0$ and $b - 1 < 0$, therefore $b(b-1) < 0$. Since $a(a-1) < 0$ and $b(b-1) < 0$, their sum will also be negative $a(a-1) + b(b-1) < 0$, this implies that indeed $a^2 + b^2 < a + b$.

Bounds for c^p_{exp}. The lower bound for c^p_{exp} is when the first term approaches zero and the scaling fraction approach 0, thus resulting in $c^p_{\text{exp}} = 0$. The upper bound is maximized when both terms are maximized, but as the second term is the inverse of the first times a scaling factor, the maximum upper bound is 1 (as $\overline{p_1} \cdot \overline{p_2} \to 1$, $(1 - \overline{p_1}) \cdot (1 - \overline{p_2}) \to 0$), resulting in:

$$0 < c^p_{\text{exp}} < 1 \tag{16}$$

Bounds for κ_p. The upper bound for κ_p is 1. In particular, κ_p will always be strictly smaller than 1, but approaching it in the limit.

Theorem: Given $\kappa_p = 1$. Then by definition:

Proof:

$$
\begin{aligned}
1 &= \frac{c^p_{\text{obs}} - c^p_{\text{exp}}}{1 - c^p_{\text{exp}}} \\
1 - c^p_{\text{exp}} &= c^p_{\text{obs}} - c^p_{\text{exp}} \\
1 &= c^p_{\text{obs}}
\end{aligned}
$$

However, as $c^p_{\text{obs}} < 1$, $\kappa_p < 1$.

Although the above implies that CAPA does not obtain 'perfect agreement' as originally defined by Cohen's k, we show that this is not a concern for our metric as (1) when model probability for the correct class approach 1, $\kappa_p \to 1$ and (2) using probabilities allows us to capture observed agreement at a more precise level:

1. Theorem: Given probabilities [a,b] and [c,d], where $a, c \to 1$ and conversely $b, d \to 0$, $\kappa_p \to 1$:

   Proof:

   $$
   \begin{aligned}
   &c^p_{\text{obs}} = a \cdot c + b \cdot d \\
   &\text{as } a \cdot c \to 1 \text{ and } b \cdot d \to 0 \\
   &c^p_{\text{obs}} \to 1
   \end{aligned}
   $$

   which confirms $\kappa_p \to 1$.

2. Geirhos et al. (2020) computes c_{obs} as $c_{obs_{i,j}} = \frac{e_{i,j}}{n}$ where $e_{i,j}$ is the number of equal responses. As such, $c_{obs_{i,j}}$ is independent of the observed output probabilities. However, for a model pair with output probabilities [0.999.. , 0.000..1] versus [0.8. 0.2] (assume the same for both models), we would like the first case to have a higher observed agreement than the second, but Geirhos et al. (2020) fails to capture this, while c^p_{obs} does:

   Theorem: Given two probabilities [a,b] and [c,d] where $0 < a, b, c, d < 1$, $a + b = 1$, $c + d = 1$, and $a > c$, $a > d$, $c > d$, $b < d$, indicates that $a \cdot a + b \cdot b > c \cdot c + d \cdot d$

   Proof:

   $$
   \begin{aligned}
   &a \cdot a + b \cdot b > c \cdot c + d \cdot d \\
   &a^2 + (1-a)^2 > c^2 + (1-c)^2 \\
   &a^2 + (1-a)^2 - (c^2 + (1-c)^2) > 0 \\
   &2a^2 - 2c^2 - 2a + 2c > 0 \\
   &2(a-c)(a+c-1) > 0 \\
   &(a-c)(a+c-1) > 0 \\
   &\text{as } a > c \Rightarrow (a-c) > 0 \\
   &\text{as } a > d \text{ and } c + d = 1 \Rightarrow d = 1 - c, a > 1 - c \Rightarrow a + c > 1, \text{ thus}, \Rightarrow (a + c - 1) > 0,
   \end{aligned}
   $$

   therefore, $a \cdot a + b \cdot b > c \cdot c + d \cdot d$.

The lower bound for κ_p is -1. In particular, κ_p will always be strictly greater than -1.

Theorem: $\kappa_p \geq -1$, given $0 < c^p_{\text{exp}} < 1$, and $0 < c^p_{\text{obs}} < 1$.

Proof:

$$\frac{c^p_{\text{obs}} - c^p_{\text{exp}}}{1 - c^p_{\text{exp}}} \geq -1$$
$$c^p_{\text{obs}} - c^p_{\text{exp}} \geq -(1 - c^p_{\text{exp}})$$
$$c^p_{\text{obs}} + 1 - 2c^p_{\text{exp}} \geq 0$$
$$c^p_{\text{obs}} \geq 2c^p_{\text{exp}} - 1$$
$$\text{minimal possible } c^p_{\text{obs}} \to 0 \text{ (complete disagreement)}$$
$$0 \geq 2c^p_{\text{exp}} - 1$$
$$1 \geq 2c^p_{\text{exp}}$$
$$0.5 \geq c^p_{\text{exp}}$$

therefore, $\kappa_p \geq -1$. Even though, the theoretical lower bound for $\kappa_p = -1$, to achieve $\kappa_p = -1$ in practice c^p_{obs} must be 0 (both models perfectly oppose each other), leading that $c^p_{\text{obs}} = 2c^p_{\text{exp}} - 1, \to c^p_{\text{exp}} = 0.5$. As c^p_{obs} is computed based on probabilities its value is $c_{\text{obs}} < 1$, therefore, the actual lower bound for $\kappa_p > -1$.

Altogether, the bounds for CAPA are as follows:

$$-1 < \kappa_p < 1 \tag{17}$$

A.7 CAPA COMPARISON WITH OTHER INTER-RATER METRICS

Numerical Example For a simple mathematical example consider two models with 2 data samples with the following probability distributions, model 1 = [[0.9,0.1],[0.8, 0.2]] and model 2 = [[0.7,0.3],[0.6, 0.4]]. The underlying ground truth index is [0,1]. For Cohen's k and Scott's π we treat this is example as a binary classification with option A and B, converting the probabilities to model 1= [A,A], model 2 = [A, A] (these metrics do not take accuracy into account). The accuracy for both models is 50%. In table 5 we report the computed similarity for each metric as well specify the exact computation values. As it can be noted, all other metrics suffer from the following limitations: (1) Cohen's κ and Scott's π treat the problem as a classification, as such both metrics report that the similarity between models is 0.00, indicating no relationship as $P_o = P_e$, (2) Probabilistic versions of the metrics slightly deviate from 0.00 however still undermine model similarity, (3) Error consistency over estimates model similarity by ignoring model output probabilities in its c_{obs} calculation. As such, only CAPA is able to accurately account for the observed sample level similarity across the two models.

Table 5: Numerical Example

Metric	Similarity	Computation
κ	0.00	$P_o = \frac{2}{2} = 1.0$, $P_e = \frac{2}{2} \cdot \frac{2}{2} + \frac{0}{2} \cdot \frac{0}{2} = 1.0$
Probabilistic κ	0.01	$P_o = \frac{1}{2}(0.9 \cdot 0.7 + 0.1 \cdot 0.3 + 0.8 \cdot 0.6 + 0.2 \cdot 0.4) = 0.61$
		$P_e = \frac{0.9+0.8}{2} \cdot \frac{0.7+0.6}{2} + \frac{0.1+0.2}{2} \cdot \frac{0.3+0.4}{2} = 0.605$
π	0.00	$P_o = 1.00$, $P_e = (\frac{2+2}{2 \cdot 2})^2 + (\frac{0+0}{2 \cdot 2})^2 = 1.0$
Probabilistic π	-0.04	$P_o = \frac{1}{2}(0.9 \cdot 0.7 + 0.1 \cdot 0.3 + 0.8 \cdot 0.6 + 0.2 \cdot 0.4) = 0.61$
		$P_e = ((\frac{0.9+0.8}{2} + \frac{0.7+0.6}{2})\frac{1}{2})^2 + ((\frac{0.1+0.2}{2} + \frac{0.3+0.4}{2})\frac{1}{2})^2 = 0.625$
error consistency	1.00	$c_{\text{obs}} = 1.00$, $c_{\text{exp}} = 0.5 \cdot 0.5 + (1 - 0.5)(1 - 0.5) = 0.5$
CAPA	0.21	$c^p_{\text{obs}} = \frac{1}{2}(0.9 \cdot 0.7 + 0.1 \cdot 0.3 + 0.8 \cdot 0.6 + 0.2 \cdot 0.4) = 0.61$
		$\overline{p}_1 = \frac{1}{2}(0.9 + 0.2) = 0.55$, $\overline{p}_2 = \frac{1}{2}(0.7 + 0.4) = 0.55$
		$c_{\text{exp}} = 0.55 \cdot 0.55 + \frac{1}{2}\frac{2}{2-1}(1 - 0.55)(1 - 0.55) = 0.51$

Simulation Experiment Furthermore, we design a simulation experiment to compare the 'behavior' of the above listed inter-rater metrics with our novel contribution CAPA. In particular, we limit the simulation to a binary classification problem as standard metrics like Cohen's k and Scott's π are

ill-suited for multiple choice question settings. In total we investigate the performance of 4 metrics: Cohen's k Probabilistic, Scott's π Probabilistic, Error consistency, and CAPA. We simulate N=10000 observations for 2 models. For the first model we set it's accuracy to 90%, it always favors the 1st option, and has a high calibration, 0.99, meaning the model is highly confident in it's predictions (e.g. single data point is [0.99, 0.01]). For the second model we iteratively increase it's accuracy by adjusting it's calibration from 0.01 to 0.99 for the first option, as such, making the models more similar artificially.

The first observation from the results reported in Fig. 5 is that both standard inter-rater metrics, Cohen's κ and Scott's π (even when adjusted to take into account probabilities) are ill suited for the present use-case: capturing model similarity. The main issue stems from the fact that the computation of P_e if simply adjusted to probabilistic setting without taking into account model accuracy, obtains a similar computational value as P_o (in this case equal to c^p_{obs}). P^p_e computes marginal class probabilities as indicated in Section A.5, which is ill suited when the model attributes all it's probability mass to a single option (always prefers option A in MCQ setting). Furthermore, whilst error consistency improves upon Cohen's κ and Scott's π it over estimates model similarity. In particular, when both models reach 90% accuracy error consistency reports perfect agreement, while in reality model output probabilities differ, [0.99, 0.01] and [0.65, 0.35] respectively. As such, our metric is the only one that is able to capture model observed agreement c^p_{obs} increasing beyond model accuracy levels and reaching 1 when models are highly calibrated, e.g. [0.99, 0.01] and [0.99, 0.01].

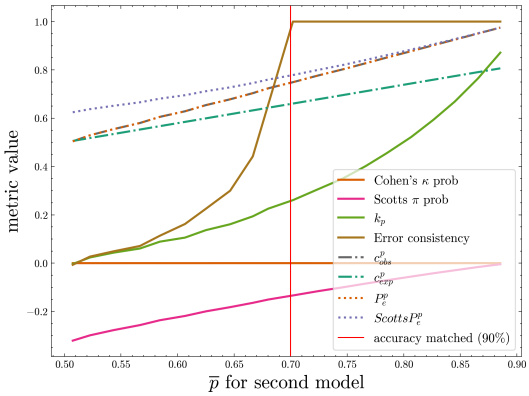

Figure 5: Metric comparison when models tend towards agreement. We compare different metric values for two models in a binary setting. For first model we set 90% accuracy and calibration to 0.99 (meaning the model is highly confident in its answers). For the second model, we increase it's calibration from 0.01 to 0.99 to approach the same distribution as the first model. On y-axis we are plotting metric value on x-axis we are reporting $\overline{p}$ for the second model which as the model becomes more calibrated approaches accuracy of the first model.

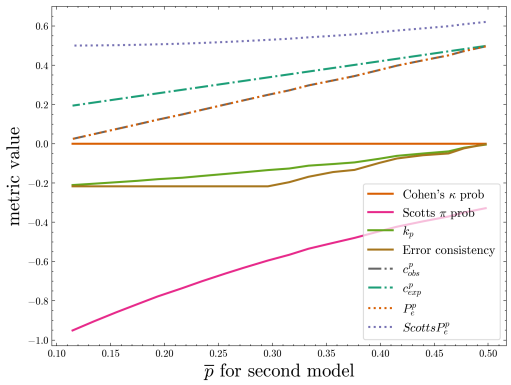

Figure 6: Metric comparison when models tend towards disagreement (Read plot from right to left). We compare different metric values for two models in a binary setting. For the first model, we set accuracy to 90% and calibration to 0.99 (the model is highly confident in its answers). For the second model, we incrementally increase its disagreement with model one by pushing its probability mass to the second option and increasing its calibration to 0.99.

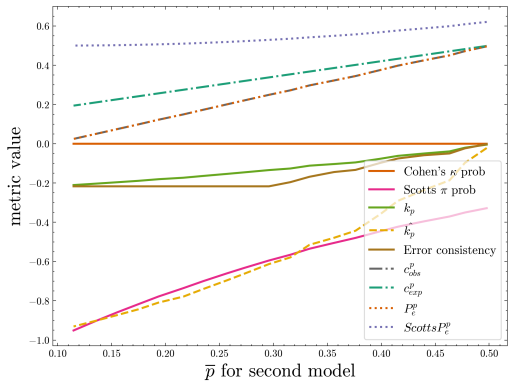

Figure 7: Metric comparison when models tend towards disagreement with adjusted κ_p. Replication of fig. 6 but with adjusted κ_p as as $\hat{\kappa_p}$, computation following eq. 18.

Limitations of CAPA. In addition, we investigated the 'behavior' of the above listed metrics as the models become increasingly dissimilar. In this set up we change that the second model always prefers the second option. Thus, by iteratively increasing its calibration we obtain models that maximally differ in their probability distribution, e.g. [0.99, 0.01] and [0.01, 0.99] respectively. As such, also the accuracy of the second model decreases overtime from random chance (50%) to 0.10 %, and we would like to obtain metric of -1. As it can be seen in Fig. 6, CAPA never reaches -1. Importantly, the same issue also can be observed for error consistency. This observation comes from the fact that both metrics use the original Cohen's κ equation. As explained in Section A.6, $\kappa_p = -1$ iff $c^p_{\text{exp}} = 0.5$. For probabilistic Cohen's κ we see the same observation as in Fig. 5, the marginal probability computation is not suited for the given problem. Interestingly, probabilistic Scott's π is the only metric that approaches -1. Whilst a desired final outcome, Scott's π overestimates model disagreement when model probabilities are independent, [0.99, 0.01] and [0.5, 0.5].

Possible solution for lower bound. In the context of the current work, the above limitation is not an issue, as models are trained to maximize accuracy, hence, there will always be some level of agreement. However, if CAPA would be used in settings like preference judgments, we would advise to adjust the computation of c^p_{exp} as described by Safak (2020):

$$\kappa_p = \begin{cases} \frac{c^p_{\text{obs}} - c^p_{\text{exp}}}{1 - c^p_{\text{exp}}} & c^p_{\text{obs}} \geq c^p_{\text{exp}} \\ \frac{c^p_{\text{obs}} - c^p_{\text{exp}}}{c^p_{\text{exp}} - c^p_{\text{obs-min}}} & c^p_{\text{obs}} < c^p_{\text{exp}} \end{cases} \tag{18}$$

where $c^p_{\text{obs-min}}$ is computed as $c^p_{\text{obs-min}} = \max(0, \overline{p_1} + \overline{p_2} - 1)$. This resolves the observed limitation of CAPA over the negative domain, see Fig. 7. Now, as the models become increasingly dissimilar $\hat{\kappa_p}$ approaches -1.

B LLM-AS-A-JUDGE

In this section, we extend the LLM-as-a-judge experiments introduced in Section 3. First, we compare CAPA with the related concept of error consistency (Geirhos et al., 2020), demonstrating its advantages in this context. We then present additional experiments to analyze the quality and behavior of the judges, as well as the performance of the evaluated models on the open-style MMLU-Pro benchmark.

To validate our findings, we provide detailed results from the statistical tests summarized in Table 6. Specifically, we conduct Shapiro-Wilk and Breusch-Pagan tests to confirm that the assumptions of normality and homoscedasticity required for partial correlation and multiple regression analyses are satisfied.

Additionally, we outline the experimental setup, including: (1) the filtering process for MMLU-Pro to obtain open-style questions only, (2) the methodology for free-form chain-of-thought inference on this benchmark, and (3) the design of the LLM-as-a-judge evaluation framework. To ensure full reproducibility, we include all prompts and specify the language models used as judges and evaluated models at the end of this section.

B.1 Comparison of Judge Scores for Our Similarity vs Error Consistency

In Figure 8 we compare the relationship of judgment scores on the filtered MMLU-Pro dataset using different similarity metrics. On the left, we use CAPA and on the right, we compare against the original error consistency of Geirhos et al. (2020). In both cases, we can see a correlation between the judge scores and the similarity of the LLM-as-a-judge and the model being evaluated. However, the relationship for CAPA is stronger, as shown by a mean Pearson r of 0.9 which is greater than the one of 0.85 if error consistency is used.

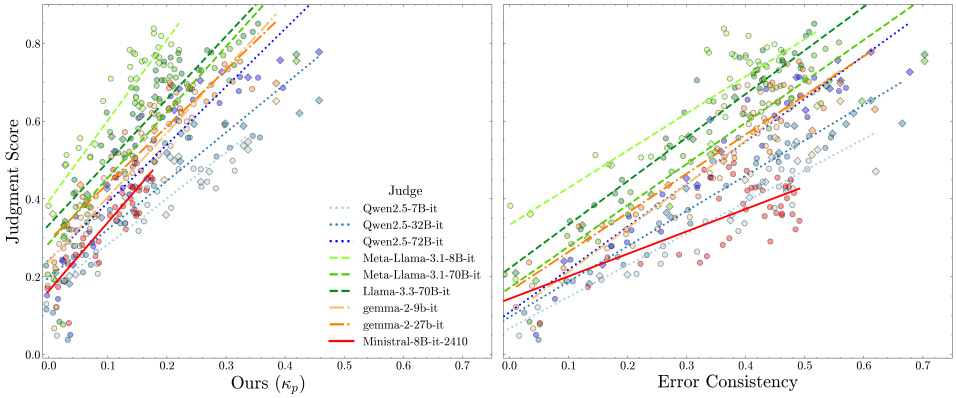

Figure 8: **Judgment Scores vs CAPA and vs Error Consistency.** We compare the relationship of judge scores on the filtered MMLU-Pro to our improved error consistency and to the original version of Geirhos et al. (2020).

B.2 Evaluating Judge Scores Against Ground-Truth

B.2.1 MCQ Ground-Truth

Since we source MCQ evaluations from Huggingface OpenLLM Leaderboard 2 throughout the paper, we use their default method to obtain probabilities across MCQ options. For MMLU-Pro and BBH they report the log-likelihood of each option. We apply a softmax to normalize these to 1. We checked this leads to calibrated predictions for base models and overconfident predictions for instruct models, consistent with prior observations about uncertainty of language models (OpenAI, 2024).

B.2.2 Judge Ensemble with Access to Reference Answers

Since we are evaluating model responses given in open style on filtered MMLU-Pro questions using LM-as-a-judge, it is important to investigate whether the responses of the evaluated models are reasonable. To ensure that qualitative differences between models of different sizes and families remain, we compare their performance using free-form responses to the multiple-choice accuracy on the same set of questions. This is shown in Figure 9. Using the same question base for free-form and MCQ evaluation draws a direct connection between functional similarity and the behavior of LLM-as-judges. Focusing on a setting where we have access to ground-truth responses is important to accurately analyze the affinity biases of different LMs when used as evaluators.

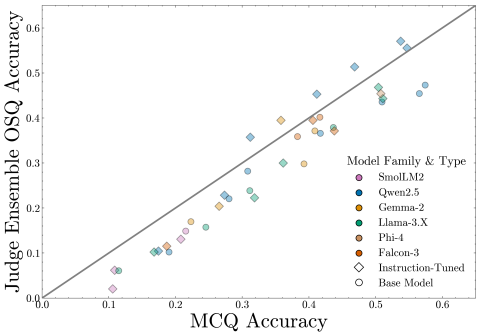

Figure 9: **Accuracy of free-form responses compared with multiple-choice accuracy on MMLU-Pro.** The free-form responses were rated using an ensemble of five capable LM judges. Each judge was given access to the original MMLU-Pro reference answers and their decisions whether a given response is correct or not were aggregated using majority voting.

Experimental Setup Every response is evaluated using an ensemble of five capable LMs used as LLM-as-a-judge from a range of different model families. The judge is given access to the question, the model's free-form response and all MMLU-Pro reference options. For each option we indicate if it is the correct or a wrong option. Using this information, the judge has to decide whether the model's response is correct or wrong. The prompt can be seen in Prompt B.8.2. For every per-sample response, we aggregate the five binary decisions using majority voting. Since there are five judges and it is a binary decision task, there are no ties. A qualitative analysis has shown the high quality of this process in determining the correctness of responses. The judges used are `gemma-2-27b-it`, `Qwen2.5-32B-Instruct`, `Qwen2.5-72B-Instruct`, `Llama-3.1-70-Instruct` and `Llama-3.3-70B-Instruct` (Gemma Team, 2024; Qwen Team, 2025; Llama Team, 2024a;c).

Open-style and Multiple Choice Correlate As we can see in Figure 9, there is a high alignment between the performance in MCQ style compared to free-form. For the majority of models, the ordering with MCQ accuracy and open-style accuracy is very similar. There is a consistent trend that performance on the more challenging open evaluation is approximately 5-10% lower. The exception is the instruction-tuned models from the Qwen2.5 and Gemma-2 model families that performed particularly well when giving free-form responses. For all other model families, the instruction tuned and base models show similar performance.

B.2.3 Judge Score Validity Against Reference-Based Ensemble

To evaluate the quality of different judges and to analyze their similarities and differences, we compare judge scores to the correctness assessments of the previously introduced ensemble of judges. The results are shown in Figure 10. As we can see, most models used as LLM-as-a-judge are able to correctly rank capable and less capable models.

Capability-Dependent Affinity Effects Even if the ordinal ranking of evaluated models is mostly accurate, there is a consistent trend that too many wrong responses are judged as being right. The exact behavior varies from judge to judge. Consider the small `Llama-3.1-8B-Instruct` for instance: it has a consistent positivity bias and ranks too many wrong responses as correct, even for models of low capability. `Qwen2.5-72B-Instruct` on the other hand appears to be much more capable in identifying the wrong responses of low-capability models. However, as the evaluated LMs become stronger, it exhibits the same bias as the smaller Llama judge. This aligns with the findings of Section 3 that LLM-as-judges show an affinity bias, because more capable models are also more similar to `Qwen2.5-72B-Instruct`.

B.3 Statistical Testing

This section provides detailed statistical validation of the affinity bias observed in Section 3. We confirm that judge-model similarity correlates with judgment scores even after controlling for MCQ ground-truth accuracy, using partial correlation and multiple regression. Additionally, we verify the statistical assumptions (normality, homoscedasticity) required for these tests across all nine judges.

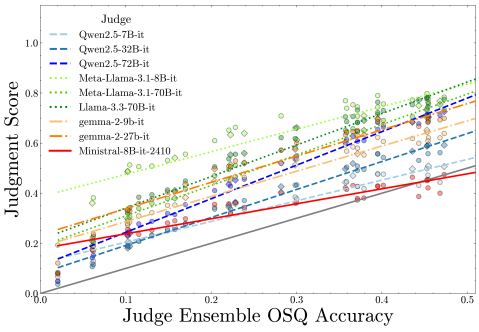

Figure 10: **Judgment Scores compared with the ensemble judgment accuracy given access to reference answers.** We compare the judgment scores of each judge using only their own knowledge and capabilities to the rating of a judge ensemble that has access to the ground-truth options. The latter is a good proxy of the real correctness of responses.

B.3.1 Quantifying Correlation Strength Using Partial Correlation

We compute partial correlations between judge scores and judge-model similarity while controlling for ground-truth accuracy. All judges show statistically significant positive correlations (Table B.3.1), with coefficients ranging from $r = 0.35$ (`Llama-3.3-70B-Instruct`) to $r = 0.65$ (`Llama-3.1-8B-Instruct`). The strongest correlations occur for smaller judges from the same gemma-2 family (`gemma-2-27b-it` and `gemma-2-9b-it`), while larger Qwen2.5 judges exhibit moderate correlations ($r = 0.42$ and $r = 0.43$). All p-values remain significant ($p < 0.05$), with the most robust results for the larger gemma judge ($p = 0.00001$).

Detailed Partial Correlation Results

Judge	n	r	CI 95%	p-val
Qwen2.5-7B-Instruct	38	0.60043	[0.34 0.77]	0.00009
Qwen2.5-32B-Instruct	38	0.43376	[0.13 0.66]	0.00732
Qwen2.5-72B-Instruct	38	0.42353	[0.12 0.66]	0.00900
Meta-Llama-3.1-8B-Instruct	38	0.65172	[0.42 0.81]	0.00001
Meta-Llama-3.1-70B-Instruct	38	0.44770	[0.14 0.67]	0.00546
Llama-3.3-70B-Instruct	38	0.34882	[0.03 0.6]	0.03435
gemma-2-9b-it	38	0.64639	[0.41 0.8]	0.00002
gemma-2-27b-it	38	0.64808	[0.41 0.8]	0.00001
Ministral-8B-Instruct-2410	39	0.59745	[0.34 0.77]	0.00007

B.3.2 Multiple Regression

We perform multiple regression analysis with judgment scores as the dependent variable, using model similarity and ground-truth accuracy from the filtered set of MCQ questions as independent variables. Key results across all judges include:

- **Coefficient Significance:** Both similarity and accuracy show statistically significant effects ($p < 0.05$) for all judges. The similarity coefficients range from $\beta = 0.35$ for the large `Llama-3.3-70B-Instruct` to $\beta = 1.15$ for the smaller `Meta-Llama-3.1-8B-Instruct`, while accuracy coefficients span $\beta = 0.43$ for the small `Ministral-8B-Instruct-2410` to $\beta = 1.04$ for the large `Qwen2.5-72B-Instruct`.
- **Model Fit:** All regressions achieve high explanatory power with adjusted R^2 values between 0.87 (`Ministral-8B`) and 0.92 (`gemma-2-9b-it`).
- **Assumption Verification:**
  - *Normality:* Residuals are normally distributed (Shapiro-Wilk $p > 0.05$) for 7 of 9 judges. Exceptions: `Meta-Llama-3.1-8B-Instruct` ($p = 0.002$) and `Ministral-8B` ($p = 0.012$).

– *Homoscedasticity:* All models satisfy constant variance assumptions (Breusch-Pagan $p > 0.05$).

For example, the `Qwen2.5-7B-Instruct` judge model shows:

- Significant positive effects for both similarity ($\beta = 0.59$, $p < 0.001$) and accuracy ($\beta = 0.51$, $p < 0.001$)
- Strong model fit ($R^2 = 0.91$, $F(2, 35) = 182.9$, $p = 2.95 \times 10^{-19}$)
- Normally distributed residuals (Shapiro-Wilk $p = 0.690$)

Full regression outputs for all judges are provided in the Tables below. We present detailed regression results for each judge model. Each judge's statistical analysis includes three components: (1) Test summary, (2) Coefficient estimates, and (3) Diagnostic statistics. The consistent significance of similarity coefficients confirms that affinity bias persists even when controlling for actual model capability.

Judge: `Qwen2.5-7B-Instruct` (Qwen Team, 2025)			
Model:	OLS	Adj. R-squared:	0.908
Dependent Variable:	scores	AIC:	-134.3091
Date:	2025-01-30 11:42	BIC:	-129.3963
No. Observations:	38	Log-Likelihood:	70.155
Df Model:	2	F-statistic:	182.9
Df Residuals:	35	Prob (F-statistic):	2.95e-19
R-squared:	0.913	Scale:	0.0015837

	Coef.	Std.Err	t	P¿—t—	95% CI	
Intercept	0.092	0.019	4.885	0.000	0.054	0.131
similarity	0.586	0.132	4.442	0.000	0.318	0.853
accuracy	0.506	0.098	5.185	0.000	0.308	0.704

Omnibus:	2.363	Durbin-Watson:	2.097
Prob(Omnibus):	0.307	Jarque-Bera (JB):	1.400
Skew:	-0.437	Prob(JB):	0.496
Kurtosis:	3.348	Condition No.:	27

Normality & Homoscedasticity: Shapiro-Wilk Test for Normality: Statistic=0.979, (p-value=0.690). Residuals are likely normally distributed. Breusch-Pagan test for homoscedasticity: Lagrange Multiplier statistic: 0.456 (p-value: 0.796), F-value: 0.213 (p-value: 0.809). No evidence of heteroscedasticity (the residuals have a constant variance, homoscedasticity met).

Judge: `Qwen2.5-32B-Instruct` (Qwen Team, 2025)			
Model:	OLS	Adj. R-squared:	0.907
Dependent Variable:	scores	AIC:	-114.7801
Date:	2025-01-30 11:42	BIC:	-109.8674
No. Observations:	38	Log-Likelihood:	60.390
Df Model:	2	F-statistic:	182.2
Df Residuals:	35	Prob (F-statistic):	3.14e-19
R-squared:	0.912	Scale:	0.0026477

	Coef.	Std.Err	t	P¿—t—	95% CI	
Intercept	0.045	0.028	1.620	0.114	-0.011	0.101
similarity	0.414	0.145	2.848	0.007	0.119	0.709
accuracy	0.861	0.132	6.513	0.000	0.593	1.129

Omnibus:	0.227	Durbin-Watson:	2.052
Prob(Omnibus):	0.893	Jarque-Bera (JB):	0.411
Skew:	0.127	Prob(JB):	0.814
Kurtosis:	2.558	Condition No.:	25

Normality & Homoscedasticity: Shapiro-Wilk Test for Normality: Statistic=0.989, (p-value=0.965). Residuals are likely normally distributed. Breusch-Pagan test for homoscedasticity: Lagrange Multiplier statistic: 3.097 (p-value: 0.213), F-value: 1.553 (p-value: 0.226). No evidence of heteroscedasticity (the residuals have a constant variance, homoscedasticity met).

Judge: `Qwen2.5-72B-Instruct` (Qwen Team, 2025)

Model:	OLS	Adj. R-squared:	0.913
Dependent Variable:	scores	AIC:	-103.8097
Date:	2025-01-30 11:42	BIC:	-98.8969
No. Observations:	38	Log-Likelihood:	54.905
Df Model:	2	F-statistic:	195.4
Df Residuals:	35	Prob (F-statistic):	1.03e-19
R-squared:	0.918	Scale:	0.0035339

	Coef.	Std.Err	t	P¿—t—	95% CI	
Intercept	0.064	0.032	2.038	0.049	0.000	0.128
similarity	0.474	0.171	2.766	0.009	0.126	0.822
accuracy	1.043	0.156	6.702	0.000	0.727	1.359

Omnibus:	0.139	Durbin-Watson:	1.776
Prob(Omnibus):	0.933	Jarque-Bera (JB):	0.286
Skew:	-0.124	Prob(JB):	0.867
Kurtosis:	2.655	Condition No.:	25

Normality & Homoscedasticity: Shapiro-Wilk Test for Normality: Statistic=0.989, (p-value=0.968). Residuals are likely normally distributed. Breusch-Pagan test for homoscedasticity: Lagrange Multiplier statistic: 3.562 (p-value: 0.168), F-value: 1.810 (p-value: 0.179). No evidence of heteroscedasticity (the residuals have a constant variance, homoscedasticity met).

Judge: `Meta-Llama-3.1-8B-Instruct` (Llama Team, 2024a)

Model:	OLS	Adj. R-squared:	0.881
Dependent Variable:	scores	AIC:	-114.9610
Date:	2025-01-30 11:42	BIC:	-110.0482
No. Observations:	38	Log-Likelihood:	60.481
Df Model:	2	F-statistic:	138.6
Df Residuals:	35	Prob (F-statistic):	2.34e-17
R-squared:	0.888	Scale:	0.0026351

	Coef.	Std.Err	t	P¿—t—	95% CI	
Intercept	0.327	0.023	14.309	0.000	0.281	0.374
similarity	1.149	0.226	5.083	0.000	0.690	1.608
accuracy	0.532	0.106	5.035	0.000	0.317	0.746

Omnibus:	23.344	Durbin-Watson:	2.611
Prob(Omnibus):	0.000	Jarque-Bera (JB):	52.336
Skew:	-1.424	Prob(JB):	0.000
Kurtosis:	7.994	Condition No.:	31

Normality & Homoscedasticity: Shapiro-Wilk Test for Normality: Statistic=0.892, (p-value=0.002). Residuals are likely not normally distributed. Breusch-Pagan test for homoscedasticity: Lagrange Multiplier statistic: 4.186 (p-value: 0.123), F-value: 2.166 (p-value: 0.130). No evidence of heteroscedasticity (the residuals have a constant variance, homoscedasticity met).

Judge: `Meta-Llama-3.1-70B-Instruct` (Llama Team, 2024a)			
Model:	OLS	Adj. R-squared:	0.903
Dependent Variable:	scores	AIC:	-103.3457
Date:	2025-01-30 11:42	BIC:	-98.4329
No. Observations:	38	Log-Likelihood:	54.673
Df Model:	2	F-statistic:	172.4
Df Residuals:	35	Prob (F-statistic):	7.60e-19
R-squared:	0.908	Scale:	0.0035773

	Coef.	Std.Err	t	P¿—t—	95% CI	
Intercept	0.140	0.031	4.533	0.000	0.077	0.202
similarity	0.615	0.208	2.962	0.005	0.193	1.036
accuracy	0.917	0.157	5.827	0.000	0.598	1.237

Omnibus:	4.624	Durbin-Watson:	1.984
Prob(Omnibus):	0.099	Jarque-Bera (JB):	3.237
Skew:	-0.616	Prob(JB):	0.198
Kurtosis:	3.724	Condition No.:	28

Normality & Homoscedasticity: Shapiro-Wilk Test for Normality: Statistic=0.974, (p-value=0.502). Residuals are likely normally distributed. Breusch-Pagan test for homoscedasticity: Lagrange Multiplier statistic: 2.975 (p-value: 0.226), F-value: 1.487 (p-value: 0.240). No evidence of heteroscedasticity (the residuals have a constant variance, homoscedasticity met).

Judge: `Llama-3.3-70B-Instruct` Llama Team (2024c)			
Model:	OLS	Adj. R-squared:	0.884
Dependent Variable:	scores	AIC:	-94.3204
Date:	2025-01-30 11:42	BIC:	-89.4077
No. Observations:	38	Log-Likelihood:	50.160
Df Model:	2	F-statistic:	142.6
Df Residuals:	35	Prob (F-statistic):	1.49e-17
R-squared:	0.891	Scale:	0.0045363

	Coef.	Std.Err	t	P¿—t—	95% CI	
Intercept	0.162	0.036	4.544	0.000	0.089	0.234
similarity	0.487	0.221	2.202	0.034	0.038	0.935
accuracy	1.022	0.177	5.770	0.000	0.662	1.381

Omnibus:	4.168	Durbin-Watson:	1.898
Prob(Omnibus):	0.124	Jarque-Bera (JB):	2.830
Skew:	-0.584	Prob(JB):	0.243
Kurtosis:	3.652	Condition No.:	27

Normality & Homoscedasticity: Shapiro-Wilk Test for Normality: Statistic=0.978, (p-value=0.642). Residuals are likely normally distributed. Breusch-Pagan test for homoscedasticity: Lagrange Multiplier statistic: 2.500 (p-value: 0.287), F-value: 1.232 (p-value: 0.304). No evidence of heteroscedasticity (the residuals have a constant variance, homoscedasticity met).

Judge: `gemma-2-9b-it` (Gemma Team, 2024)			
Model:	OLS	Adj. R-squared:	0.917
Dependent Variable:	scores	AIC:	-122.8074
Date:	2025-01-30 11:42	BIC:	-117.8946
No. Observations:	38	Log-Likelihood:	64.404
Df Model:	2	F-statistic:	206.0
Df Residuals:	35	Prob (F-statistic):	4.36e-20
R-squared:	0.922	Scale:	0.0021435

	Coef.	Std.Err	t	P¿—t—	95% CI	
Intercept	0.134	0.021	6.356	0.000	0.091	0.177
similarity	0.763	0.152	5.012	0.000	0.454	1.072
accuracy	0.688	0.097	7.129	0.000	0.492	0.884

Omnibus:	6.751	Durbin-Watson:	1.901
Prob(Omnibus):	0.034	Jarque-Bera (JB):	5.969
Skew:	-0.621	Prob(JB):	0.051
Kurtosis:	4.492	Condition No.:	25

Normality & Homoscedasticity: Shapiro-Wilk Test for Normality: Statistic=0.959, (p-value=0.179). Residuals are likely normally distributed. Breusch-Pagan test for homoscedasticity: Lagrange Multiplier statistic: 2.550 (p-value: 0.279), F-value: 1.259 (p-value: 0.297). No evidence of heteroscedasticity (the residuals have a constant variance, homoscedasticity met).

Judge: `gemma-2-27b-it` (Gemma Team, 2024)

Model:	OLS	Adj. R-squared:	0.919
Dependent Variable:	scores	AIC:	-121.3075
Date:	2025-01-30 11:42	BIC:	-116.3947
No. Observations:	38	Log-Likelihood:	63.654
Df Model:	2	F-statistic:	212.0
Df Residuals:	35	Prob (F-statistic):	2.76e-20
R-squared:	0.924	Scale:	0.0022298

	Coef.	Std.Err	t	P¿—t—	95% CI	
Intercept	0.191	0.022	8.655	0.000	0.146	0.235
similarity	0.705	0.140	5.034	0.000	0.421	0.989
accuracy	0.677	0.106	6.407	0.000	0.462	0.892

Omnibus:	8.920	Durbin-Watson:	1.882
Prob(Omnibus):	0.012	Jarque-Bera (JB):	8.659
Skew:	-0.791	Prob(JB):	0.013
Kurtosis:	4.722	Condition No.:	24

Normality & Homoscedasticity: Shapiro-Wilk Test for Normality: Statistic=0.945, (p-value=0.062). Residuals are likely normally distributed. Breusch-Pagan test for homoscedasticity: Lagrange Multiplier statistic: 1.645 (p-value: 0.439), F-value: 0.792 (p-value: 0.461). No evidence of heteroscedasticity (the residuals have a constant variance, homoscedasticity met).

Judge: `Ministral-8B-Instruct-2410` (Mistral AI, 2024)

Model:	OLS	Adj. R-squared:	0.868
Dependent Variable:	scores	AIC:	-146.8086
Date:	2025-01-30 11:42	BIC:	-141.8179
No. Observations:	39	Log-Likelihood:	76.404
Df Model:	2	F-statistic:	125.6
Df Residuals:	36	Prob (F-statistic):	5.80e-17
R-squared:	0.875	Scale:	0.0012608

	Coef.	Std.Err	t	P¿—t—	95% CI	
Intercept	0.117	0.016	7.187	0.000	0.084	0.150
similarity	0.825	0.185	4.470	0.000	0.451	1.199
accuracy	0.432	0.063	6.803	0.000	0.303	0.560

Omnibus:	9.707	Durbin-Watson:	1.766
Prob(Omnibus):	0.008	Jarque-Bera (JB):	8.755
Skew:	-0.999	Prob(JB):	0.013
Kurtosis:	4.180	Condition No.:	36

Normality & Homoscedasticity: Shapiro-Wilk Test for Normality: Statistic=0.925, (p-value=0.012). Residuals are likely not normally distributed. Breusch-Pagan test for homoscedasticity: Lagrange Multiplier statistic: 1.270 (p-value: 0.530), F-value: 0.606 (p-value: 0.551). No evidence of heteroscedasticity (the residuals have a constant variance, homoscedasticity met).

B.4 Experimental Setup for Filtering MMLU-Pro

We evaluate or models and judges on a set of questions that can be answered as MCQ as well as in open-style without access to reference options. This benchmark is obtained by using the filtering process proposed by Myrzakhan et al. (2024) on MMLU-Pro, whereas it was originally used to filter MMLU (Hendrycks et al., 2021; Wang et al., 2024). Every question is evaluated twice using a `Qwen-2.5-32B-Instruct` LM: first, it is judged in a binary way whether it is possible to answer the question without access to the MCQ options. In the second iteration, the judge gives a fine-grained confidence score. If either the binary decision is positive or the confidence is above a threshold, the question becomes part of our filtered benchmark. After this filtering process, 8707 of the original 12032 questions remain. The detailed prompts are described in Prompts B.8.5 and B.8.6.

B.5 Experimental Setup to Perform Free-Form Inference on Filtered MMLU-Pro

To obtain the per-sample responses of every model on the filtered MMLU-Pro benchmark, we evaluate them using a custom task on the LM Evaluation Harness (Gao et al., 2023). Whereas the MCQ results from the Open LLM Leaderboard were generated using 5-shot evaluation without chain-of-thought (CoT) prompt, we included CoTs when performing free-form inference (Myrzakhan et al., 2024). This was necessary to ensure sufficient instruction following and response quality even for small base models, because free-form generation is more challenging than MCQ evaluation, where access to reference answers is given.

We modified every 5-shot CoT prompt by removing the answer options from the end of the question and replacing every reference to them in the CoT with the corresponding answer text. An example of this process is shown in Prompts B.8.3 and B.8.4. Our benchmark is implemented as a task for the LM Eval Harness (Gao et al., 2023). Every CoT response is generated until a stop condition is met. The final response that is judged is extracted using regex matching. We use vLLM as the backend for the LM Eval Harness (Kwon et al., 2023). Even for instruction-tuned models, the options `--apply_chat_template` and `--fewshot_as_multiturn` were omitted because for the majority of LMs inspected the quality of responses decreased slightly to severely. However, we did not thoroughly investigate whether this is the case for every single model.

B.6 Experimental Setup for LLM-as-a-Judge on Filtered MMLU-Pro

This section describes the setup of the experiment for Figure 2. On the x-axis we show the similarity between our LLM-as-a-judge and the LM that is being evaluated, whereas the y-axis shows how the given responses of that model were rated by the same judge. The list of judges is shown in Table 6 and the pool of models evaluated can be seen in Table 7.

For the computation of similarities, we use the logs of the official evaluation runs of Myrzakhan et al. (2024) that are provided on huggingface.co. The set of responses is filtered to include only those questions that were rated as answerable in open-style without access to the reference options, as previously described in Section B.4. Using the logarithmic probabilities of the models for the answer options of this set of questions, we compute CAPA and other similarities. In addition, for each model-judge pair data samples where the ground truth option differed were excluded from the final analysis, for the final sample count per pair see from table 8 to table 16.

Next, the judgment scores are obtained by prompting each LLM-as-a-judge to decide whether a given response to a question is correct or not. To mimic more common, but ungrounded settings for automatic AI evaluation, such as Arena-hard-auto or AlpacaEval 2.0, we do not provide the judge with access to ground-truth responses or MCQ answer options (Li et al., 2024b; Dubois et al., 2024). Since ground-truth responses for each question are available, it is possible to analyze the affinity bias of different judges and determine if there is any unfair preference. The prompt given to the judge is shown in Section B.8.1. Each final decision was given as token “0” (incorrect) or “1” (correct). Instruction-following is exceptional for the models used as LLM-as-a-judge, so the amount

of discarded samples due to invalid responses is negligible. Finally, the *Judge Score* of an evaluated model is computed by averaging the judge decisions across the set of questions.

B.7 List of Judges and Evaluated Language Models

Our judge preference experiments were performed using nine high-capability, open-weight models from four different model families. The models that represent the current state-of-the-art of open-weight language models from very small up to models with 72 billion parameters. Whereas the judges are all instruction-tuned, the list of evaluated models contains base models as well.

Whenever possible, we evaluated both the base and the instruction-tuned model for every combination of size and model family. Sometimes this was not possible, because the base model's weights were not available on huggingface, evaluations on the Open LLM Leaderboard v2 were not provided or the LM consistently crashed in vLLM when performing inference (Myrzakhan et al., 2024; Kwon et al., 2023). The list below shows all models that are part of our experiments.

Table 6: **LMs used as LLM-as-a-Judge**

Judge Model Name	
`google/gemma-2-9b-it`	(Gemma Team, 2024)
`google/gemma-2-27b-it`	(Gemma Team, 2024)
`Qwen/Qwen2.5-7B-Instruct`	(Qwen Team, 2025)
`Qwen/Qwen2.5-32B-Instruct`	(Qwen Team, 2025)
`Qwen/Qwen2.5-72B-Instruct`	(Qwen Team, 2025)
`meta-llama/Meta-Llama-3.1-8B-Instruct`	(Llama Team, 2024a)
`meta-llama/Meta-Llama-3.1-70B-Instruct`	(Llama Team, 2024a)
`meta-llama/Llama-3.3-70B-Instruct`	(Llama Team, 2024c)
`mistralai/Ministral-8B-Instruct-2410`	(Mistral AI, 2024)

B.8 Prompts

B.8.1 LM-Judge Prompt without Reference Answer

Prompt for Free-Form Evaluation

```
Your task is to judge whether the given response to a
question is correct or not.  You are only given a question
and the response you are judging.

Possible judgments:
"0":  The response is incorrect.
"1":  The response is correct.

Question:  "[Insert the question here]"
Response:  "[Insert the response here]"

To the best of your knowledge:  Does the provided response
answer the question correctly?  This is part of an automated
evaluation process, therefore you must only output a single
word:  "0" or "1".  Do not justify your decision.

Evaluation (0/1):
```

Table 7: **LMs Evaluated on the Filtered MMLU-Pro Benchmark**

Model Name	
Base Models	**Instruction-tuned Models**
Gemma-2 Family (Gemma Team, 2024)	
google/gemma-2-2b	google/gemma-2-2b-it
google/gemma-2-9b	google/gemma-2-9b-it
google/gemma-2-27b	google/gemma-2-27b-it
SmolLM2 Family (Allal et al., 2024)	
	HuggingFaceTB/SmolLM2-135M-Instruct
	HuggingFaceTB/SmolLM2-360M-Instruct
HuggingFaceTB/SmolLM2-1.7B	HuggingFaceTB/SmolLM2-1.7B-Instruct
Llama 3.1/3.2/3.3 Model Family (Llama Team, 2024a;b;c)	
meta-llama/Meta-Llama-3.1-8B	meta-llama/Meta-Llama-3.1-8B-Instruct
meta-llama/Meta-Llama-3.1-70B	meta-llama/Meta-Llama-3.1-70B-Instruct
meta-llama/Llama-3.2-1B	meta-llama/Llama-3.2-1B-Instruct
meta-llama/Llama-3.2-3B	meta-llama/Llama-3.2-3B-Instruct
	meta-llama/Llama-3.3-70B-Instruct
Phi-4 Family (Microsoft Research, 2024)	
	microsoft/phi-4
Qwen2.5 Family (Qwen Team, 2025)	
Qwen/Qwen2.5-0.5B	Qwen/Qwen2.5-0.5B-Instruct
Qwen/Qwen2.5-1.5B	Qwen/Qwen2.5-1.5B-Instruct
Qwen/Qwen2.5-3B	Qwen/Qwen2.5-3B-Instruct
Qwen/Qwen2.5-7B	Qwen/Qwen2.5-7B-Instruct
Qwen/Qwen2.5-14B	Qwen/Qwen2.5-14B-Instruct
Qwen/Qwen2.5-32B	Qwen/Qwen2.5-32B-Instruct
Qwen/Qwen2.5-72B	Qwen/Qwen2.5-72B-Instruct
Falcon-3 Model Family (Technology Innovation Institute, 2024)	
	tiiuae/Falcon3-1B-Instruct
tiiuae/Falcon3-7B-Base	tiiuae/Falcon3-7B-Instruct
tiiuae/Falcon3-10B-Base	tiiuae/Falcon3-10B-Instruct

Table 8: Final Sample Count (N) for Qwen2.5-7B-Instruct on Similarity Computation of Filtered MMLU-Pro

judge	model	N
Qwen2.5-7B-Instruct	HuggingFaceTB/SmolLM2-1.7B	8707
	HuggingFaceTB/SmolLM2-1.7B-Instruct	8706
	HuggingFaceTB/SmolLM2-135M-Instruct	8707
	HuggingFaceTB/SmolLM2-360M-Instruct	8707
	Qwen/Qwen2.5-0.5B	8707
	Qwen/Qwen2.5-0.5B-Instruct	8707
	Qwen/Qwen2.5-1.5B	8707
	Qwen/Qwen2.5-1.5B-Instruct	8707
	Qwen/Qwen2.5-14B	8707
	Qwen/Qwen2.5-14B-Instruct	8707
	Qwen/Qwen2.5-32B	8707
	Qwen/Qwen2.5-32B-Instruct	8707
	Qwen/Qwen2.5-3B	8707
	Qwen/Qwen2.5-3B-Instruct	8707
	Qwen/Qwen2.5-72B	8707
	Qwen/Qwen2.5-72B-Instruct	8707
	Qwen/Qwen2.5-7B	8707
	google/gemma-2-27b	8702
	google/gemma-2-27b-it	8702
	google/gemma-2-2b	8702
	google/gemma-2-2b-it	8685
	google/gemma-2-9b	8702
	google/gemma-2-9b-it	8702
	meta-llama/Llama-3.2-1B	8707
	meta-llama/Llama-3.2-1B-Instruct	8707
	meta-llama/Llama-3.2-3B	8707
	meta-llama/Llama-3.2-3B-Instruct	8707
	meta-llama/Llama-3.3-70B-Instruct	8706
	meta-llama/Meta-Llama-3.1-70B	8685
	meta-llama/Meta-Llama-3.1-70B-Instruct	8685
	meta-llama/Meta-Llama-3.1-8B	8685
	meta-llama/Meta-Llama-3.1-8B-Instruct	8702
	microsoft/phi-4	8706
	tiiuae/Falcon3-10B-Base	8706
	tiiuae/Falcon3-10B-Instruct	8706
	tiiuae/Falcon3-1B-Instruct	8706
	tiiuae/Falcon3-7B-Base	8706
	tiiuae/Falcon3-7B-Instruct	8706

Table 9: Final Sample Count (N) for Qwen2.5-32B-Instruct on Similarity Computation of Filtered MMLU-Pro

judge	model	N
Qwen2.5-32B-Instruct	HuggingFaceTB/SmolLM2-1.7B	8707
	HuggingFaceTB/SmolLM2-1.7B-Instruct	8706
	HuggingFaceTB/SmolLM2-135M-Instruct	8707
	HuggingFaceTB/SmolLM2-360M-Instruct	8707
	Qwen/Qwen2.5-0.5B	8707
	Qwen/Qwen2.5-0.5B-Instruct	8707
	Qwen/Qwen2.5-1.5B	8707
	Qwen/Qwen2.5-1.5B-Instruct	8707
	Qwen/Qwen2.5-14B	8707
	Qwen/Qwen2.5-14B-Instruct	8707
	Qwen/Qwen2.5-32B	8707
	Qwen/Qwen2.5-3B	8707
	Qwen/Qwen2.5-3B-Instruct	8707
	Qwen/Qwen2.5-72B	8707
	Qwen/Qwen2.5-72B-Instruct	8707
	Qwen/Qwen2.5-7B	8707
	Qwen/Qwen2.5-7B-Instruct	8707
	google/gemma-2-27b	8702
	google/gemma-2-27b-it	8702
	google/gemma-2-2b	8702
	google/gemma-2-2b-it	8685
	google/gemma-2-9b	8702
	google/gemma-2-9b-it	8702
	meta-llama/Llama-3.2-1B	8707
	meta-llama/Llama-3.2-1B-Instruct	8707
	meta-llama/Llama-3.2-3B	8707
	meta-llama/Llama-3.2-3B-Instruct	8707
	meta-llama/Llama-3.3-70B-Instruct	8706
	meta-llama/Meta-Llama-3.1-70B	8685
	meta-llama/Meta-Llama-3.1-70B-Instruct	8685
	meta-llama/Meta-Llama-3.1-8B	8685
	meta-llama/Meta-Llama-3.1-8B-Instruct	8702
	microsoft/phi-4	8706
	tiiuae/Falcon3-10B-Base	8706
	tiiuae/Falcon3-10B-Instruct	8706
	tiiuae/Falcon3-1B-Instruct	8706
	tiiuae/Falcon3-7B-Base	8706
	tiiuae/Falcon3-7B-Instruct	8706

Table 10: Final Sample Count (N) for Qwen2.5-72B-Instruct on Similarity Computation of Filtered MMLU-Pro

judge	model	N
Qwen2.5-72B-Instruct	HuggingFaceTB/SmolLM2-1.7B	8707
	HuggingFaceTB/SmolLM2-1.7B-Instruct	8706
	HuggingFaceTB/SmolLM2-135M-Instruct	8707
	HuggingFaceTB/SmolLM2-360M-Instruct	8707
	Qwen/Qwen2.5-0.5B	8707
	Qwen/Qwen2.5-0.5B-Instruct	8707
	Qwen/Qwen2.5-1.5B	8707
	Qwen/Qwen2.5-1.5B-Instruct	8707
	Qwen/Qwen2.5-14B	8707
	Qwen/Qwen2.5-14B-Instruct	8707
	Qwen/Qwen2.5-32B	8707
	Qwen/Qwen2.5-32B-Instruct	8707
	Qwen/Qwen2.5-3B	8707
	Qwen/Qwen2.5-3B-Instruct	8707
	Qwen/Qwen2.5-72B	8707
	Qwen/Qwen2.5-7B	8707
	Qwen/Qwen2.5-7B-Instruct	8707
	google/gemma-2-27b	8702
	google/gemma-2-27b-it	8702
	google/gemma-2-2b	8702
	google/gemma-2-2b-it	8685
	google/gemma-2-9b	8702
	google/gemma-2-9b-it	8702
	meta-llama/Llama-3.2-1B	8707
	meta-llama/Llama-3.2-1B-Instruct	8707
	meta-llama/Llama-3.2-3B	8707
	meta-llama/Llama-3.2-3B-Instruct	8707
	meta-llama/Llama-3.3-70B-Instruct	8706
	meta-llama/Meta-Llama-3.1-70B	8685
	meta-llama/Meta-Llama-3.1-70B-Instruct	8685
	meta-llama/Meta-Llama-3.1-8B	8685
	meta-llama/Meta-Llama-3.1-8B-Instruct	8702
	microsoft/phi-4	8706
	tiiuae/Falcon3-10B-Base	8706
	tiiuae/Falcon3-10B-Instruct	8706
	tiiuae/Falcon3-1B-Instruct	8706
	tiiuae/Falcon3-7B-Base	8706
	tiiuae/Falcon3-7B-Instruct	8706

Table 11: Final Sample Count (N) for Meta-Llama-3.1-8B-Instruct on Similarity Computation of Filtered MMLU-Pro

judge	model	N
Meta-Llama-3.1-8B-Instruct	HuggingFaceTB/SmolLM2-1.7B	8702
	HuggingFaceTB/SmolLM2-1.7B-Instruct	8701
	HuggingFaceTB/SmolLM2-135M-Instruct	8702
	HuggingFaceTB/SmolLM2-360M-Instruct	8702
	Qwen/Qwen2.5-0.5B	8702
	Qwen/Qwen2.5-0.5B-Instruct	8702
	Qwen/Qwen2.5-1.5B	8702
	Qwen/Qwen2.5-1.5B-Instruct	8702
	Qwen/Qwen2.5-14B	8702
	Qwen/Qwen2.5-14B-Instruct	8702
	Qwen/Qwen2.5-32B	8702
	Qwen/Qwen2.5-32B-Instruct	8702
	Qwen/Qwen2.5-3B	8702
	Qwen/Qwen2.5-3B-Instruct	8702
	Qwen/Qwen2.5-72B	8702
	Qwen/Qwen2.5-72B-Instruct	8702
	Qwen/Qwen2.5-7B	8702
	Qwen/Qwen2.5-7B-Instruct	8702
	google/gemma-2-27b	8707
	google/gemma-2-27b-it	8707
	google/gemma-2-2b	8707
	google/gemma-2-2b-it	8690
	google/gemma-2-9b	8707
	google/gemma-2-9b-it	8707
	meta-llama/Llama-3.2-1B	8702
	meta-llama/Llama-3.2-1B-Instruct	8702
	meta-llama/Llama-3.2-3B	8702
	meta-llama/Llama-3.2-3B-Instruct	8702
	meta-llama/Llama-3.3-70B-Instruct	8701
	meta-llama/Meta-Llama-3.1-70B	8690
	meta-llama/Meta-Llama-3.1-70B-Instruct	8690
	meta-llama/Meta-Llama-3.1-8B	8690
	microsoft/phi-4	8701
	tiiuae/Falcon3-10B-Base	8701
	tiiuae/Falcon3-10B-Instruct	8701
	tiiuae/Falcon3-1B-Instruct	8701
	tiiuae/Falcon3-7B-Base	8701
	tiiuae/Falcon3-7B-Instruct	8701

Table 12: Final Sample Count (N) for Meta-Llama-3.1-70B-Instruct on Similarity Computation of Filtered MMLU-Pro

judge	model	N
Meta-Llama-3.1-70B-Instruct	HuggingFaceTB/SmolLM2-1.7B	8685
	HuggingFaceTB/SmolLM2-1.7B-Instruct	8684
	HuggingFaceTB/SmolLM2-135M-Instruct	8685
	HuggingFaceTB/SmolLM2-360M-Instruct	8685
	Qwen/Qwen2.5-0.5B	8685
	Qwen/Qwen2.5-0.5B-Instruct	8685
	Qwen/Qwen2.5-1.5B	8685
	Qwen/Qwen2.5-1.5B-Instruct	8685
	Qwen/Qwen2.5-14B	8685
	Qwen/Qwen2.5-14B-Instruct	8685
	Qwen/Qwen2.5-32B	8685
	Qwen/Qwen2.5-32B-Instruct	8685
	Qwen/Qwen2.5-3B	8685
	Qwen/Qwen2.5-3B-Instruct	8685
	Qwen/Qwen2.5-72B	8685
	Qwen/Qwen2.5-72B-Instruct	8685
	Qwen/Qwen2.5-7B	8685
	Qwen/Qwen2.5-7B-Instruct	8685
	google/gemma-2-27b	8690
	google/gemma-2-27b-it	8690
	google/gemma-2-2b	8690
	google/gemma-2-2b-it	8707
	google/gemma-2-9b	8690
	google/gemma-2-9b-it	8690
	meta-llama/Llama-3.2-1B	8685
	meta-llama/Llama-3.2-1B-Instruct	8685
	meta-llama/Llama-3.2-3B	8685
	meta-llama/Llama-3.2-3B-Instruct	8685
	meta-llama/Llama-3.3-70B-Instruct	8684
	meta-llama/Meta-Llama-3.1-70B	8707
	meta-llama/Meta-Llama-3.1-8B	8707
	meta-llama/Meta-Llama-3.1-8B-Instruct	8690
	microsoft/phi-4	8684
	tiiuae/Falcon3-10B-Base	8684
	tiiuae/Falcon3-10B-Instruct	8684
	tiiuae/Falcon3-1B-Instruct	8684
	tiiuae/Falcon3-7B-Base	8684
	tiiuae/Falcon3-7B-Instruct	8684

Table 13: Final Sample Count (N) for Llama-3.3-70B-Instruct on Similarity Computation of Filtered MMLU-Pro

judge	model	N
Llama-3.3-70B-Instruct	HuggingFaceTB/SmolLM2-1.7B	8706
	HuggingFaceTB/SmolLM2-1.7B-Instruct	8707
	HuggingFaceTB/SmolLM2-135M-Instruct	8706
	HuggingFaceTB/SmolLM2-360M-Instruct	8706
	Qwen/Qwen2.5-0.5B	8706
	Qwen/Qwen2.5-0.5B-Instruct	8706
	Qwen/Qwen2.5-1.5B	8706
	Qwen/Qwen2.5-1.5B-Instruct	8706
	Qwen/Qwen2.5-14B	8706
	Qwen/Qwen2.5-14B-Instruct	8706
	Qwen/Qwen2.5-32B	8706
	Qwen/Qwen2.5-32B-Instruct	8706
	Qwen/Qwen2.5-3B	8706
	Qwen/Qwen2.5-3B-Instruct	8706
	Qwen/Qwen2.5-72B	8706
	Qwen/Qwen2.5-72B-Instruct	8706
	Qwen/Qwen2.5-7B	8706
	Qwen/Qwen2.5-7B-Instruct	8706
	google/gemma-2-27b	8701
	google/gemma-2-27b-it	8701
	google/gemma-2-2b	8701
	google/gemma-2-2b-it	8684
	google/gemma-2-9b	8701
	google/gemma-2-9b-it	8701
	meta-llama/Llama-3.2-1B	8706
	meta-llama/Llama-3.2-1B-Instruct	8706
	meta-llama/Llama-3.2-3B	8706
	meta-llama/Llama-3.2-3B-Instruct	8706
	meta-llama/Meta-Llama-3.1-70B	8684
	meta-llama/Meta-Llama-3.1-70B-Instruct	8684
	meta-llama/Meta-Llama-3.1-8B	8684
	meta-llama/Meta-Llama-3.1-8B-Instruct	8701
	microsoft/phi-4	8707
	tiiuae/Falcon3-10B-Base	8707
	tiiuae/Falcon3-10B-Instruct	8707
	tiiuae/Falcon3-1B-Instruct	8707
	tiiuae/Falcon3-7B-Base	8707
	tiiuae/Falcon3-7B-Instruct	8707

Table 14: Final Sample Count (N) for gemma-2-9b-it on Similarity Computation of Filtered MMLU-Pro

judge	model	N
gemma-2-9b-it	HuggingFaceTB/SmolLM2-1.7B	8702
	HuggingFaceTB/SmolLM2-1.7B-Instruct	8701
	HuggingFaceTB/SmolLM2-135M-Instruct	8702
	HuggingFaceTB/SmolLM2-360M-Instruct	8702
	Qwen/Qwen2.5-0.5B	8702
	Qwen/Qwen2.5-0.5B-Instruct	8702
	Qwen/Qwen2.5-1.5B	8702
	Qwen/Qwen2.5-1.5B-Instruct	8702
	Qwen/Qwen2.5-14B	8702
	Qwen/Qwen2.5-14B-Instruct	8702
	Qwen/Qwen2.5-32B	8702
	Qwen/Qwen2.5-32B-Instruct	8702
	Qwen/Qwen2.5-3B	8702
	Qwen/Qwen2.5-3B-Instruct	8702
	Qwen/Qwen2.5-72B	8702
	Qwen/Qwen2.5-72B-Instruct	8702
	Qwen/Qwen2.5-7B	8702
	Qwen/Qwen2.5-7B-Instruct	8702
	google/gemma-2-27b	8707
	google/gemma-2-27b-it	8707
	google/gemma-2-2b	8707
	google/gemma-2-2b-it	8690
	google/gemma-2-9b	8707
	meta-llama/Llama-3.2-1B	8702
	meta-llama/Llama-3.2-1B-Instruct	8702
	meta-llama/Llama-3.2-3B	8702
	meta-llama/Llama-3.2-3B-Instruct	8702
	meta-llama/Llama-3.3-70B-Instruct	8701
	meta-llama/Meta-Llama-3.1-70B	8690
	meta-llama/Meta-Llama-3.1-70B-Instruct	8690
	meta-llama/Meta-Llama-3.1-8B	8690
	meta-llama/Meta-Llama-3.1-8B-Instruct	8707
	microsoft/phi-4	8701
	tiiuae/Falcon3-10B-Base	8701
	tiiuae/Falcon3-10B-Instruct	8701
	tiiuae/Falcon3-1B-Instruct	8701
	tiiuae/Falcon3-7B-Base	8701
	tiiuae/Falcon3-7B-Instruct	8701

Table 15: Final Sample Count (N) for gemma-2-27b-it on Similarity Computation of Filtered MMLU-Pro

judge	model	N
gemma-2-27b-it	HuggingFaceTB/SmolLM2-1.7B	8702
	HuggingFaceTB/SmolLM2-1.7B-Instruct	8701
	HuggingFaceTB/SmolLM2-135M-Instruct	8702
	HuggingFaceTB/SmolLM2-360M-Instruct	8702
	Qwen/Qwen2.5-0.5B	8702
	Qwen/Qwen2.5-0.5B-Instruct	8702
	Qwen/Qwen2.5-1.5B	8702
	Qwen/Qwen2.5-1.5B-Instruct	8702
	Qwen/Qwen2.5-14B	8702
	Qwen/Qwen2.5-14B-Instruct	8702
	Qwen/Qwen2.5-32B	8702
	Qwen/Qwen2.5-32B-Instruct	8702
	Qwen/Qwen2.5-3B	8702
	Qwen/Qwen2.5-3B-Instruct	8702
	Qwen/Qwen2.5-72B	8702
	Qwen/Qwen2.5-72B-Instruct	8702
	Qwen/Qwen2.5-7B	8702
	Qwen/Qwen2.5-7B-Instruct	8702
	google/gemma-2-27b	8707
	google/gemma-2-2b	8707
	google/gemma-2-2b-it	8690
	google/gemma-2-9b	8707
	google/gemma-2-9b-it	8707
	meta-llama/Llama-3.2-1B	8702
	meta-llama/Llama-3.2-1B-Instruct	8702
	meta-llama/Llama-3.2-3B	8702
	meta-llama/Llama-3.2-3B-Instruct	8702
	meta-llama/Llama-3.3-70B-Instruct	8701
	meta-llama/Meta-Llama-3.1-70B	8690
	meta-llama/Meta-Llama-3.1-70B-Instruct	8690
	meta-llama/Meta-Llama-3.1-8B	8690
	meta-llama/Meta-Llama-3.1-8B-Instruct	8707
	microsoft/phi-4	8701
	tiiuae/Falcon3-10B-Base	8701
	tiiuae/Falcon3-10B-Instruct	8701
	tiiuae/Falcon3-1B-Instruct	8701
	tiiuae/Falcon3-7B-Base	8701
	tiiuae/Falcon3-7B-Instruct	8701

Table 16: Final Sample Count (N) for Ministral-8B-Instruct-2410 on Similarity Computation of Filtered MMLU-Pro

judge	model	N
Ministral-8B-Instruct-2410	HuggingFaceTB/SmolLM2-1.7B	8706
	HuggingFaceTB/SmolLM2-1.7B-Instruct	8707
	HuggingFaceTB/SmolLM2-135M-Instruct	8706
	HuggingFaceTB/SmolLM2-360M-Instruct	8706
	Qwen/Qwen2.5-0.5B	8706
	Qwen/Qwen2.5-0.5B-Instruct	8706
	Qwen/Qwen2.5-1.5B	8706
	Qwen/Qwen2.5-1.5B-Instruct	8706
	Qwen/Qwen2.5-14B	8706
	Qwen/Qwen2.5-14B-Instruct	8706
	Qwen/Qwen2.5-32B	8706
	Qwen/Qwen2.5-32B-Instruct	8706
	Qwen/Qwen2.5-3B	8706
	Qwen/Qwen2.5-3B-Instruct	8706
	Qwen/Qwen2.5-72B	8706
	Qwen/Qwen2.5-72B-Instruct	8706
	Qwen/Qwen2.5-7B	8706
	Qwen/Qwen2.5-7B-Instruct	8706
	google/gemma-2-27b	8701
	google/gemma-2-27b-it	8701
	google/gemma-2-2b	8701
	google/gemma-2-2b-it	8684
	google/gemma-2-9b	8701
	google/gemma-2-9b-it	8701
	meta-llama/Llama-3.2-1B	8706
	meta-llama/Llama-3.2-1B-Instruct	8706
	meta-llama/Llama-3.2-3B	8706
	meta-llama/Llama-3.2-3B-Instruct	8706
	meta-llama/Llama-3.3-70B-Instruct	8707
	meta-llama/Meta-Llama-3.1-70B	8684
	meta-llama/Meta-Llama-3.1-70B-Instruct	8684
	meta-llama/Meta-Llama-3.1-8B	8684
	meta-llama/Meta-Llama-3.1-8B-Instruct	8701
	microsoft/phi-4	8707
	tiiuae/Falcon3-10B-Base	8707
	tiiuae/Falcon3-10B-Instruct	8707
	tiiuae/Falcon3-1B-Instruct	8707
	tiiuae/Falcon3-7B-Base	8707
	tiiuae/Falcon3-7B-Instruct	8707

B.8.2 LM-JUDGE PROMPT WITH MCQ OPTIONS

Prompt for Free-Form Evaluation with Access to MCQ Reference Options

```
Your task is to judge whether the given response to a
question is correct or not.  You are given a question, a
ground truth response, incorrect options and the response
you are judging.

Possible judgments:
"0":  The response is incorrect.  It does not match the
ground-truth answer or is more similar to any of the
incorrect options than to the ground-truth answer.
"1":  The response is correct.  It matches the ground-truth.

Question:  "[Insert the question here]"
Ground truth:  "[Insert the ground-truth option here]"
Incorrect option (1):  "[Insert the 1st wrong option here]"
...
Incorrect option (9):  "[Insert the 9th wrong option here]"
Response:  "[Insert the response here]"

To the best of your knowledge:  Does the provided response
answer the question correctly, taking the ground-truth
and wrong answer options into account?  This is part of an
automated evaluation process, therefore you must only output
a single word:  "0" or "1".  Do not justify your decision.

Evaluation (0/1):
```

B.8.3 ORIGINAL MCQ COT PROMPT

We describe how an original MCQ prompt on MMLU-Pro is transformed into an open-style prompt for free-form inference without access to the reference options. The original chain-of-thought (CoT) prompt consists of general information about the task, a few-shot list of questions-answer pairs and finally the actual question that is to be solved.

Each question is preceded by the keyword "Question:", followed by the question text and the list of answer options. Every option text is marked with a letter. Next, a reference chain-of-thought is given after the key-phrase "Answer: Let's think step by step" to provide an in-context example on how to solve related questions. This CoT can include references to the answer options. The CoT answer ends with the key-phrase "The answer is (X)" where "X" is the letter of the correct option. The phrase nudges the evaluated LM to answer in the same way, allowing to extract the final response using regex matching. The number of in-context examples depends on the `--num_fewshot` parameter. In our experiment, we use five examples, but for reasons of brevity, only a single one is part of the example prompt below. Finally, the phrase that starts a CoT is repeated right before the model's response.

We automatically transform these MCQ into OSQ CoT prompts. The general information is slightly adjusted to indicate the type of task. All key-phrases remain the same. We completely omit the MCQ options at the end behind the question. Any reference to an option in the chain-of-thought is replaced with the option text itself – e.g. "(G)" is replaced with the corresponding "(The second and third pharyngeal arches)". This includes the final response: "The answer is (XYZ).". Our experiments have shown that even the smallest models evaluated are able to follow these instructions and provide free-form responses that can be automatically extracted in the vast majority of cases.

Few-shot CoT MCQ Prompt

```
The following are multiple choice questions (with answers)
about health.  Think step by step and then finish your answer
with the answer is (X) where X is the correct letter choice.

Question:  What is the embryological origin of the hyoid
bone?
Options:
A. The third and fourth pharyngeal arches
B. The fourth pharyngeal arch
C. The third pharyngeal arch
D. The second pharyngeal arch
E. The second, third and fourth pharyngeal arches
F. The first pharyngeal arch
G. The second and third pharyngeal arches
H. The first and third pharyngeal arches
I. The first, second and third pharyngeal arches
J. The first and second pharyngeal arches

Answer:  Let's think step by step.  We refer to Wikipedia
articles on anatomy for help.  Let's solve this problem
step by step.  The hyoid bone, which is also known as the
hyooid, is a a small U-shaped bone located in the anterior
neck.  In its resting position, it lies between the base of
the mandible and the third cervical vertebrae.  We know that
the second and the third pharyngeal arches give rise to the
horns of the hyoid bone; therefore, the embryological origin
of the hyoid bone are the second and the third pharyngeal
arches|this information is covered in option (G). Therefore,
we conclude that (G) must be the correct answer.  The answer
is (G)

Question:  ...

Question:  Which disease do polyomaviruses predominantly
cause?
Options:
A. Tumours
B. Brain pathology
C. No disease at all
D. Kidney infections

Answer:  Let's think step by step.
```

B.8.4 OPEN-STYLE COT PROMPT

Few-shot CoT OSQ Prompt

```
The following are multiple choice questions (with answers)
about health.  Think step by step and then finish your answer
with the answer is (X) where X is the correct letter choice.

Question:  What is the embryological origin of the hyoid
bone?

Answer:  Let's think step by step.  We refer to Wikipedia
articles on anatomy for help.  Let's solve this problem
step by step.  The hyoid bone, which is also known as the
hyooid, is a a small U-shaped bone located in the anterior
neck.  In its resting position, it lies between the base of
the mandible and the third cervical vertebrae.  We know that
the second and the third pharyngeal arches give rise to the
horns of the hyoid bone; therefore, the embryological origin
of the hyoid bone are the second and the third pharyngeal
arches|this information is covered in option (The second
and third pharyngeal arches).  Therefore, we conclude that
(The second and third pharyngeal arches) must be the correct
answer.  The answer is (The second and third pharyngeal
arches)

Question:  ...

Question:  Which disease do polyomaviruses predominantly
cause?

Answer:  Let's think step by step.
```

These are the two prompts used for coarse and fine-grained filtering to get the OSQ version of MMLU-Pro. They almost exactly match the original ones provided by Myrzakhan et al. (2024), but we performed minimal adjustments to make them more suitable to MMLU-Pro.

B.8.5 COARSE FILTERING PROMPT

Coarse Prompt

```
Your task is to review a series of multiple-choice questions
and evaluate their ability to be answered without the
provided answer choices.

For questions that begin with an incomplete sentence (e.g.,
"During swallowing, ..."), use your knowledge to attempt
to complete the sentence accurately.  For direct questions
that ask for specific information or identification (e.g.,
"Which of the following structures is part of the small
intestine?"), assess whether the question is formulated
clearly enough that an informed answer can be given without
seeing the multiple-choice options.  For mathematical or
analytical questions (e.g., "Find all cosets of the subgroup
4Z of 2Z"), determine if the question provides enough context
and information for a solution to be formulated without
additional options.

Please follow this format for your evaluation:

QUESTION: [Insert the question here]

VERDICT: Respond with "YES" if the question is clear and can
be directly answered based on its content alone, or "NO" if
it relies on the answer choices to be understood or answered.
Your response should include only the verdict without any
justification or reasoning.
```

B.8.6 FINE-GRAINED FILTERING PROMPT

Fine-grained Prompt

```
You will assign a numerical score from 1 to 10 based on how
confidently it can be answered without the choices.  The
scoring criteria are as follows:

1:  The question is entirely dependent on its choices for
an answer, making it impossible to answer without them.
Example:  'Which of the following statements is correct?'

10:  The question can be easily and confidently answered
based solely on the question stem,without any need to refer
to the provided options.  Example:  'What is the first law of
thermodynamics in physics?'

Intermediate Scores:

2-4:  The question stem gives very little information and is
highly reliant on the choices forcontext.  Example:  'Which
of these is a prime number?'  'The _______ perspective on
sustainability resulted from growth models that analysed the
carrying capacity of the planet, overall concluding that the
finite capacity of the earth and _______, _______ and _______ by
current and past generations could reduce quality of life for
future generations.'
5:  The question provides some context or information,
that gives a moderate possibility to answer the question.
Example:  'Which of the following best describes the
structure that collects urine in the body?'
6:  The question provides a good amount of context or
information, that gives a moderate possibility to answer
the question.  Example:  'Statement 1 | A factor group of
a non-Abelian group is non-Abelian.  Statement 2 | If K is a
normal subgroup of H and H is a normal subgroup of G, then K
is a normal subgroup of G.'
7:  The question provides a good amount of context or
information, that gives a high possibility to answer the
question.  Example:  'The element (4, 2) of Z_12 x Z_8 has
order'
8-9:  The question provides a good amount of context or
information, that gives a high possibility to answer the
question.  Example:  'A "dished face" profile is often
associated with'

ONLY GIVE THE VALUE BETWEEN 1-10 AS YOUR ANSWER. DO NOT
INCLUDE ANY OTHER INFORMATION IN YOUR RESPONSE.
```

C WEAK-TO-STRONG TRAINING

C.1 SETUP

We follow the weak to strong generalization setup proposed in Burns et al. (2024), focusing on NLP tasks. The original paper reported results with GPT (Radford et al., 2019) model versions. Instead, we use larger, more capable and recent open-weight models to make observations at the frontier. For this, we used the codebase of Scherlis et al. (2024) that uses open-weight models on Huggingface instead. We now describe the full setup here.

Table 17: Datasets, Weak Models and Strong Models Used in the Weak to Strong Experiments.

Models	Datasets
Weak Models	sciq (Welbl et al., 2017)
google/gemma-2-2b (Gemma Team, 2024)	anli-r2 (Nie et al., 2019)
Qwen/Qwen2.5-1.5B (Qwen Team, 2025)	boolq (Clark et al., 2019)
meta-llama/Llama-3.2-1B (Llama Team, 2024a)	cola (Warstadt et al., 2019)
microsoft/phi-2 (Li et al., 2023)	ethics-utilitarianism (Hendrycks et al., 2020)
Strong Models	sst2 (Socher et al., 2013)
google/gemma-2-9b	twitter-sentiment (Zhang et al., 2019)
Qwen/Qwen2.5-7B	dream (Sun et al., 2019)
meta-llama/Llama-3.1-8B	mc-taco (Zhou et al., 2019)
	multirc (Khashabi et al., 2018)
	quail (Rogers et al., 2020)
	quartz (Tafjord et al., 2019)
	social-i-qa (Sap et al., 2019)
	wic (Pilehvar & Camacho-Collados, 2018)
	cosmos-qa (Huang et al., 2019)

The setup uses a pretrained weak base model W, a pretrained strong base model S and a dataset D, where D_{tr}, D_{val}, D_{te} are the training (10,000 samples), validation (1,000 samples) and test (5,000 samples) datasplits respectively. D_{tr} is divided into two halves, independently assigning each sample to D_{tr1}, D_{tr2} with 50% probability each. All the datasets studied convert standard NLP MCQ datasets into binary classification, by randomly sampling one of the wrong options. Predictions ≥ 0.5 are considered as class 1, and < 0.5 as class 0. We highlight the models and datasets used in our study in Table 17.

First, the weak base model W is finetuned on ground-truth labels in D_{tr1} to obtain the weak supervisor W_s. In the original setup, this is meant to simulate a human that is an expert at the given task. Then, W_{gt} annotates samples in D_{tr2}, and the strong student model S is finetuned on these annotations to obtain the Weak to Strong trained model S_{w2s}. In the original setup, the strong base model simulates a future model with superhuman intelligence, but not finetuned for specific domain knowledge.

Finetuning Methodology: For the above finetuning steps we use Low Rank Adapters (LoRA) (Hu et al., 2021) due to budget constraints, and train a binary classifier the same as Scherlis et al. (2024). We use the confidence weighted loss proposed by Burns et al. (2024). This loss encourages the strong model's predictions to align with both a weaker model and its own "hardened" predictions. The hardened predictions are derived by thresholding the strong model's output. The loss function is defined as:

$$\mathcal{L}(f) = (1-\alpha) \cdot \text{CE}(f(x), f_w(x)) + \alpha \cdot \text{CE}(f(x), \hat{f}(x)) \tag{19}$$

where $f(x)$ is the strong model's output, $f_w(x)$ is the weak model's output, $\hat{f}(x) = \mathbb{I}[f(x) > t]$ represents the hardened predictions using an adaptive threshold t, and α is a weight that increases over the initial phase of training.

Following Scherlis et al. (2024) we use a cosine learning rate schedule, with 40 warmup steps, the learning rates for the weak, strong model are $5 \times 10^{-4}, 8 \times 10^{-5}$ respectively, and we train for 3 epochs which is sufficient for the train and validation loss to stabilize.

Weak to Strong Gain Metric: We wish to study the gain achieved from weak to strong training for the strong student model. To characterize the initial accuracy of the strong student model, we train a binary classifier head to obtain S_b. The weak to strong gain is then quantified as:

$$Acc(S_{w2s}) - Acc(S_b) \tag{20}$$

Note that this is different from the PGR metric reported by Burns et al. (2024). Their goal was to show weak to strong training can make the strong student cross the accuracy of the weak supervisor. Thus, they measured accuracy gained over the weak supervisor $Acc(S_{w2s}) - Acc(W_{gt})$, normalizing it by an "upper-bound" obtained by training the strong student on ground-truth labels on D_{tr2}, giving $PGR = \frac{Acc(S_{w2s}) - Acc(W_{gt})}{Acc(S_{gt}) - Acc(W_{gt})}$. In our work, we show that leveraging complementary knowledge

effectively might actually allow $S_{w2s} > S_{gt}$, questioning their "upper-bound". Thus we stick to reporting how much the student model improved as described in Equation 20.

Similarity vs Weak to Strong Gain: In Figure 12 we reported weak-to-strong gain (Equation 20) on the Y-axis, and similarity (κ_p) on the X-axis. We plot linear grouped by model pair, thus varying the task within each model pair for the linear fit. Figure 12 shows the same scatter points but colored based on the dataset. This shows that weak-to-strong gain is consistently higher for tasks where models are less similar, and how similar two models are depends mostly on the task, i.e. there is not much variance in similarity across the model pairs for a fixed task.

Discarded Results: We had initially run experiments with three more weak models: SmolLM 1.7B, Qwen-2.5-0.5B, Llama-3.2-1B against the same list of strong models reported above. However, we found that on some tasks, the weak-to-strong gain was negative. The weak supervisor (W_{gt}) models had lower accuracy compared to the strong student S_b, leading to a decrease in accuracy for the strong student after weak to strong training. We thus removed these weak models from our analysis. Similarly, we had also tried the Hellaswag dataset, but found that both weak and strong models had very low accuracies, often below 60% where chance is 50% for binary classification, consistent with Scherlis et al. (2024), and decided to not include it in our analysis.

C.2 Elicitation vs Complementary Knowledge

Table 18: **Models and Sources of Knowledge in Complementary Knowledge vs Elicitation Comparison**.

Model	Ground-truth labels in D_{tr1}	Latent Knowledge of W	Latent Knowledge of S
W_{gt}	✓	✓	✗
S_{gt}	✓	✗	✓
S_{w2s}	✓[4]	✓	✓

Figure 3a points to the fact that similarity or difference between the weak supervisor and the initial strong student are strong predictors of weak-to-strong gain. However, the initially proposed explanation of weak-to-strong generalization is "elicitation", i.e. the strong student has latent capabilities that are brought out by finetuning on weak annotations (Burns et al., 2024). To quantify the contribution of these two sources for weak-to-strong gain, elicitation and complementary knowledge, we establish the following setup.

First, our functional similarity metric cannot capture latent knowledge in the strong student's representations. For this, we follow Burns et al. (2024) and finetune the strong student S on ground-truth labels of D_{tr1} to obtain the elicited strong student model S_{gt}. Note that we use D_{tr1} instead of D_{tr2} here so that the training set of S_{w2s}, D_{tr2}, remains held-out, and we can analyze the relative effect of eliciation and complementary knowledge on both the train and test set.

Table 18 summarizes sources of knowledge for the weak supervisor W_{gt}, strong elicited S_{gt}, and weak-to-strong trained student S_{w2s} in our setup. S_{w2s} benefits from the latent knowledge of S, complementary knowledge transfer of latent knowledge of W, and distillation of knowledge in D_{tr1} from W_{gt}. It learns imperfectly from all three sources of knowledge. Given this, we now discuss how Figure 3b compares elicitation and complementary knowledge transfer:

- **Bottom-Left = Elicitation**: W_{gt} does not benefit from latent knowledge of S, so S_{w2s} accuracy on samples where it is wrong but S_{gt} is correct signify knowledge that could only be from elicitation.
- **Top-Right = Complementary Knowledge Transfer**: S_{gt} does not benefit from the latent knowledge of W, so S_{w2s} accuracy on samples where it is wrong but W_{gt} is correct signify knowledge that could only be from complementary knowledge transfer.
- **Top-Left = Could be Both**: Accuracy of S_{w2s} on samples where both W_{gt}, S_{gt} are correct could come from both their latent knowledge, and the ground-truth annotations in D_{tr1}. Thus, these could be both elicitation and complementary knowledge transfer, or also learning from the finetuning data.
- **Bottom-Right = Random flips**: We find that 10% predictions can flip even when finetuning W, S on ground-truth labels from D_{tr2} instead of D_{tr1}, which were split into two halves

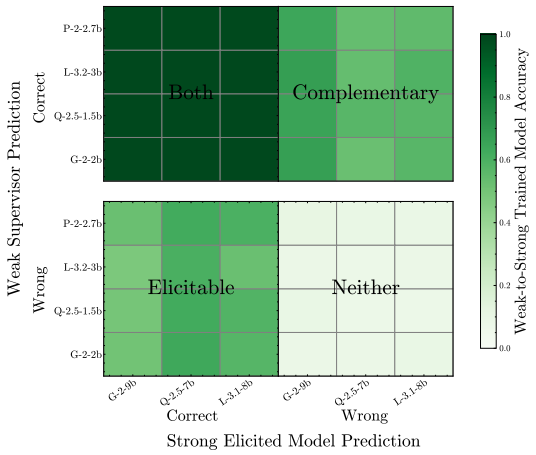

Figure 11: We decompose the accuracy of the weak to strong trained model on four parts of the train data distribution based on whether the weak supervisor and an oracle strong elicited model (using ground-truth annotations) are correct or wrong. All results are averaged over 15 datasets. Sub-rectangles represent weak, strong model pairs. On the train dataset, complementary knowledge transfer (mean accuracy 0.59) plays an equal role as elicitation (mean accuracy 0.56).

at random from D_{tr}. Thus, the roughly 10% accuracy on samples that both W_{gt}, S_{gt} got wrong could just be random flips to the correct prediction (since its a binary classification setting).

Behavior on the Train Set: Figure 11 reports the same comparison of elicitation and complementary knowledge transfer but on D_{tr2} on which the weak-to-strong training occurs. This set is unseen for both the weak supervisor W_{gt} and the strong elicited model S_{gt}. We find that in fitting the training data complementary knowledge transfer plays an equal or bigger role than elicitation. This is to be expected as S_{w2s} is trained by fitting on W_{gt}'s annotations of D_{tr2}. The weak-to-strong trained student however still generalizes more similarly to the strong elicited model than the weak supervisor, though complementary knowledge transfer is also visible on test set predictions as seen in Figure 3b.

C.3 Effect of Different similarity metrics

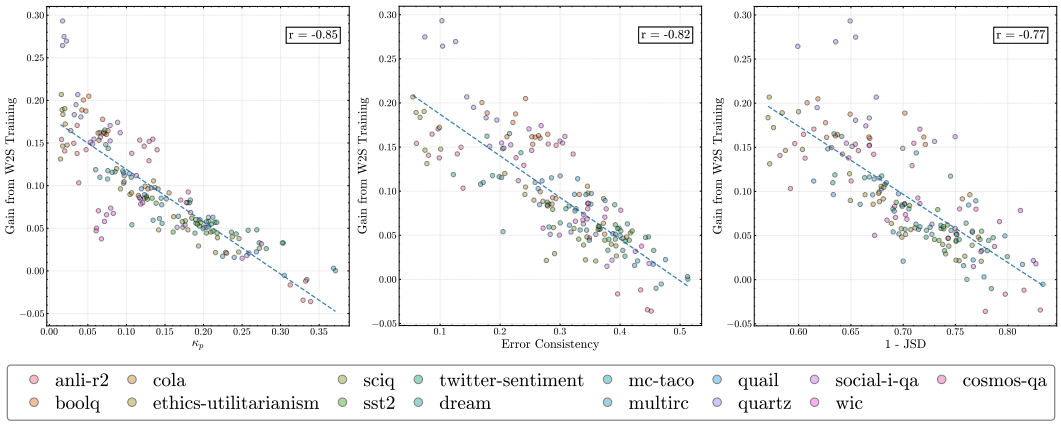

Figure 12: **Various Similarity Metrics vs Weak-to-Strong gain**. The highest correlation is seen for CAPA κ_p, though in the binary classification setup of weak-to-strong generalization the probabilistic information does not add much value compared to error consistency. $1 - JSD$ gives a more noisy scatter plot, with lower correlation (r).

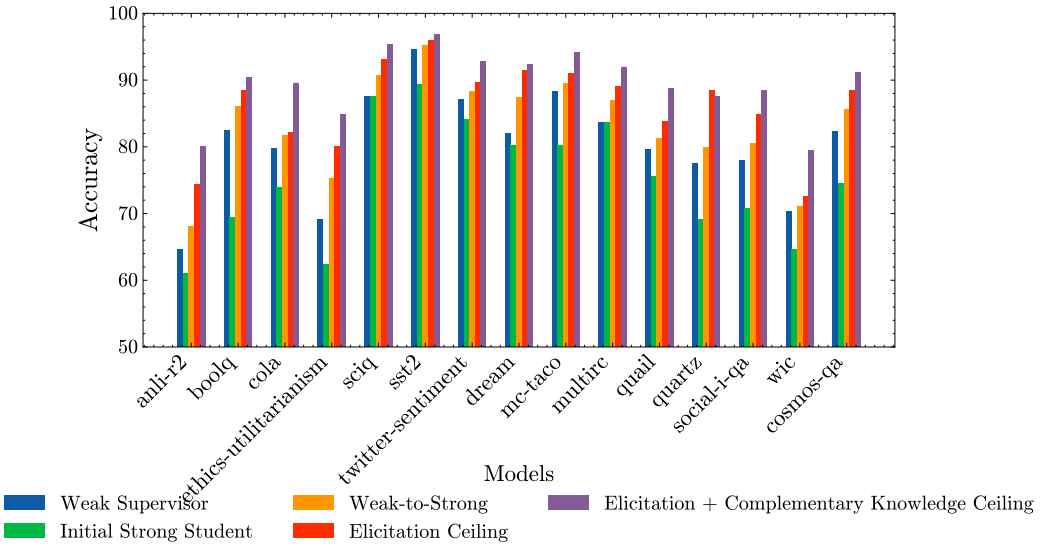

Figure 13: **Test Accuracies for various models and ceiling estimates in Weak-to-Strong training**. The accuracies are averaged over 12 model pairs. The initial strong student model has consistently lower accuracy than the weak supervisor consistent with Burns et al. (2024); Scherlis et al. (2024). The weak-to-strong trained student surpasses the weak-supervisor across datasets. However it has lower accuracy than the elicitation ceiling which trains the strong student on ground-truth annotations. Finally, our new estimated ceiling which incorporates the complementary knowledge of the weak supervisor has even higher accuracies, showing even more scope for improvements.

We now report similarity vs weak-to-strong gain for various alternate similarity metrics. Here, we color the scatter points by dataset instead of model pair, and fit a single line, for ease of interpretation. We report the following similarity metrics:

- Error Consistency - In this setting of binary classification, this is equivalent to the non-probabilistic version of CAPA, as there is only one incorrect option so models cannot disagree when both are incorrect on a sample.
- CAPA (κ_p) - Our metric which incorporates probabilistic information into error consistency.
- $1 - JSD$ - Since Jensen-Shannon Distance measures difference between distributions and is normalized between 0 and 1, by subtracting it from 1 we can obtain a similarity metric for ease of comparison with the previous metrics.

In Figure 12 we see that all metrics can show the same trend, that is, tasks where models differ more have larger gain from weak-to-strong training. The highest correlation is seen for CAPA, though in the binary classification setup of weak-to-strong generalization the probabilistic information does not add much value compared to error consistency. $1 - JSD$ gives a more noisy scatter plot, with lower correlation (r).

C.4 Accuracies in Weak-to-Strong Training

In Figure 13 we report average across the 12 model pairs for all 15 datasets. Consistently, the ordering is as follows: the initial strong student has lower accuracy than the weak supervisor, but surpasses it after weak-to-strong training. However, it is not able to match the performance ceiling of ground-truth elicitation. Finally, if the take a union over the correct predictions of the weak supervisor and strong elicited model, the performance ceiling can be even higher.

C.5 Weak-to-strong Accuracy Value Details in Elicitation vs Complementary Knowledge Analysis

In Table 19 and Table 20 we report the underlying numbers for Figure 3b and Figure 11 respectively. The astute observer may be confused about the around 12% accuracy on the test set when when both the weak supervisor and strong elicited model are wrong (bottom-right quadrant). We find that merely finetuning on a different random subset of training data leads to around 11% predictions being flipped. Thus, much of this accuracy could just be due to random chance because of the binary classification setup. This also indicates that complementary knowledge transfer explains much of the beyond-chance accuracy not accounted for by elicitation.

Table 19: **Weak-to-strong trained model's accuracies on four parts of the test data distribution, based on relative mistakes of weak-supervisor, strong elicited model**. This table reports the underlying numbers for Figure 3b, with accuracy averaged across the 15 datasets studied for each model pair. We see that the weak-to-strong model is almost always correct when both the weak-supervisor, strong elicited model are correct. It is more correct when the strong elicited model is correct and the weak-supervisor is wrong than vice-versa. This indicates weak-to-strong training currently exploits more of the possible gains from elicitation, but less of the possible gains from complementary knowledge transfer.

Common Knowledge		**Complementary Knowledge Transfer**	
Pair	**Acc (%)**	**Pair**	**Acc (%)**
(gemma-2-2b, gemma-2-9b)	97.4	(gemma-2-2b, gemma-2-9b)	45.2
(gemma-2-2b, Qwen2.5-7B)	97.1	(gemma-2-2b, Qwen2.5-7B)	34.9
(gemma-2-2b, Llama-3.1-8B)	97.0	(gemma-2-2b, Llama-3.1-8B)	40.1
(Qwen2.5-1.5B, gemma-2-9b)	97.1	(Qwen2.5-1.5B, gemma-2-9b)	47.1
(Qwen2.5-1.5B, Qwen2.5-7B)	97.4	(Qwen2.5-1.5B, Qwen2.5-7B)	36.9
(Qwen2.5-1.5B, Llama-3.1-8B)	96.5	(Qwen2.5-1.5B, Llama-3.1-8B)	39.6
(Llama-3.2-3B, gemma-2-9b)	97.6	(Llama-3.2-3B, gemma-2-9b)	46.2
(Llama-3.2-3B, Qwen2.5-7B)	97.5	(Llama-3.2-3B, Qwen2.5-7B)	36.2
(Llama-3.2-3B, Llama-3.1-8B)	97.3	(Llama-3.2-3B, Llama-3.1-8B)	41.7
(phi-2, gemma-2-9b)	97.3	(phi-2, gemma-2-9b)	50.2
(phi-2, Qwen2.5-7B)	97.3	(phi-2, Qwen2.5-7B)	44.2
(phi-2, Llama-3.1-8B)	97.4	(phi-2, Llama-3.1-8B)	44.2
Elicitation		**Both Wrong**	
Pair	**Acc (%)**	**Pair**	**Acc (%)**
(gemma-2-2b, gemma-2-9b)	71.0	(gemma-2-2b, gemma-2-9b)	12.9
(gemma-2-2b, Qwen2.5-7B)	75.0	(gemma-2-2b, Qwen2.5-7B)	10.7
(gemma-2-2b, Llama-3.1-8B)	72.3	(gemma-2-2b, Llama-3.1-8B)	13.0
(Qwen2.5-1.5B, gemma-2-9b)	69.4	(Qwen2.5-1.5B, gemma-2-9b)	11.4
(Qwen2.5-1.5B, Qwen2.5-7B)	73.3	(Qwen2.5-1.5B, Qwen2.5-7B)	11.6
(Qwen2.5-1.5B, Llama-3.1-8B)	72.1	(Qwen2.5-1.5B, Llama-3.1-8B)	13.5
(Llama-3.2-3B, gemma-2-9b)	71.0	(Llama-3.2-3B, gemma-2-9b)	12.5
(Llama-3.2-3B, Qwen2.5-7B)	77.2	(Llama-3.2-3B, Qwen2.5-7B)	11.2
(Llama-3.2-3B, Llama-3.1-8B)	73.4	(Llama-3.2-3B, Llama-3.1-8B)	13.8
(phi-2, gemma-2-9b)	67.9	(phi-2, gemma-2-9b)	12.3
(phi-2, Qwen2.5-7B)	71.1	(phi-2, Qwen2.5-7B)	11.6
(phi-2, Llama-3.1-8B)	69.0	(phi-2, Llama-3.1-8B)	11.5

D Similarity Trends with Increasing Capabilities

D.1 Setup Details

We utilize two prominent benchmark datasets from the OpenLLM leaderboard to explore the relationship between model similarity and capability: MMLU Pro and BBH. For the BBH dataset,

Table 20: **Weak-to-strong trained model's accuracies on four parts of the train data distribution, based on relative mistakes of weak-supervisor, strong elicited model**. This table reports the underlying numbers for Figure 11, with accuracy averaged across the 15 datasets studied for each model pair. On the train distribution, the weak-to-strong model is almost equally correct on the only-elicitable and only learnable from complementary knowledge samples, with a slight lean towards the latter. Yet, Table 19 showed it generalizes more similarly to the strong elicited model.

Common Knowledge		**Complementary Knowledge Transfer**	
Pair	**Acc (%)**	**Pair**	**Acc (%)**
(gemma-2-2b, gemma-2-9b)	98.6	(gemma-2-2b, gemma-2-9b)	66.8
(gemma-2-2b, Qwen2.5-7B)	98.6	(gemma-2-2b, Qwen2.5-7B)	52.5
(gemma-2-2b, Llama-3.1-8B)	98.5	(gemma-2-2b, Llama-3.1-8B)	56.8
(Qwen2.5-1.5B, gemma-2-9b)	98.5	(Qwen2.5-1.5B, gemma-2-9b)	65.2
(Qwen2.5-1.5B, Qwen2.5-7B)	98.6	(Qwen2.5-1.5B, Qwen2.5-7B)	56.9
(Qwen2.5-1.5B, Llama-3.1-8B)	98.5	(Qwen2.5-1.5B, Llama-3.1-8B)	57.0
(Llama-3.2-3B, gemma-2-9b)	98.7	(Llama-3.2-3B, gemma-2-9b)	67.2
(Llama-3.2-3B, Qwen2.5-7B)	98.7	(Llama-3.2-3B, Qwen2.5-7B)	53.8
(Llama-3.2-3B, Llama-3.1-8B)	98.5	(Llama-3.2-3B, Llama-3.1-8B)	58.8
(phi-2, gemma-2-9b)	98.0	(phi-2, gemma-2-9b)	64.4
(phi-2, Qwen2.5-7B)	98.4	(phi-2, Qwen2.5-7B)	53.7
(phi-2, Llama-3.1-8B)	98.2	(phi-2, Llama-3.1-8B)	54.8

Elicitation		**Both Wrong**	
Pair	**Acc (%)**	**Pair**	**Acc (%)**
(gemma-2-2b, gemma-2-9b)	50.7	(gemma-2-2b, gemma-2-9b)	8.6
(gemma-2-2b, Qwen2.5-7B)	63.5	(gemma-2-2b, Qwen2.5-7B)	8.3
(gemma-2-2b, Llama-3.1-8B)	57.3	(gemma-2-2b, Llama-3.1-8B)	9.5
(Qwen2.5-1.5B, gemma-2-9b)	49.2	(Qwen2.5-1.5B, gemma-2-9b)	9.6
(Qwen2.5-1.5B, Qwen2.5-7B)	62.2	(Qwen2.5-1.5B, Qwen2.5-7B)	7.4
(Qwen2.5-1.5B, Llama-3.1-8B)	58.2	(Qwen2.5-1.5B, Llama-3.1-8B)	7.7
(Llama-3.2-3B, gemma-2-9b)	47.9	(Llama-3.2-3B, gemma-2-9b)	8.8
(Llama-3.2-3B, Qwen2.5-7B)	60.3	(Llama-3.2-3B, Qwen2.5-7B)	7.9
(Llama-3.2-3B, Llama-3.1-8B)	52.4	(Llama-3.2-3B, Llama-3.1-8B)	8.5
(phi-2, gemma-2-9b)	52.6	(phi-2, gemma-2-9b)	10.8
(phi-2, Qwen2.5-7B)	62.3	(phi-2, Qwen2.5-7B)	9.4
(phi-2, Llama-3.1-8B)	60.1	(phi-2, Llama-3.1-8B)	9.1

we aggregate 23 distinct tasks that can be studied as multiple-choice questions from the Big-Bench Hard benchmark to ensure that each model is evaluated on sufficient questions, thereby ensuring statistically significant results. The MMLU Pro dataset consists of MCQs across 14 different subjects, with varying numbers of options per question. Notably, some questions are repeated with shuffled option orders. To maintain consistency, we filter the dataset by retaining only those questions for which both the question text and the correct option index remain consistent across all models. This filtering process yields a refined dataset of 11,828 questions.

To analyze trends across model capabilities, we divide 130 models (Table 22) into five bins based on their individual accuracy percentiles. This binning strategy is followed for all experimental setups and ensures an approximately equal distribution of models per bin, maintaining a consistent sample size across bins. We select model pairs within each bin and compute their similarity and average accuracy. This approach ensures that the average accuracy of the pairs remains representative of the individual model accuracies within the bin. We do not consider model pairs from the same family to avoid confounding effects of model similarity being attributed to model family rather than the capability.

D.2 WHY ARE MODEL MISTAKES BECOMING MORE SIMILAR? A PRELIMINARY ANALYSIS

D.2.1 INSTRUCTION-TUNING EXACERBATES THE TREND

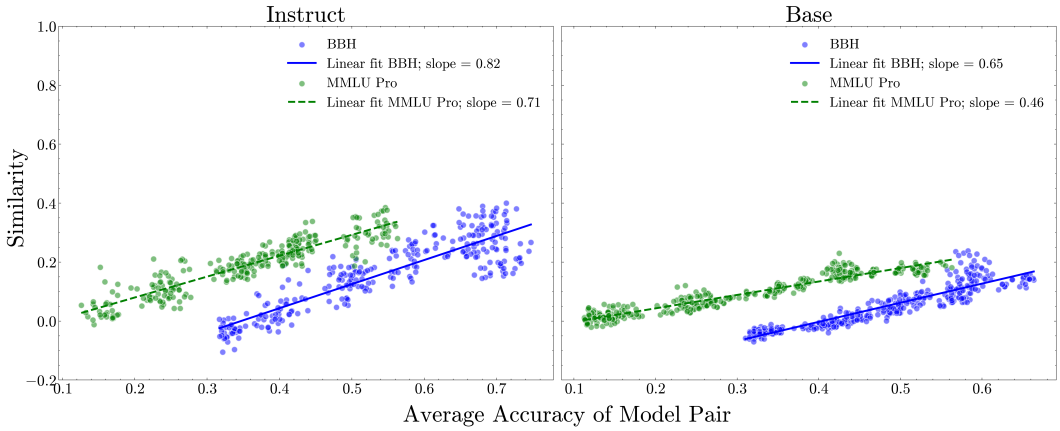

Figure 14: **LM Similarity (κ_p) vs Capabilities in Instruct-tuned and Base models on MMLU pro and BBH**. After applying the same model binning stratergy and pairwise similarity, a steeper trend is observed in the instruct-tuned models compared to base models for both datasets.

Instruction-tuned models are base models that have been fine-tuned on instruction datasets and their corresponding outputs, enhancing their ability to follow user instructions accurately. Among the models analyzed for the capability-similarity trend, we categorize them into instruction-tuned and base models. Using the same binning strategy as discussed in the previous section, we first assign all models to bins based on their accuracy percentiles. When computing pairwise similarity and accuracy, we restrict to pairs of the same model type— base-base and instruct-instruct models. As illustrated in Fig. 14, instruction-tuned model pairs exhibit a stronger similarity trend with a steeper slope compared to base models. This can likely be attributed to the fact that instruction-tuned models may have been fine-tuned on similar instruction datasets, leading to a higher similarity trend among them.

D.2.2 IS THE TREND CONFOUNDED BY QUESTION DIFFICULTIES?

To address the potential confounder that models might exhibit higher similarity as their capability increases simply due to their inherent ability to solve harder problems, we analyze the relationship between question hardness and model similarity on MMLU Pro and BBH. Question hardness is determined by the percentage of models that answer a question correctly, with harder questions being those that fewer models answer correctly. We split the data samples into percentile bins based on question hardness and compute the average similarity across all capability bins of the initial setting, as illustrated in Fig. 15(a).

Fig. 15(a) demonstrates that the overall average similarity remains consistent across different levels of question hardness, with only a slight increase observed for the hardest questions (100th percentile). This consistency indicates that the hardness of the questions does not significantly confound the observed trend of increasing similarity with model capability. These findings reinforce the hypothesis that the growing similarity among models is not merely a byproduct of their ability to solve harder problems but reflects a deeper trend in model behavior as their capabilities improve.

D.2.3 CAN CHANGING ARCHITECTURE REDUCE MODEL SIMILARITY?

To study the effect of model similarities across different architectures, we analyze Falcon3 Mamba 7B base and instruct models by computing their CAPA values with Falcon3 7B transformer, Mistral 7Bv0.3, and Llama 3.1 8B base and instruct models. We ensure that the accuracies of the non-Falcon3 transformers are within ±5% of the Mamba model to ensure comparable capabilities.

In Table 21, $Similarity_1$ presents the CAPA between the Falcon3 Mamba and Falcon3 Transformer, $Similarity_2$ the CAPA between Falcon3 Mamba and Llama/Mistral Transformer, and $Similarity_3$

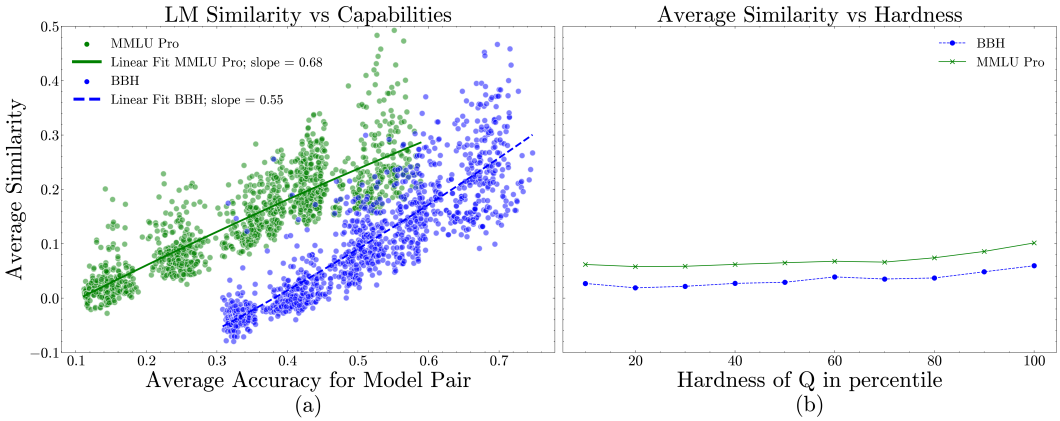

Figure 15: **Role of question difficulty in similarity-capability trend.** We plot in parallel (a) Scatter plot with model pairs, illustrating the increasing trend of similarity (κ_p) with model capability. (b) Average similarity (κ_p) across all capability bins for different levels of question hardness. CAPA is mostly consistent across question hardness, with a slight increase on the hardest questions. This shows that question difficulty is not a significant confounder for increasing similarity in mistakes.

between Falcon3 Transformer and Llama/Mistral Transformers. The results reveal that base models exhibit lower overall similarity compared to instruction-tuned models, with pairwise similarity between Falcon3 Mamba and non-Falcon Mistral/Llama Transformers showing the least similarity. Within the base model category, Falcon3 Mamba and Falcon Transformers demonstrate the highest similarity. For instruction-tuned models, Falcon3 Transformer and Mistral/Llama Transformer pairs exhibit the highest similarity, followed closely by Falcon3 Mamba and Falcon3 Transformer.

The Falcon Mamba-Falcon Transformers maintain higher similarity overall, potentially due to their shared model family, despite differences in their underlying architectures. This observation highlights that architectural differences may play a less significant role in model similarity compared to factors such as training data and fine-tuning procedures. From the earlier section, instruction-tuned models exhibit a stronger similarity trend, similar to as observed in this setting.

Table 21: **Analyzing the effect of difference in architecture on CAPA κ_p.** Using base and instruct variants of Falcon3 Mamba and Falcon3 Transformer of size 7B, we compare it with transformers with similar size and accuracy from a different model family- LLama and Mistral. $Similarity_1$ consistently has an overall higher similarity due to models belonging to the same family. In instruct-tuned models, $Similarity_3$ is the highest, possibly due to the instruct-tuning.

Falcon Mamba	**Falcon Transformer**	**Transformer Model**	$Similarity_1$	$Similarity_2$	$Similarity_3$
7B Base	7B Base	Llama 3.1 8B	0.0619	0.0167	0.0422
		Mistral v0.3 7B		0.0105	0.0235
7B Instruct	7B Instruct	Llama 3.1 8B Instruct	0.1111	0.0665	0.173
		Mistral v0.3 7B Instruct		0.0582	0.1584

D.3 Alternative Similarity Metrics

As discussed in earlier sections, multiple metrics can be employed to quantify the similarity between models, each with its own strengths and limitations. In this analysis, we evaluate several alternative metrics under the same experimental setting used for CAPA, including the binning and averaging strategies, for the two benchmark datasets. Fig. 17a presents the results for discrete κ_p, which does not utilize logit information, while Fig. 17b demonstrates a similar trend using κ_p for $M > 2$ (κ_p extended for more than 2 models). Additionally, Fig. 16 includes results for Jensen-Shannon Divergence (JSD) and Error Consistency Geirhos et al. (2020).

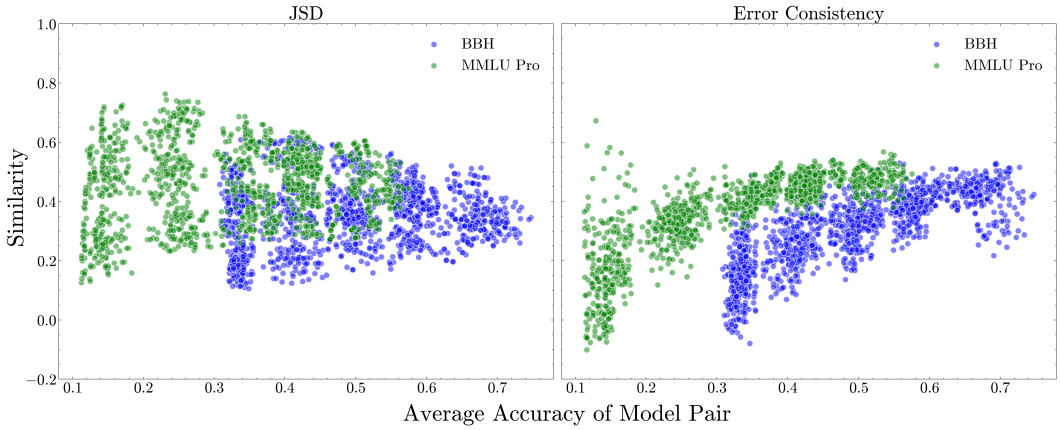

Figure 16: **Error consistency and JSD for model similarity on BBH and MMLU Pro.** The y-axis represents the similarity computed using JSD and Error consistency. JSD exhibits high variance and a flat trend, whereas Error Consistency shows an increasing trend with model capability, similar to the trend observed in κ_p.

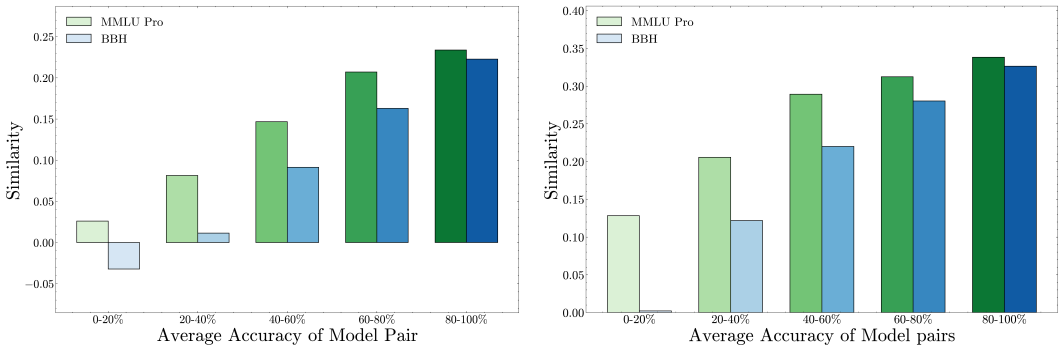

(a) **LM Similarity (κ_p for $M > 2$) vs Average Accuracy of Model Pairs in each Capability bin**

(b) **LM Similarity (Discrete κ_p) vs Average Accuracy of Model Pairs in each Capability bin**

Figure 17: Discrete κ_p and κ_p for $M > 2$ values computed on the MMLU Pro and BBH dataset. An increasing trend in similarity is observed across both datasets in accordance with the hypothesis. Discrete κ_p uses similar averaging idea as used in κ_p while in κ_p for $M > 2$, the similarity is computed using all models in a capability bin at once.

Discrete κ_p exhibits an increasing trend with model capability, closely mirroring the trend observed with κ_p. Similarly, κ_p for $M > 2$, which leverages probabilistic information, unlike Discrete κ_p, shows a strong upward trend. Unlike other metrics, κ_p for $M > 2$ provides a direct measure of similarity that quantifies agreement among all models within a bin, eliminating the need for averaging pairwise similarities. Models of same family within the same bin are retained when computing the metric. In contrast, JSD does not exhibit a clear trend and remains flat with high variance across the capability axis. Error Consistency, however, aligns with the upward trend observed in other metrics, further supporting the hypothesis that model similarity increases with capability.

D.4 Model capability vs similarity across domains

The scatter plot in Fig 4 shows the increasing similarity trend after aggregating across the subjects (MMLU pro) and tasks (BBH). Fig 18 and Fig 19 show the observed trend within each individual subject and task for MMLU Pro and BBH respectively.

In the MMLU Pro dataset, the trend of increasing average similarity within each bin as model capability improves is consistently observed across all individual subjects. For the BBH tasks, while the trend is not as pronounced in some tasks, it remains significant in the majority of them. This

Figure 18: **LM Similarity (κ_p) vs Capability on MMLU pro for each subject.** The increasing trend holds for all 14 subjects in MMLU pro. The similarity trend is therefore not a consequence of a particular domain or subject in MMLU Pro.

weaker trend in certain BBH tasks can be attributed to the limited number of questions per task for each model, with a maximum of 250 questions per task, which reduces the reliability of the results compared to the more robust MMLU Pro dataset. This is also visible through the high confidence interval in the BBH tasks, unlike MMLU pro subjects.

D.5 LIST OF MODELS

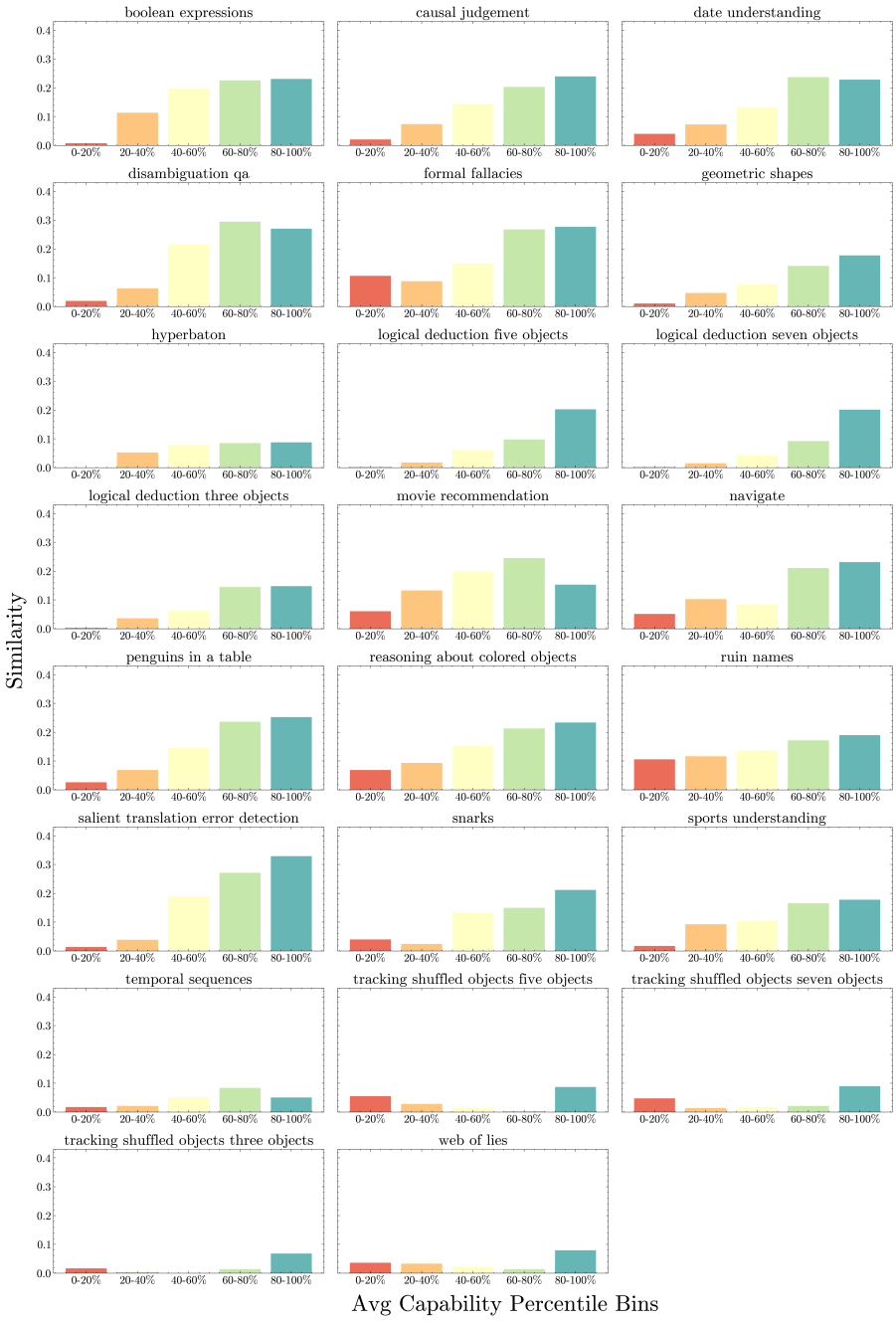

Figure 19: **LM Similarity (κ_p) vs Capability on each Big-Bench Hard task.** The increasing trend holds for most BBH tasks. Each task has atmost 250 questions, resulting in minimal data to compute similarity for the individual tasks.

Table 22: **Models from OpenLLM leaderboard used to study the capability-similarity trend**. Models across different families, architectures, size and versions were used to ensure robustness in the experimental results. The models included are both base and fine-tuned versions where available.

Dev	Model Family	Size	Type
01-ai	Yi-1.5	9B, 34B	Base, Instruct
	Yi	34B	Base, Instruct
CohereForAI	c4ai-command-r-plus	–	Base, Instruct
	aya-expanse	32b	Base
EleutherAI	Pythia	160m, 410m, 2.8b, 6.9b, 12b	Base
Google	Gemma	2b, 7b	Base, Instruct
	Gemma-1.1	2b, 7b	Instruct
	Gemma-2	2b, 9b, 27b	Base, Instruct
	Flan-T5	Small, Base, Large, XL, XXL	Base
Meta	Llama-2	7b, 13b, 70b	Base, Instruct
	Llama-3.2	1B, 3B	Base, Instruct
	Llama-3	8B, 70B	Base, Instruct
	Llama-3.1	8B, 70B	Instruct
	Llama-3.3	70B	Instruct
Mistral AI	Mistral-7B	v0.1, v0.2, v0.3	Base, Instruct
	Mixtral-8x7B	v0.1	Base, Instruct
	Mistral-Large	–	Instruct
Nvidia	Mistral-NeMo-Minitron	8B	Base, Instruct
Qwen	Qwen2	0.5B, 1.5B, 7B, 72B	Base, Instruct
	Qwen2.5	0.5B, 1.5B, 3B, 7B, 14B, 32B, 72B	Base, Instruct
	Qwen2-Math	7B, 72B	Base, Instruct
	Qwen2-VL	7B, 72B	Instruct
	Qwen2.5-Coder	7B	Base, Instruct
	Qwen1.5	32B, 110B	Base, Chat
Tiiuae	Falcon	7b, 11B, 40b	Base, Instruct
	Falcon3	7B, 10B	Base, Instruct
	Falcon-mamba	7b	Base
Upstage	solar-pro-preview	–	Instruct